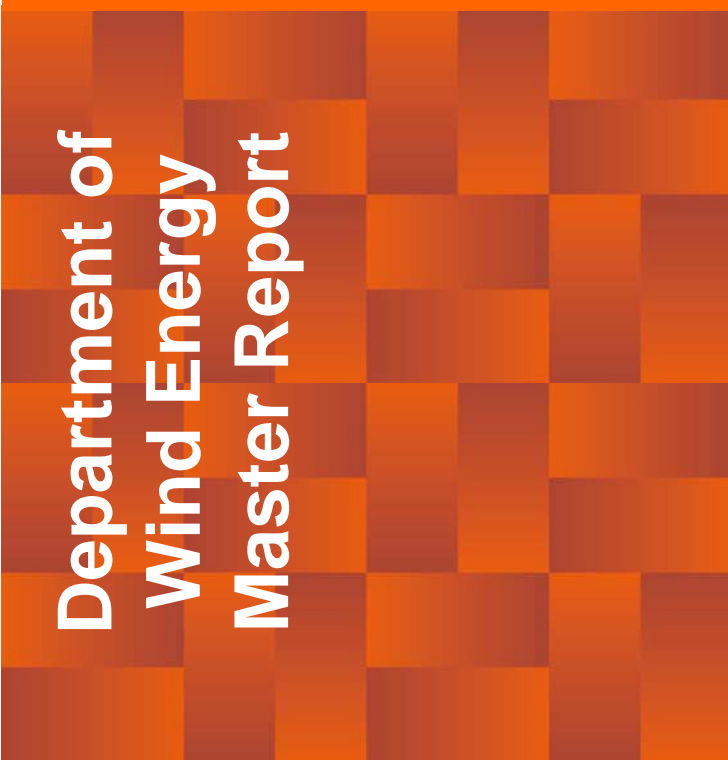


# Frequency control in power systems without must-run units



## Department of Wind Energy Master Report

Guillermo Dominguez Lopez

DTU Wind Energy-M-0156

June 2017

**DTU Wind Energy**  
Department of Wind Energy

---



**Authors:** Guillermo Dominguez Lopez

**Title:** Frequency control in power systems without must-run units

**DTU Wind Energy-M-0156**

**June 2017**

**Project Period:**

**January - June 2017**

**ECTS: 30**

**Education: Master of Science**

**Supervisors:**

Anca D. Hansen

Kaushik Das

Müfit Altin

**DTU Wind Energy**

**Remarks:**

This report is submitted as partial fulfillment of the requirements for graduation in the above education at the Technical University of Denmark.

DTU Wind Energy is a department of the Technical University of Denmark with a unique integration of research, education, innovation and public/private sector consulting in the field of wind energy. Our activities develop new opportunities and technology for the global and Danish exploitation of wind energy. Research focuses on key technical-scientific fields, which are central for the development, innovation and use of wind energy and provides the basis for advanced education at the education.

We have more than 240 staff members of which approximately 60 are PhD students. Research is conducted within nine research programmes organized into three main topics: Wind energy systems, Wind turbine technology and Basics for wind energy.

**Technical University of Denmark**

Department of Wind Energy

Frederiksborgvej 399

4000 Roskilde

Denmark

[www.vindenergi.dtu.dk](http://www.vindenergi.dtu.dk)

# Abstract

Nowadays, most of the ancillary services such as reserve capacity, inertia and frequency control relies on large conventional power plants. Approaching future power systems with high penetration of renewable energy sources (RES) has resulted in imperative need for the evaluation of ancillary services. This research focuses on the frequency stability which must be ensured in order to maintain the grid stability against imbalances between generation and load. This large conventional power plants that provide ancillary services are called “must-run” units. These facilities are generation power plants necessary during certain operating conditions and they are responsible for providing enough ancillary services to ensure a reliable operation of power systems. Given a high RES penetration in the future, must-run units are expected to be reduced or totally decommissioned reducing the power system inertia. This may result in insecure operation threatening the reliability of the power supply. This project investigates the frequency stability support from renewable energy generation such as wind power plants (WPPs) and solar photovoltaic systems (SPVs) in future power systems with high penetration of RES and without must-run units. Sensitivity studies for frequency stability are performed on a simulated 2030 scenario for western Denmark (DK1) power system.

The objective of this master thesis is to study the DK1 power system to analyse the ability of modern controllable WPPs to provide frequency stability without must-run units in a future scenario dominated by RES generation. This project examines the primary frequency control in DK1 simulating an overfrequency event islanding DK1 from the CE power system with high wind forecast.

The main results of this project reveal that the fast deploy of active power by the RES generation counterbalances the reduced inertia in the power system, which can operate without a lack of stability of the power supply for overfrequency events without must-run units. However, there are technical capabilities and limitations that curtail the RES penetration. Recommendations on the parameters of the WPPs frequency control are made according to the droop, the ramp rate and the RES penetration. The virtual inertia is recommended for frequency control of WPPs and increases its importance when the RES penetration is high. The support of HVDC interconnections is an interesting facility to increase the RES penetration allowing the power system to operate with even less inertia online maintaining a stable supply. Although, the measurement and communication delay by the frequency controllers increases its importance when increasing the RES penetration as faster power deploy is needed.



# Acknowledgments

I would like to express my special gratitude and thanks to my supervisors: Anca Daniela Hansen, Kaushik Das and Müfit Altin for their guidance, coaching, support, encouragement and valuable contributions throughout my master thesis. This project would not be possible without the continuous support from my supervisors, who are always disposed to discuss ideas and share knowledge.

I am thankful to José Luis Domínguez García<sup>1</sup>, Oriol Gomis Bellmunt<sup>2</sup> and specially Mikel de Prada Gil<sup>1</sup> from Catalonia Institute for Energy Research (IREC)<sup>1</sup> and CITCEA<sup>2</sup> for their advice on doing the master thesis in DTU and for introducing me to my main supervisor in this project, Anca Daniela Hansen.

I gratefully acknowledge *Escola Tècnica Superior d'Enginyeria Industrial de Barcelona* (ETSEIB) to give me the possibility of doing the master thesis in Denmark.

I would also like to thank to my colleagues, master students and PhD students, which I met in DTU for their knowledge sharing, friendship and very good times together. It has been a privilege to know such an amazing people and I enjoyed the experience of studying abroad thanks to them.

Special thanks to my family: Miguel, Pilar, Miki and Sergio. Words cannot express how grateful I am to my parents and brothers for all the sacrifices that they have made on my behalf. I would like to mention my girlfriend Mònica for her unconditional support in every step of the project and for me she was what sustained me thus far. I would also like to thank to all my relatives and friends that also support me through this stage of my life. I love you all.



# Table of contents

Abstract .....	i
Acknowledgments .....	iii
Table of contents .....	v
List of Figures .....	1
List of Tables .....	3
List of abbreviations and symbols .....	4
Chapter 1 Introduction .....	6
1.1. Background and motivation .....	6
1.2. Objectives .....	10
1.3. Assumptions and Limitations .....	11
1.4. Content of the report .....	12
Chapter 2 Frequency control aspects .....	14
2.1. Primary frequency control .....	15
2.2. Primary frequency control performance .....	19
2.2.1. Conventional power plants .....	19
2.2.2. Solar PV systems (SPVSs) .....	21
2.2.3. Wind power plants (WPPs) .....	22
Chapter 3 Modelling of western Danish power system .....	24
3.1. Power system characterization .....	25
3.2. Modelling the system interconnections .....	33
3.3. Modelling CHP and must-run units .....	34
3.4. Modelling DCHP units .....	36
3.5. Modelling the SPVSs .....	37
3.6. Modelling the WPPs .....	40
3.7. Single bus model, load model and outage .....	42
Chapter 4 Scenario description and test cases .....	45
4.1. Definition of the scenario .....	45
4.2. Definition of test cases .....	48
4.3. Definition of key parameters and success criteria .....	51
4.4. Danish islanding event 29.05.2007 .....	52

Chapter 5 Sensitivity studies ..... 55

- 5.1. Simulation of the base case..... 55
- 5.2. Study on the droop and the ramp rate..... 56
- 5.3. Study on the virtual inertia implementation ..... 62
- 5.4. Study on frequency support of the HVDC cross-border connections ..... 67
- 5.5. Study on the delay in the measurement and communications ..... 69
- 5.6. Summary..... 72

Chapter 6 Conclusions and future work..... 74

- 6.1. Main conclusions..... 74
- 6.2. Future work ..... 76

References ..... 78

Appendix: Model parameters..... 86

# List of Figures

Figure 1.1 Power system operating states [6] .....	7
Figure 1.2 Classification of power system stability with instability phenomena by major incidents [9] .....	8
Figure 2.1 The three steps of frequency control over time [28] .....	14
Figure 2.2 Frequency excursion for an overfrequency event [30] .....	15
Figure 2.3 Frequency power characteristics of a generating unit .....	17
Figure 2.4 Load sharing by parallel units with different droop .....	17
Figure 2.5 Overall requirements for active power production for frequency and voltage fluctuations for conventional power plants [34] .....	19
Figure 2.6 Primary frequency control for a conventional power plant [34] .....	20
Figure 2.7 Primary frequency control for SPVSs [35] .....	21
Figure 2.8 Primary frequency control for WPPs [36].....	22
Figure 3.1 Simplified illustration of DK1 delta and per-unit model.....	24
Figure 3.2 Danish map of international cable connections [38] .....	25
Figure 3.3 CHP and DCHP locations in Denmark by production [51] .....	29
Figure 3.4 Wind power electricity production and wind share in the net electricity production [57] [58]....	31
Figure 3.5 Wind power installed capacity and number of turbines active [57] [58].....	31
Figure 3.6 Aggregated CHP and must-run generic model .....	34
Figure 3.7 Speed governor for the must-run and CHP units .....	35
Figure 3.8 General turbine model for the must-run and CHP units .....	35
Figure 3.9 GAST model to simulate the aggregated DCHP units.....	37
Figure 3.10 Aggregated SPVS model .....	38
Figure 3.11 Aggregated WPP model.....	41
Figure 4.1 The four scenarios for the Danish energy system in 2030 [26] [82] .....	46
Figure 4.2 DK1 2030 scenario considered for the study based on data from [42].....	47
Figure 4.3 Measurement values for the Danish islanding in 29/05/2007 [9] .....	53
Figure 5.1 Frequency excursion for the base case with and without RES participation .....	55
Figure 5.2 Comparison between the base case and the test case with the same RES penetration .....	56
Figure 5.3 Frequency excursion for 0,5 pu/s ramp rate and 0,04 pu droop by RES penetration .....	57
Figure 5.4 Maximum instantaneous frequency by ramp rate, droop and RES penetration .....	58
Figure 5.5 Maximum frequency by droop and ramp rate in 70% and 85% RES penetration .....	60

Figure 5.6 RoCoF contour plot by droop and ramp rate in 70% and 85% RES penetration.....	60
Figure 5.7 Frequency excursion for the base case and 67% RES penetration by virtual inertia gain (Kd).....	62
Figure 5.8 a) Maximum frequency reached in every simulation with and without virtual inertia. b) Maximum frequency contour plot with virtual inertia (Kd=60) .....	63
Figure 5.9 Maximum instantaneous frequency in 67% RES penetration by virtual inertia gain.....	64
Figure 5.10 Area with maximum frequency below 51 Hz by virtual inertia in 85% RES penetration .....	64
Figure 5.11 Oscillations in the frequency excursion by using a too low droop.....	65
Figure 5.12 Frequency excursion in 80% RES penetration for 60 pu, 30 pu and 0 gain for virtual inertia .....	66
Figure 5.13 RoCoF contour plot for 85% RES penetration with and without virtual inertia (Kd=60) .....	66
Figure 5.14 Maximum instantaneous frequency by ramp rate, RES penetration and HVDC capacity .....	67
Figure 5.15 Frequency excursion in 85% RES penetration by HVDC capacity available .....	69
Figure 5.16 Maximum frequency deviation by ramp rate, RES penetration and time delay.....	70
Figure 5.17 Frequency excursion in 80% REs penetration with and without virtual inertia.....	71

# List of Tables

Table 3.1 Planned system interconnection capacities for 2030 scenario in DK1 by type of connection and country [42] .....	26
Table 3.2 Future conventional power generation in Danish power system by 2015 predictions [45] .....	27
Table 3.3 Capacity and type of fuel for CHPs of DK1 [46] [47] [48] [49] .....	28
Table 4.1 Installed Capacities for Denmark and DK1 in 2030 in the Green Europe scenario [42] .....	46
Table 4.2 Power flow of the specific hour in 2030 scenario chosen [42].....	47
Table 4.3 Test cases to be simulated in the sensitivity studies .....	50
Table 5.1 Recommended droop for WPPs by RES penetration and ramp rate performed .....	61
Table A.1 Parameters of the aggregated CHP and must-run unit.....	87
<i>Table A.2 Parameters of the aggregated DCHP unit .....</i>	<i>88</i>
Table A.3 Parameters of the aggregated SPVS.....	89
Table A.4 Parameters of the aggregated WPP .....	90
Table A.5 Parameters of the aggregated HVCD interconnector and outage simulated .....	91

# List of abbreviations and symbols

<b>Abbreviation/symbol</b>	<b>Definition</b>
AC	Alternative Current
CE	Continental Europe
CHP	Combined Heat and Power
D	Damping
DCHP	Decentralized Combined Heat and Power
DK1	Western Danish grid
DK2	Eastern Danish grid
ENTSO-E	European Network of Transmission System Operators for Electricity
FCR	Frequency containment reserves
FFR	Fast frequency response
FRR	Frequency restoration reserves
HVDC	High Voltage Direct Current
Hz	Hertz
Kd	Virtual inertia gain constant
KPI	Key performance indicator
M(2H)	Inertia constant
MPPT	Maximum power point tracking
ms	Millisecond
MVA	Mega volt ampere
MW	Megawatt
NE	Northern Europe
PCC	Point of common coupling
PI	Proportional integral
pu	Per unit
R	Governor Droop setting or droop
RES	Renewable Energy Sources
RoCoF	Rate of change of frequency
RR	Replacement reserves
SPVS	Solar Photovoltaic System

$T_f$	Measurement and communication delay
TSO	Transmission System Operator
TYNDP	Ten-Year Network Development Plan
WPP	Wind Power Plant
WT	Wind Turbine
$\Delta f$	Frequency deviation
$\Delta P$	Power deviation
$\beta$	Power system frequency characteristic

# Chapter 1

## Introduction

This chapter describes the background and objectives of this project. The motivation, assumptions and limitations of the project are explained as well.

### 1.1. Background and motivation

Many modern power systems are intensifying efforts on reducing their needs in fossil fuels and moving towards a 100% renewable generation [1]. This strategic change has been given as a consequence of the raising engagement for meeting environmental challenges and sustainable development.

Historically, the Danish power system, as many others, based the energy production on fossil fuels and it was not since late 90s when the renewable generation became relevant in electricity production [2]. Since then, the renewable energy sources (RES) have been increasing over the years and Denmark is involved into a green transition from a system based on large central fossil fired power plants towards an entirely renewable energy based system in 2050 [3]. Furthermore, the government's goal for being independent of fossil fuels in electricity and heating generation was set in 2035 [4].

The power system stability is defined as the ability of a power system to recover a state of operating balance after being disturbed, with most system variables confined in certain boundaries, thereby, the entire system remains practically intact for given initial operating conditions [5]. According to [6] and [7], there are five operating states for power system security and stability purposes: Normal state, Alert state, Emergency state, Black out and Restoration. The illustration of these states is presented in Figure 1.1. In case of highly reliable system protection schemes, the power system operation could be shifted from normal state to alert state. The violation of the operational limits in case of extreme events, such as N-2 or more, would bring the system to an emergency state and there is risk of black out in case of loss of stability. The "N", "N-1" or "N-2" terminology refers to number of failures for single or multiple elements that are linked and failed together as one where "N" is the normal operation of the power system [8].

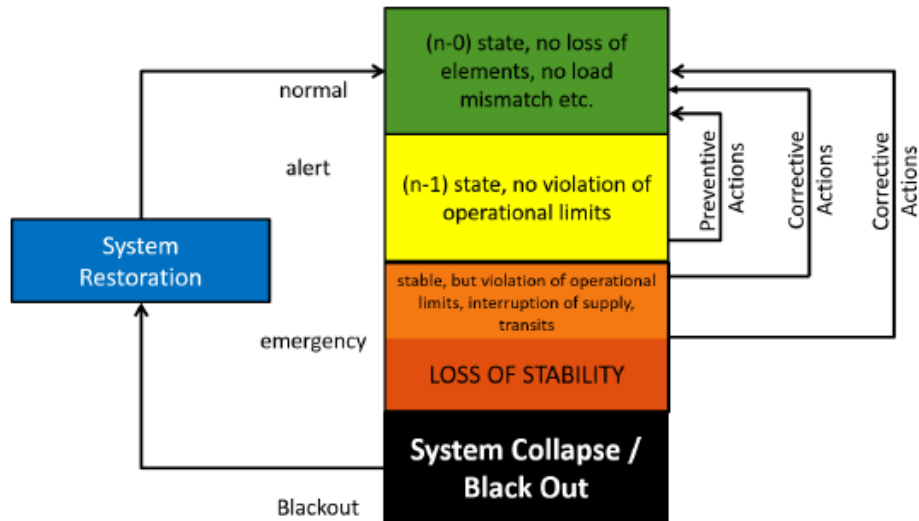


Figure 1.1 Power system operating states [6]

Power systems are very complex since they are continuously growing to satisfy an increasing demand. Furthermore, power systems are interconnected with each other, so an instability phenomena that appears in one particular power system can end up being a global threat. Normal operation of the whole interconnected power systems can be threatened by a single instability in one of them. Figure 1.2 shows a classification of the power system stability [9]. For each classified stability issue, the different causes of instability phenomena are underlined. Examples of major incidents by each instability can be seen, like large disturbances and black outs which took place on the European Network of Transmission System Operators for Electricity (ENTSO-E) and in the United States power systems.

This study is focused on the frequency stability. Frequency stability refers to the ability of a power system to maintain a steady frequency after a severe disturbance resulting in a significant imbalance between generation and load [5]. A severe power imbalance in a power system generally results not only in large excursions of frequency, but outages in power flows, voltage and other system variables. These circumstances invoke the controls and protections, such as boiler and steam turbine dynamics, and the coordination of these controls must be considered. In highly interconnected power systems like Denmark, frequency stability is most commonly associated with islanding events leaded by the disconnection of AC lines between the western Danish power system (DK1) and Continental Europe (CE). The disconnection of multiple generators is usually correlated to handle with frequency stability as well. A power system islanding is an extreme event and some challenges are associated as long as the frequency is a system parameter and while one power system will manage an overfrequency event, the other will handle an underfrequency event.

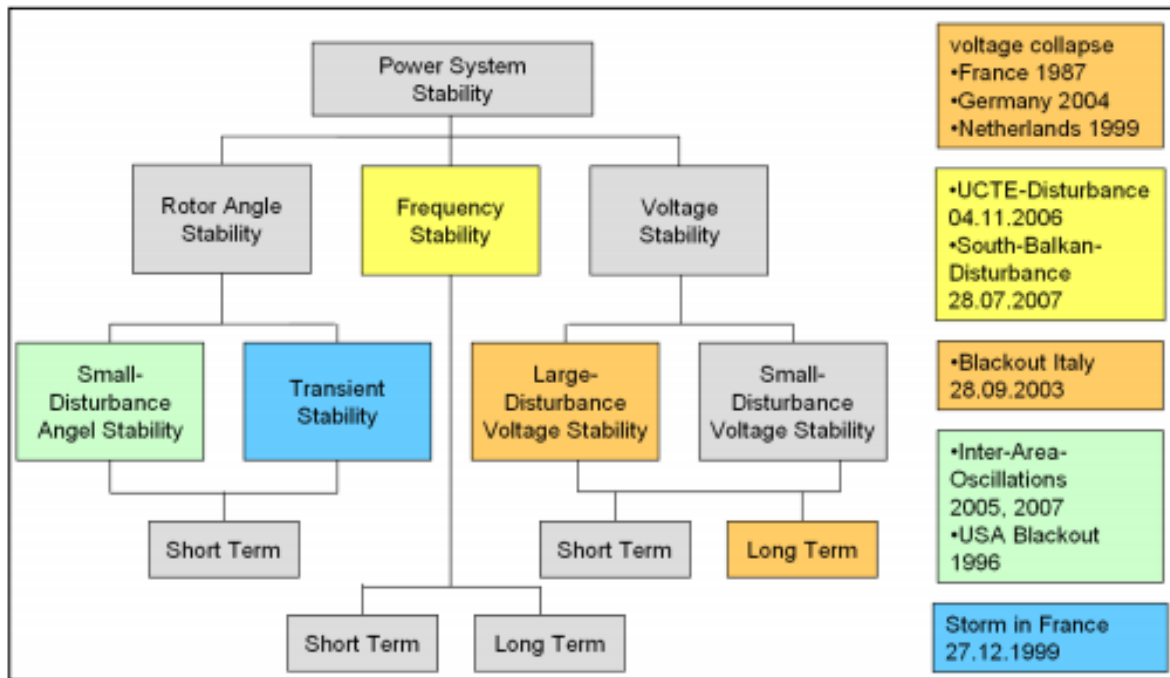


Figure 1.2 Classification of power system stability with instability phenomena by major incidents [9]

Nowadays, the power system stability is mainly ensured and maintained through the so called “must-run units”. These units are necessary to provide ancillary services. There are different definitions for the ancillary services, but the definition considered in this study is that ancillary services are all the support services required by the power system to maintain the integrity of the transmission or distribution grid that ensures a stable and reliable power system operation. Examples of ancillary services are the voltage stability, the inertia or the frequency stability. The term “must-run units” is explained in literature [10], [11] and [12], as large conventional power plants which are required to be online in order to provide ancillary services and are also required to run for technical reasons. It is known as conventional power plant all the power plants that are based on the combustion of fossil fuels and, in this study, the term includes: the must-run units, combined heat and power (CHP) units and decentralized CHP (DCHP) units. The must-run units can be classified in two types according to the covered need:

- Units which provide voltage control and grid stability that can supply ancillary services.
- Combined heat and power (CHP) units which are required because of the heat production.

These units provide support to increase the flexibility in a power system. The flexibility describes the ability of a power system to handle with variability and uncertainty in both generation and demand showing imbalances up, while maintaining a satisfactory level of reliability at a reasonable cost, over different time

horizons [13]. Due to the adaptability of the CHP, these power plants are currently starting not to be considered as must-run units, hence they can shift production using heat storage, produce heat on alternative units such as boilers or bypass turbines altogether and operate in heat only mode.

According to ENTSO-E, the highest growth in generation capacity between 2020 and 2025 at the whole Pan-European zone correspond to both wind and solar where the wind generation is the one which has the highest net growth [14]. On the other hand, the fossil fuel based generation decreases, despite the gas fired power plants are the only one that increase its sharing. The energy scenarios developed by ENTSO-E following this transition plan imply that must-run and CHPs are likely going to be phased out and, consequently, this might result in an insecure operation of a power system without appropriate ancillary services provided by RES. The increment share of RES over the years together with the fact that these must-run units are very costly have already resulted in the decommissioning of these units [15]. For example, in Denmark, the transmission system operator (TSO, Energinet.dk) remunerates intensively for the ancillary services to secure and maintain the stability of the power system, and there are consequently strong financial incentives to significantly reduce the number and operational duration of must-run units [16]. Furthermore, the increasing use of electric boilers, heat pumps and heat storage reduce generation from CHP and also provides flexibility to the system increasing or decreasing power demand. Moreover, must-run units can be sometimes replaced by synchronous condensers when only voltage control is needed.

As a result, the requirements from must-run units have been reduced to the usage of 1 unit in the western Danish grid (DK1) and in the eastern Danish grid (DK2) to 2 units [15]. Last year, for the first time, the Danish TSO tested the operation of the Danish power system without any must-run units for one day. It was demonstrated that it is possible to operate the Danish power system without must-run units for a short period. However, for this to become a day to day reality in the future when power system will operate with very high penetration of RES, many challenges for ensuring and maintaining the stability of the system should be investigated and solved.

Must-run units traditionally have been playing major role in both frequency regulation and frequency control following a large disturbance. The frequency regulation refers to the power adjustment in order to control the frequency around the nominal value in normal operation. The frequency control is the automatic performance, upward or downward adjustment of active power, after a large imbalance when a certain threshold in the frequency is reached to ensure the grid stability. Their unavailability in the future can therefore have a severe impact on the power system frequency without appropriate contribution from RES sources, such as wind power, because of the appearance of new challenges when the complexity of the power system is increased by adding the RES frequency stability support [17] [18] [19]. Many solutions

contributing to the green transition through ancillary services provision from RES have already been intensively investigated in the academia and industry in recent years [20] [21] [22]. However, the literature review reveals that until now the research into the capabilities of RES delivering critical properties to the power system has been conducted based on the assumption that the power system operates with must-run units. Furthermore, the research to date has not been focused on the possibility to exploit a joint and coordinated system support contribution from RES. This means that a through insight and understanding of the increasing complexity of a RES dominated Danish power system without must-run units is missing in the current research activities. Additionally, modern power electronics interfaced WPPs are capable of providing ancillary services [23] [24] [25]. However, the required responses from these WPPs should be identified through different control parameters and sensitivity studies.

## 1.2. Objectives

The main objective of thesis is to answer the following question: Can the power system operate without the must-run units? And if so, which are the technical capabilities and limitations that allow the system to operate without must-run units?

The future scenario with a high RES penetration joined together with the electrification of the heat demand and the appearance of new consumptions like the electric vehicle will be a reality in the near future. These will increase the power generation, highly relied on variable power sources as wind and solar generation. Currently, CHPs and must-run units are in charge of providing support on frequency stability and other ancillary services and they will be decommissioned due to the increasing RES penetration and the high cost of maintaining a power plant online which only provides ancillary services. TSOs must ensure a secure operation against power imbalances on their power systems and, with the decommissioning of the must-run units, there is a need for the evaluation of the ancillary services. This project investigates the wind power frequency stability support in future power systems with very high penetration of RES without the must-run units. The aim of this study is to develop recommendations and new understanding on the frequency stability support performed by modern controllable WPPs in a low inertia scenario. In this study, primary frequency control is focused in a 2030 DK1 scenario and parameters for the frequency control for WPPs are studied focusing on overfrequency events.

Summarizing, the future 2030 DK1 power system operation without must-run units is evaluated. Recommendations on control strategies and control parameters are developed and tested to evaluate the technical capabilities and limitations in a power system with high penetration of RES in a low inertia

scenario. In order to meet the main objective of the project, specific objectives are defined. First, primary frequency control characteristics for DK1 power system are identified to provide the state of the art for this ancillary service of frequency stability. Then, a model of DK1 for a severe overfrequency event is modelled where a power imbalance take place in 2030 scenario when islanding DK1 from CE. The WPPs' capabilities to provide ancillary services participating in primary frequency control are studied when the power system is operating with low inertia. Key parameters, such as power system inertia, are identified and their sensitivity is studied for frequency stability. The HVDC cross-border connectors are introduced in the power system frequency control and the coordinated frequency control of these connectors with the WPPs in a high RES penetration scenario is studied. Finally, a set of recommendations for overfrequency control for WPPs on a power system without must-run units and dominated by wind are proposed.

### 1.3. Assumptions and Limitations

This study will focus on the 2030 scenario for DK1 based on the Ten-Year Network Development Plan (TYNDP) presented by ENTSO-E [26]. It is difficult to predict how the grid will develop until 2030. However, four scenarios were developed by ENTSO-E for 2030 and the scenario with the highest RES capacity is chosen for this research. The installed power capacity, the power demand and data from the cross-border power exchange between DK1 and the neighbour countries are established from [26] and [27]. When choosing the scenario with the highest RES penetration of the four developed by ENTSO-E for this study, a European focus on energy policies to be on track of the 2050 roadmap to achieve a fossil fuel free power system is considered.

High penetration of RES generation in a power system will be a challenge for TSOs to ensure the stability of the grid. Additionally, in a system leaded by wind and solar generation, not only frequency stability is affected, but rotor angle and voltage stability will present challenges to be solved in the future. However, the scope for this project is the study of the frequency stability and not the other forms of stabilities.

Even though the frequency stability involves three different controls (primary, secondary and tertiary control), this research gives recommendations of better practices for primary frequency control on a high wind penetration power system based on test cases. The primary frequency control maintains the frequency in an acceptable range when a power imbalance take place in the first 30 seconds after the imbalance happens. The secondary and tertiary control are related to bring the system frequency into its nominal value and rescheduling the power hourly, but these two controls are out of the scope of this work.

The simulations of the case studies are made under the general assumption that the power system has enough frequency containment reserves to handle the power imbalance in the system. The worst case to be considered in frequency stability is an islanding event and the imbalance studied is an extreme event (i.e. N-4) where DK1 is islanded from CE due to a failure in all the AC lines. This study considers a base case where the must-run units are online and different test cases are developed by increasing the RES penetration and decommissioning first, the must-runs and then, the rest of the power plants that provide inertia to the system.

Aggregated models are developed with the available data of the power plants that will compose the future 2030 DK1 power system to simplify the mathematical effort of the simulations. So, the general conditions assumed in this study such as the high wind forecast are generalized while every WPP would have a different wind condition in the real scenario. Also, by aggregating the models, the congestion on the lines are neglected and it is assumed that they can handle all the power deviations.

This study is made under the assumption that the must-run, CHP and DCHP units are operating in a high set point (90% of the total capacity) and all the wind power is available, but it is curtailed to meet the hourly power dispatched. This assumption is made since there is not a market model providing the hour ahead generation. It can be a conservative consideration because, if the conventional power plants work in a low set point (and they probably will do), for the same power delivered, the capacity online of these power plants will increase together with the system inertia since the RES power online will not change.

Finally, the study is planned so the DK1 power system is capable to handle the outage and maintain the system frequency in an acceptable range even if it is in an emergency state without the need of a defence plan like a tripping strategy for the generators. This assumption is made because it is considered that providing the system to have enough reserves (i.e. downgrading the power in overfrequency events) is a cheaper solution than having a large tripping strategy of generators.

## 1.4. Content of the report

The report is organised as follows:

In chapter 2, an overview of the frequency control aspects for this study is given. The key parameters for the primary frequency control are introduced. Moreover, the primary frequency control is explained for each power source provided in the Danish grid codes in which the frequency controllers of the developed model are based on.

In chapter 3, the DK1 power system, in which the simulation model is based on, is presented. A general structure of the facilities and interconnections is introduced in the actual and future Danish grid. For each component of the power system, the model implemented for the study is shown, underlining the clue components in each technology considered.

In chapter 4, the scenario and the test cases in which the project is based on are explained. The key parameters, the specific power flow studied and the evaluation criteria are presented. An example of a severe event islanding DK1 is presented at the end of this chapter.

In chapter 5, several sensitivity studies based on the considered key parameters are shown. A summary concludes the chapter where the main results and comments are included.

In the last chapter, the main conclusions of the research are summarized and discussed. Also, some suggestions and open questions for future projects are underlined.

## Chapter 2

### Frequency control aspects

This chapter gives an overview of frequency control aspects and the state of art of the ancillary service that ensures the primary frequency stability studied in this project. The primary frequency stability for conventional power plants (must-run, CHP and DCHP) and RES generation is underlined.

TSOs must guarantee a stable operation of their grid. The generation of the power units and consumption of the loads connected to the grid needs to be controlled to secure a high-quality performance of the grid and also to maintain a balance between the generation and the consumption. During normal operation of a power system, the generation follows the load and when there is an imbalance between them, the system frequency is affected. When there is a lack of generation, the frequency goes down and when there is a surplus of generation, the frequency goes up. Frequency control is required to prevent problems led by large frequency deviations from its nominal value such as the loss of synchronism of a synchronous generator. By means of frequency stability, there are three control steps: primary frequency control, secondary frequency control and tertiary frequency control. These three steps are respectively enabled over time to ensure a good sequential operation on the frequency recovery and an illustration can be seen in Figure 2.1.

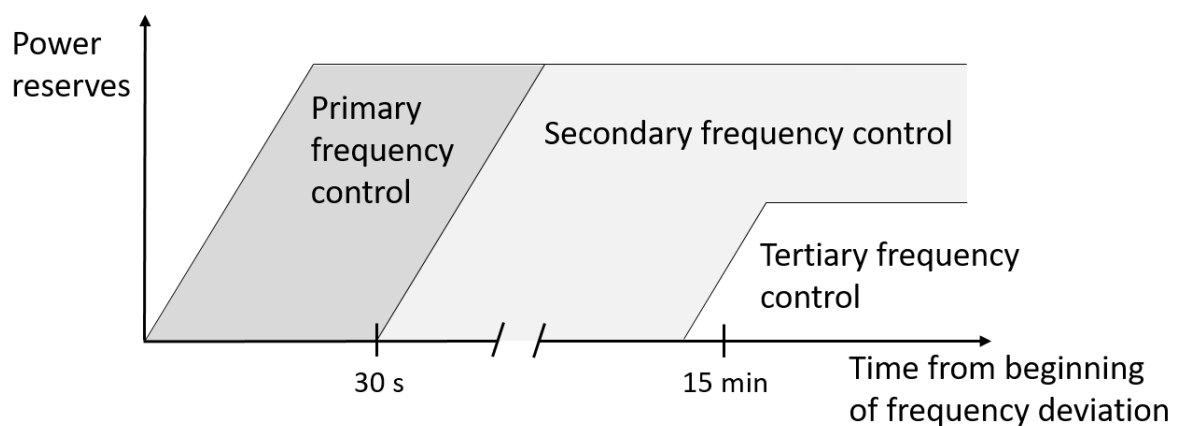


Figure 2.1 The three steps of frequency control over time [28]

Power reserves are needed for underfrequency situations to supply frequency stability services. The active power produced by the generators has to increase or decrease in order to response to the power imbalance and control the frequency deviation. This power reserves are related to the three steps of

frequency control and they are named Frequency Containment Reserves (FCR), Frequency Restoration Reserves (FRR) and Replacement Reserves (RR) respectively by each primary, secondary and tertiary control, according to ENTSO-E and the European next System Operation Guideline [29]. In this study, the name FCR is used to mention the reserves dispatched by the power plants in the primary frequency control.

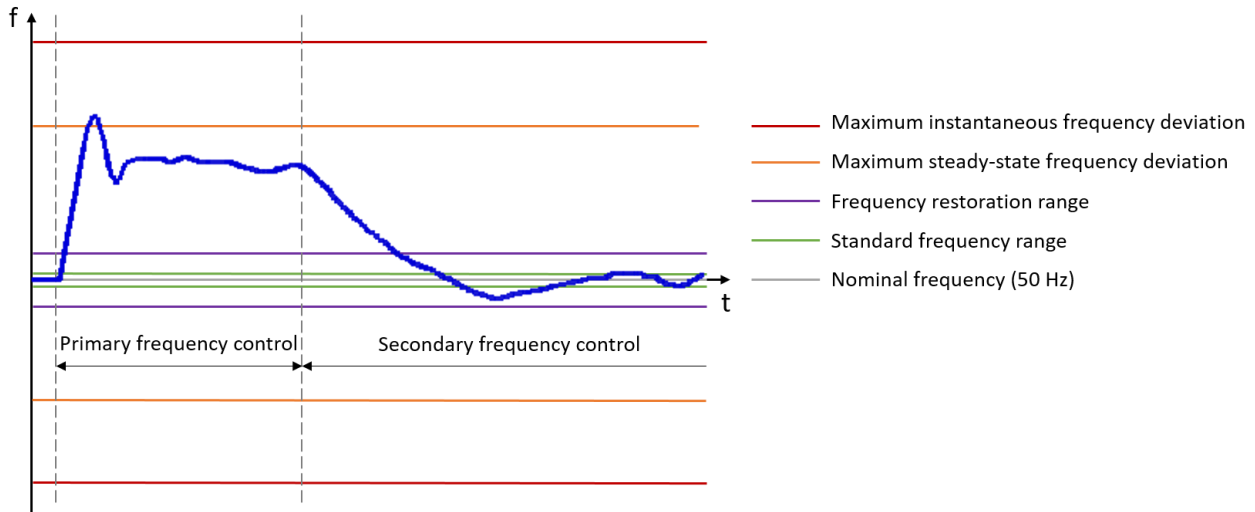


Figure 2.2 Frequency excursion for an overfrequency event [30]

In Figure 2.2, it can be seen the frequency excursion when a power imbalance takes place for an overfrequency event. The frequency excursion refers to the evolution of the frequency over time when there is a power imbalance in a power system. In this project, the primary frequency control when DK1 is islanded from CE is analysed. In the following sections, the dynamics of the primary frequency control is explained and reviewed from the Danish grid code to understand its performance to implement this control to the model developed in this study.

## 2.1. Primary frequency control

The primary frequency control enables the FCR. This control ensures the balance between generation and demand in a synchronous area during the first 30 seconds after a disturbance. It is the first step of the frequency control (Figure 2.1) and it is an automatic function performed by the speed governors and other frequency controllers implemented in the different interconnected conventional power plants. The power output of the power plants is adjusted as according to the frequency deviation stabilizing it at a stationary value. The frequency deviation appears after a precipitous disturbance or imbalance of the active power and it does not return to its nominal value until the secondary control, or a defence plan if the power

system is threatened to loss its stability, is activated. A defence plan is the last action of a power system to prevent a black out when the grid is in emergency state and threatening to loss its stability [31].

The deployment of FCR is needed to keep the frequency within the design limits when a power imbalance takes place. The FCR are delivered with an activation time up to 30 seconds. The amount of FCR established in the CE is 3000 MW [30], the same value as the reference incident defined by ENTSO-E. Denmark has to contribute with 27 MW from DK1 to CE and also the eastern Danish power system (DK2) has to contribute with 160 MW to Northern Europe (NE) since the Danish power system is synchronized separately, DK1 and DK2, to both CE and NE, respectively [32].

According to the ENTSO-E handbook, the maximum permissible quasi-steady-state frequency deviation after a reference incident is  $\pm 200$  mHz where the primary frequency control is fully activated and the FCR must be fully deployed after 30 seconds from the detection of the imbalance. The minimum and maximum instantaneous frequency after a loss of generation or load, respectively, are 49,2 Hz and 50,8 Hz that correspond to  $\pm 800$  mHz from the nominal frequency. In this study, the maximum instantaneous frequency is also referred as maximum frequency deviation or frequency peak. The maximum and minimum instantaneous frequency that will be considered in this study are 51 and 49 Hz which are limits that reach the  $\pm 800$  mHz mentioned before, so the system operates in emergency state. The limits chosen correspond to the normal operation zone for the power plants modelled according to Energinet.dk (Danish TSO) as it would be seen in following sections for conventional power plants, WPP and SPVS.

A frequency controller, speed governor in case of the conventional power plants, is implemented in the generators to perform primary frequency control. This governor implements the governor droop setting, or just droop (R), which is the main characteristic of this governor and it is the relation between the frequency deviation in the power system and the power deviation dispatched by the power plant. It is defined as the percentage of the frequency deviation required for a governor to drive a unit into a 100% change in the power output.

$$R [pu] = -\frac{\Delta f / f_n}{\Delta P / P_n} = -\frac{\Delta f [pu]}{\Delta P [pu]} \quad (1)$$

Equation (1) means that for a 6% of droop, a 6% of frequency deviation will cause a 100% change on the power output of the generating unit. In Figure 2.3, it can be seen the frequency power characteristic of a generating unit [7] [33].

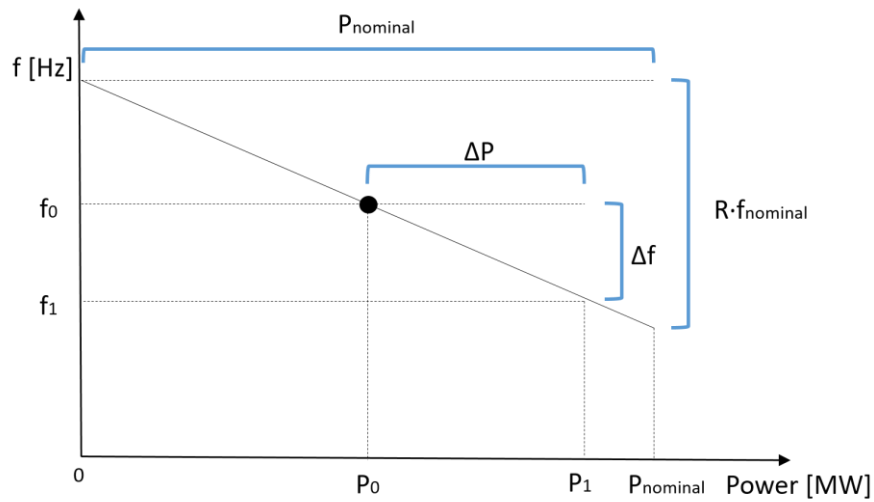


Figure 2.3 Frequency power characteristics of a generating unit

In Figure 2.4, the power deviation for two different generating units with different droop in the speed governor is shown. The same deviation on the frequency does a different power change in the generating units. The higher the droop is, the less it will respond to a frequency deviation. Furthermore, the power delivered by the two power plants is related to equation (2).

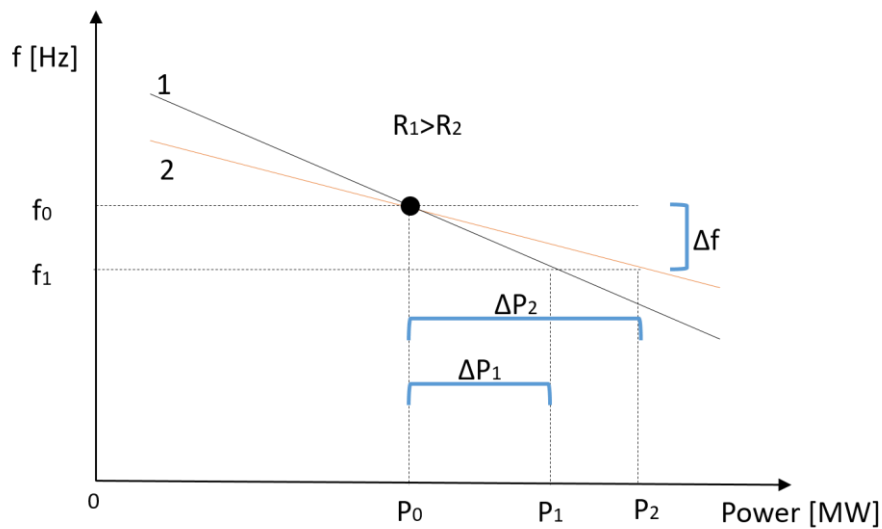


Figure 2.4 Load sharing by parallel units with different droop

$$\frac{R_1}{R_2} = \frac{\Delta P_2}{\Delta P_1} \quad (2)$$

Finally, it is worth mentioning that the operation set point of the power plant matters during a power imbalance because if the generator is working at high level, it may not have enough reserves to support a underfrequency event, for example. This also happens in overfrequency events when the generator is working at minimum level and a positive frequency deviation takes place so the power plant cannot reduce the power output and the only option to reduce the power is the disconnection of the generator.

The power system frequency characteristic ( $\beta_{PS}$ ) represents the total action of the primary frequency control provided by generators and self-regulating effects of the load. This parameter relates the steady state change in the system frequency ( $\Delta f$ ) when a power imbalance ( $\Delta P$ ) appears:

$$\beta_{PS} = -\frac{\Delta P}{\Delta f} \quad (3)$$

The power frequency characteristic is also referred as composite frequency response characteristic or the stiffness of the system and it is expressed in MW/Hz [7]. After an imbalance, the frequency goes through a transitory state before stabilizing on a steady-state value. This value does not only depend on the frequency characteristic of each single unit, but also depends on the load damping constant (D) which is supposed as 1 %/Hz of the total load in this study. Further comments about the load damping constant are given in chapter 3.

The power system frequency characteristic can be calculated as a summation of the individual frequency characteristics of every generating unit 'i' ( $\beta_i$  [MW/Hz]) and the load damping constant. To calculate the frequency characteristic for a generating unit: the droop ( $R_i$  [pu]), the nominal power ( $P_{n,i}$  [MW]) and the nominal frequency ( $f_n$  [Hz]) for each power plant is required as it is presented in equation (4) [7].

$$\beta_{PS} = \sum_{i=1}^N \beta_i + D = \frac{1}{f_n} \sum_{i=1}^N \frac{P_{n,i}}{R_i} + D \quad (4)$$

Where N is the number of generating units in the power system participating in the primary frequency control. The more generators are participating in the primary frequency control, the less frequency deviation will experience the synchronous area. The droop of the governor does not only affect the steady-state value of the frequency deviation given an imbalance in the power system, but the transient state is affected as well because this parameter defines the velocity of the power response against a frequency deviation in a power system.

## 2.2. Primary frequency control performance

The Danish power generation is spread in different technologies, but the power plants can all be aggregated in three types: conventional power plants, SPVS and WPP. From these three types of power plants, the must-run units are included in the conventional power plants. In this section, a review of the Danish grid code is presented to establish the state of art in primary frequency control for these three generation power plants.

### 2.2.1. Conventional power plants

Traditionally, the power systems rely on conventional power plants to keep the grid stable when it has to face an event that produces an imbalance. The rotating parts of this kind of generators provide inertia to the grid and it helps to have slower frequency excursions. CHPs and DCHPs are conventional power plants and they can be qualified as must-run units if they are online to provide ancillary services while selling the generation to the system. They must follow the Danish grid code to be online in the DK1 power system. In Figure 2.5, the operational limits of these power plants are illustrated. It can be seen that between 49 and 51 Hz the generator will work under normal production, but when the frequency goes below or above these limits, the generator will trip. If the frequency returns to the normal production range before the specified time, the generator will not trip.

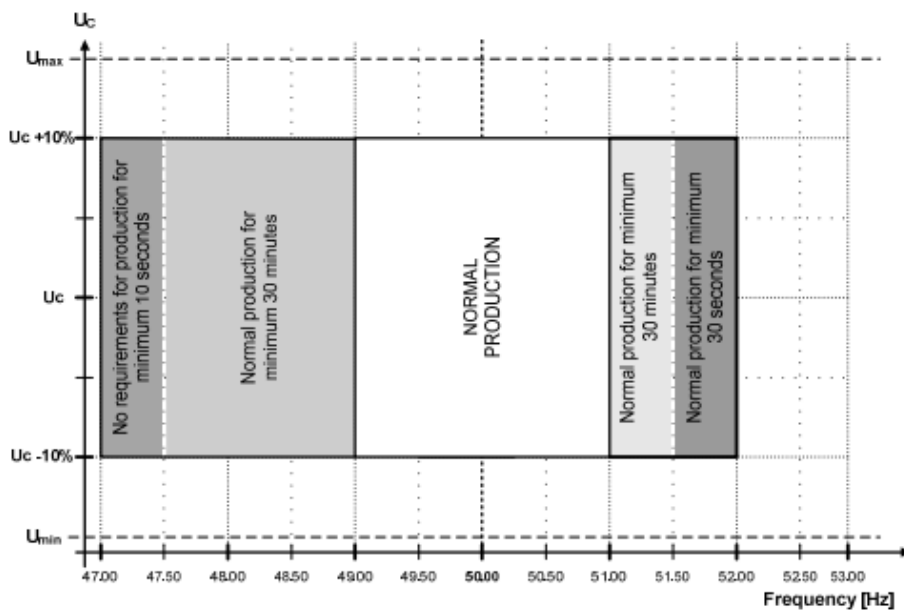


Figure 2.5 Overall requirements for active power production for frequency and voltage fluctuations for conventional power plants

[34]

With the decommissioning of conventional power plants due to the increasing RES penetration, the inertia and also the FCR provided by these generators will decrease. This means that if RES generation is increasing, a review on the calculation of the FCR is needed to allow them to participate in the primary frequency control to keep the system stable and with enough reserves. This is also challenging due to the variable generation from wind and solar and to the forecasting errors that would happen, so FCR are thought to increase in the future to counterbalance the mentioned before.

This study is focused on the frequency control, neglecting the frequency regulation, when an outage happens on the grid. The frequency control for conventional power plants above 1,5 MW is shown in Figure 2.6.

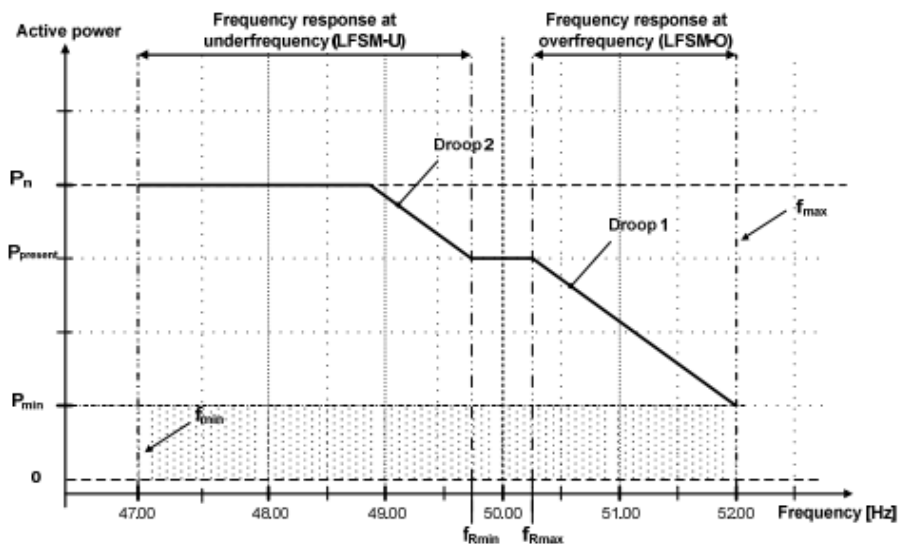


Figure 2.6 Primary frequency control for a conventional power plant [34]

In the power frequency characteristic, there is a dead band established by  $f_{rmin}$  and  $f_{rmax}$  that can be set at any value between 47,0-49,9 Hz and 50,1-52,0 Hz, respectively. Common values that are going to be used are 49,8 Hz and 50,2 Hz for  $f_{rmin}$  and  $f_{rmax}$ . The droop for the speed governor must be possible to set in the range 2-8%, while a standard value is 6%. The primary frequency control must activate within 2 seconds after a detection of a frequency deviation and the measurement of the frequency is made continuously obtaining the average value for the frequency in a 80-100 ms range. A new value of the frequency is calculated every 20 ms. Also, the limit for the rate of change of frequency (RoCoF) is  $\pm 2,5$  Hz/s. If the limit for the RoCoF is exceeded, the frequency goes below 47 Hz or above 52 Hz, the conventional power plants must be shot down with a trip time of 80 ms in the RoCoF case or 300 ms on the other two cases depending on which protective function is activated [34]. The limit for the RoCoF is the same for SPVSs and WPPs so it will not be explained again in the following sections.

## 2.2.2. Solar PV systems (SPVSs)

The SPVS generation is the less present in the Danish grid compared to wind and conventional power plants and SPVSs are not performing frequency control normally because of the need of a specific agreement with the TSO. In a European scenario where the RES penetration is increasing, SPVSs are supposed to keep growing. However, Denmark would make greater investments in WPP than in SPVS.

SPVSs can operate in normal conditions between 47,0 and 52,0 Hz, unlike the conventional power plants presented before. The SPVS generation is decoupled from the grid by a converter and it does not have any rotating mass. These are the main reasons why SPVSs can operate normally in the whole range of frequency. The frequency control of a SPVS is presented in Figure 2.7.

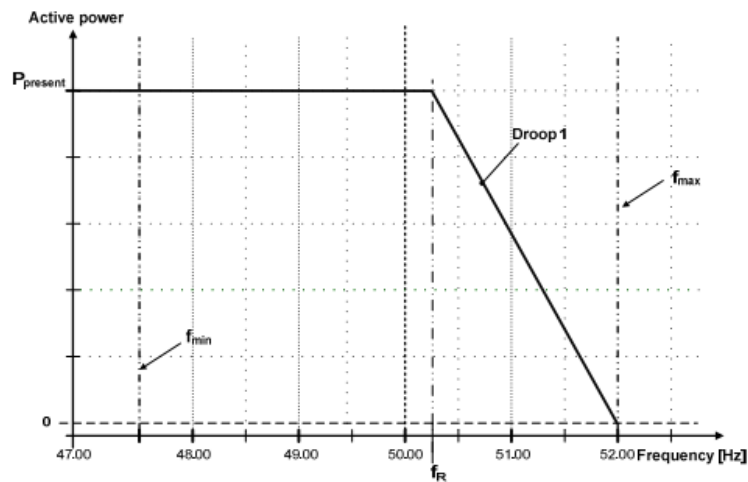


Figure 2.7 Primary frequency control for SPVSs [35]

The SPVSs downgrade the output power to maintain the grid stability when a frequency threshold is reached in overfrequency events, but its generation is set to produce all the available power so the SPVSs cannot participate in underfrequency events. The frequency threshold can be set to any value between 50,0 and 52,0 Hz range with a standard value is 50,2 Hz. The droop of the governor must be possible to set between 2-12%, while a standard value is 4%. The primary frequency control must start no later than 2 seconds after a frequency deviation and must be completed within 15 seconds [35].

### 2.2.3. Wind power plants (WPPs)

WPPs are going to become the muscle of the future Danish grid and, according to ENTSO-E, it will cover almost 66% of the installed capacity in 2030 Danish power system [26]. In this situation, the TSO has to continue ensuring the stability of the grid so the WPPs are expected to participate with ancillary services.

WPPs above 50 kW must operate in normal conditions in a 49-51 Hz range of frequency and if the frequency goes up or down these limits, the WPP must trip the generation in a established range of time. In fact, the behaviour of WPPs has to be the same as the conventional power plants seen in Figure 2.5.

Every WPP must contribute on the frequency regulation reducing active power when frequency goes above a threshold and only plants above 25 MW with a prior specific agreement with the TSO can perform frequency control [36]. By the aim of this study, WPPs are supposed to perform primary frequency control and support the grid ensuring stability when a severe disturbance happens. The primary frequency control for WPPs is presented in Figure 2.8.

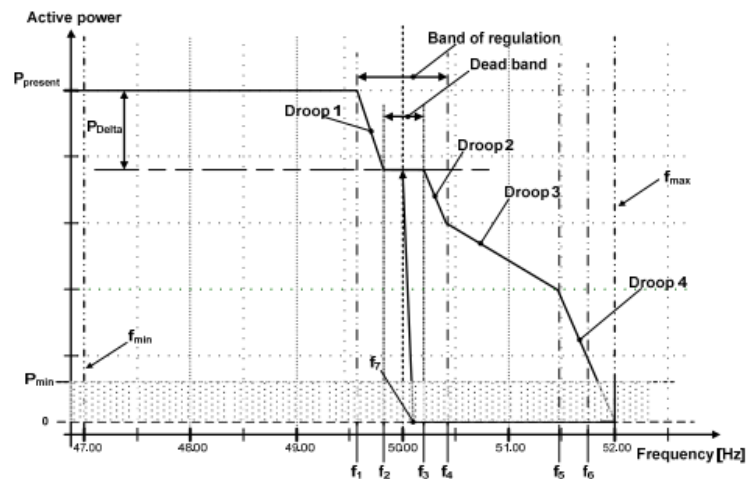


Figure 2.8 Primary frequency control for WPPs [36]

It must be possible to set  $f_{rmin}$ ,  $f_{rmax}$  and  $f_1$  to  $f_7$  that are given by Energinet.dk. The purpose of these points is to be able to produce different primary frequency control curves according to the delivery requirements. There are several droops in the curve, from droop 1 to droop 4, and they can be set between 2 and 12%, being 4% a standard value given by Energinet.dk [36]. To simplify the study, all the droops are considered to be the same value so the frequency control would be not a curve with different slopes, but a line with a constant slope that would be varied to do the sensitivity studies. Finally,  $P_{Delta}$  is the capacity

reserve that the power plant is leaving to upregulate the power and it is related to the operation point of the WPP [36].

## Chapter 3

### Modelling of western Danish power system

To study the WPP capabilities and develop sensitivity studies on the key parameters considered in this research, this chapter reviews the generating units and system interconnections on western Danish (DK1) to build up a suitable model for overfrequency studies in a 2030 scenario.

Firstly, this chapter gives an overview of the DK1 power system where the system interconnections and the different generating units are reviewed in its actual state and for 2030 future DK1 scenario. Secondly, aggregated models for the generating units are reviewed starting from the conventional power plants (must-run, CHP and DCHP) based on steam turbines and gas turbines. Also, aggregated WPP and SPVS models are developed, simplified for primary frequency control purposes, including the relevant dynamics for overfrequency event simulations. A simplified illustration of the model developed is presented in Figure 3.1. This is a delta model because both power plants and single bus model consider delta signals and it is also in per-unit.

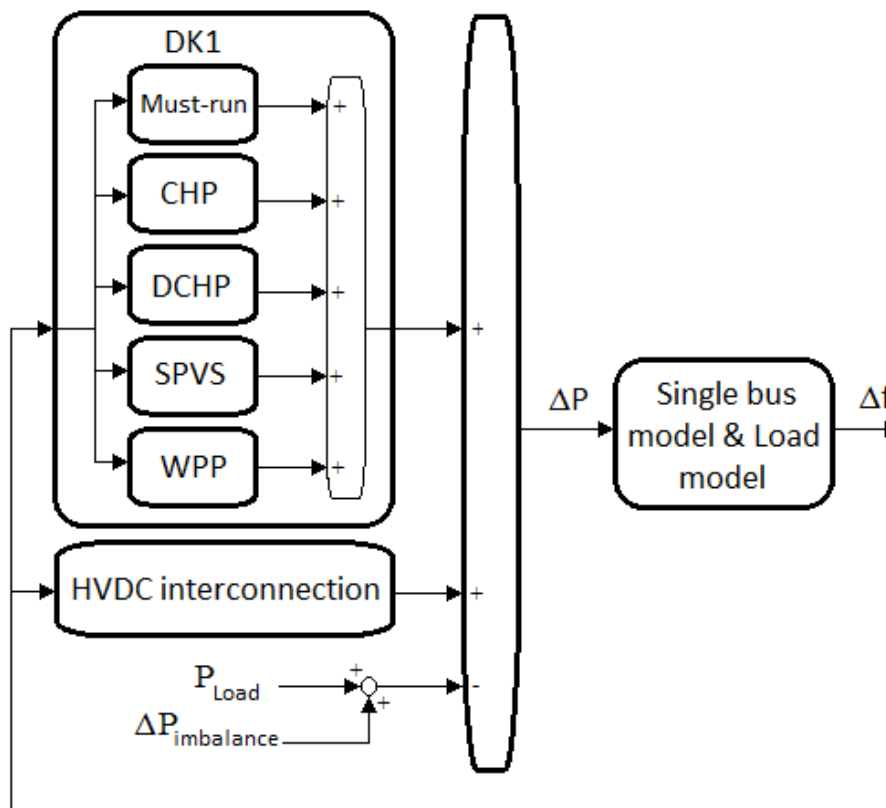


Figure 3.1 Simplified illustration of DK1 delta and per-unit model

### 3.1. Power system characterization

The Danish power system is split in 2 different synchronous zones where DK1 is connected to CE through AC lines between Germany and Denmark and DK2 is connected to NE through Sweden. Both areas are connected with an HVDC link called “Great Belt” that is a 600 MW connection. DK1 is a highly interconnected power system that consists in HVDC and AC cross-border connections, must-run units (and other CHPs), DCHPs, SPVSs and WPPs and, in this section, an overall description for every component of the power system is presented.

The system interconnections are highly important in a power system based on variable RES generation as wind or solar. As an example of this importance in a power system with high wind power penetration like DK1, the HVDC links have enough capacity to supply more power than the maximum consumption from the first 4 months recorded of 2017 in DK1 if all the interconnections import energy [37].

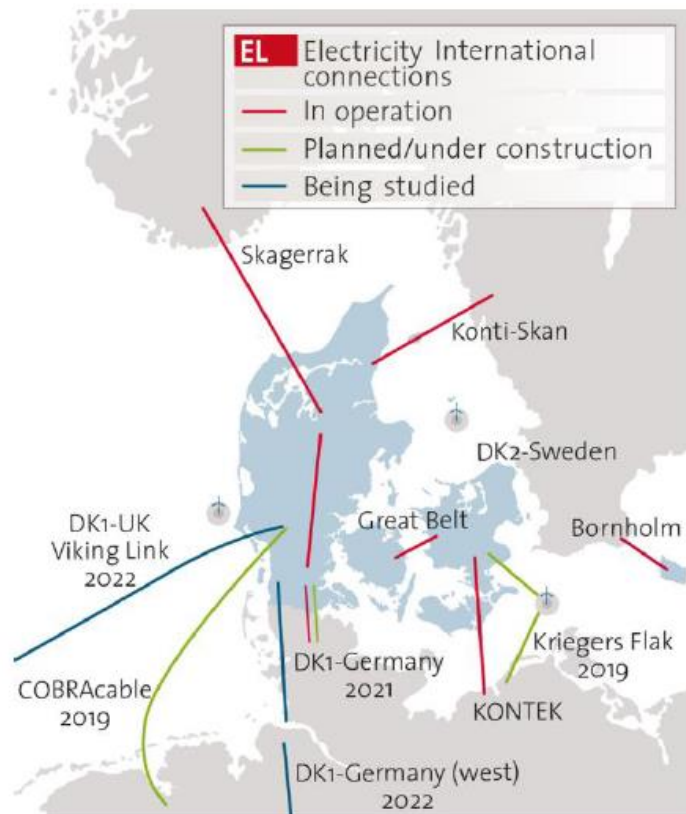


Figure 3.2 Danish map of international cable connections [38]

Some studies analyse the wind production and the power exports showing that there is a correlation between the power exported to Sweden and Norway and the wind production [15] [39] [40]. This

correlation is explained due to the hydro based NE power system and these hydro power plants are able to store the wind power generated. Then, the Danish power system exports energy during high RES generation, almost exclusively wind generation, and the Danish power system imports energy during low RES generation. Also, The Danish power system is planned to be a net exporter of renewable energy in the future. There is not a correlation between the wind production and the power exported for the exchange of power with Germany. This can be explained due to a bottleneck on the capacity of the power exchanged by the congestion on the northern part of Germany when the German WPPs are online [41]. This problem is intended to be solved by increasing the HVDC links between Denmark and CE with a new connection to the Netherlands and Great Britain. A map where all the HVDC and AC connections that permit the cross-border power exchange between DK1 and neighbour power systems in 2030 scenario is shown in Figure 3.2. Also, the planned system interconnections to DK1 are shown in Table 3.1 where the capacity for each link is presented and the type of interconnection is also outlined based on data from [42].

*Table 3.1 Planned system interconnection capacities for 2030 scenario in DK1 by type of connection and country [42]*

System interconnections	HVDC					AC
	Netherlands	Great Britain	Norway	Sweden	DK1	Germany
Capacity [MW]	700	1400	740	1640	600	3000

The activation of cross-border exchanges for power balancing is explained and used for secondary and tertiary frequency control by the European commission, but they are not extensively used for primary frequency control [29].

The HVDC connections in normal operation are performing ramp rates with different time resolutions depending on where the link is connected, to NE or to CE, because of the composition of both synchronous areas. The CE is composed by a mix of power plants that can afford higher ramp rates and the NE area needs a lower ramp rate forced by the high hydro connected in the system. The maximum ramp rate for each connection is set to a maximum value of 30 MW/min. In the CE power system, the power exchanged considers a restriction of at least 10 minutes for the duration of change of the power flow where it starts 5 minutes before and ends 5 minutes after each hour shift. However, in the NE power system, the restriction is set to 30 minutes (15 minutes before and 15 minutes after each hour shift) [43].

The conventional power generation in Denmark is typically based on three types of generators as introduced in previous chapters: CHPs, DCHPs and the must-run units, which are also facilities englobed in the CHPs, but in charge of providing inertia and frequency control, among other ancillary services.

The widespread use of district heating combined with the cogeneration of heating and electricity are the main reasons why it is possible to increase the efficiency and reduce carbon emissions in Denmark [44]. The heat and electricity generated using CHP has a significantly higher efficiency than heat and power generated separately. A CHP plant may have a total efficiency combined heating and power of 85-93% resulting in an overall fuel saving of approximately 30% compared to separate production of heat and electricity. DK1 is composed by 7 large CHPs and around 400 small and medium CHPs, DCHPs, in whole Denmark. The large CHPs are located in big cities while DCHP are located in smaller towns or centres. In DK1, there is a need of 1 must-run unit online in the system from this 7 large power plants. In 2015, the predictions made in 2015 for the future conventional power generation in the Danish power system can be seen in Table 3.2.

Table 3.2 Future conventional power generation in Danish power system by 2015 predictions [45]

	DCHP		CHP	
	Fuel	Generation capacity [MW]	Fuel	Generation capacity [MW]
<b>Eastern Danish power system (DK2)</b>	Bio Mass	124	Coal	1166
	Coal	35	Gas	560
	Gas	624	Oil	692
	Waste	96	Internal Combustion	20
	Oil	34	-	-
<b>Western Danish power system (DK1)</b>	Bio Mass	193	Bio Mass	350
	Waste	154	Coal	1130
	Gas	1261	Gas	436

In both DK1 and DK2, DCHPs are mainly using gas for electricity generation and CHPs are mainly using coal as a fuel. Other sources of generation for these power plants are waste, oil or bio mass. The electricity production of these plants has been increasing in the last years. The Danish power system is increasing its flexibility and achieving low production set points of the conventional power plants which helps the integration of the wind power generation. To provide the conventional power plants with heat storage is a short term option for flexibility and decouples the heat and the electricity demand. Also, the Danish CHPs and DCHPs can perform faster response comparing with other conventional power plants in Europe. Some examples of this increased flexibility are the improve ways of co-producing heat and electricity like allowing

a bypass for the turbines where the facility can continue providing heat while no electricity is needed without turning down the plant [13].

In Figure 3.3, the different CHP and DCHP of the Danish power system are shown. These power plants provide system inertia and reserves for the frequency control. The 7 CHPs of DK1 are briefly summarized in Table 3.3 with their capacity and type of fuel.

*Table 3.3 Capacity and type of fuel for CHPs of DK1 [46] [47] [48] [49]*

<b>Power station</b>	<b>Electricity power [MW]</b>	<b>Heating production [MJ/s]</b>	<b>Type of Fuel (Main/secondary)</b>
<b>Skærbæk Power Station</b>	392	447	Gas
<b>Studstrup Power Station</b>	714	986	Coal/Biomass
<b>Esbjerg Power Station</b>	371	460	Coal
<b>Herning Power Station</b>	88	171	Gas/Biomass
<b>Viborg Power Station</b>	57	57	Gas/Coal
<b>Fyn Power Station</b>	397	-	Coal/Biomass
<b>Nordjylland Power Station</b>	741	462	Coal/Gas

The future of the conventional power plants and the district heating in DK1 power system is to increase the flexibility of the conventional power plants. Some of these alternatives are mentioned before such as: the usage of heating storage, which allows the CHP to decrease their production when there is sufficient electricity generation; bypass the power turbines to avoid generating electricity or increasing the usage of electric boilers and heat pumps. The district heating plants can become loads to use the excess electricity from the wind directly for heating production. The increase of electric boilers will be also used to increase the demand for electricity when prices are very low by the large penetration of renewables. What is more, installing large heating storage, which is able to store heat several days, combined with the electric boilers can be also a solution for the frequency control services of the power system. Nevertheless, the remaining

conventional power plants will experience a change from coal to biomass and gas as it can be seen in [50] and probably they will not be considered must-runs anymore.

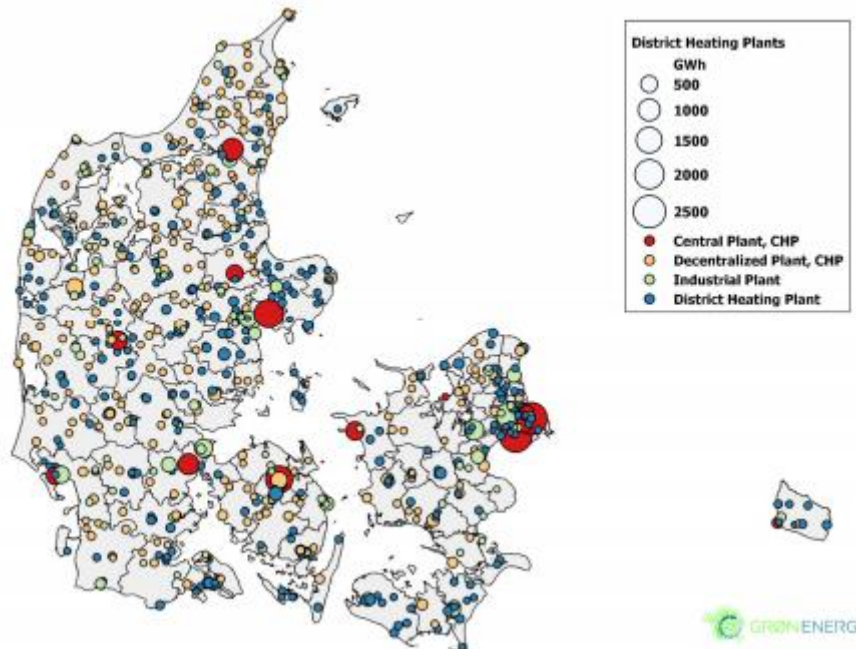


Figure 3.3 CHP and DCHP locations in Denmark by production [51]

The main focus of the renewable transition in the Danish power system is the wind integration and the solar is still seen as a minor option despite a proven growing degree of competitiveness. There is not a unified national programme for SPVSs in Denmark, but several number of projects supported by the Danish energy Authority's and Energinet.dk. In the recent years, SPVSs have been growing very fast. In 2012, the photovoltaic (PV) installed capacity grew from 13 MW to 380 MW approximately. Also, from 2014 to 2015, the PV generation grew a 30% from 602 MW to 783 MW. The main SPVS capacity by 2014 and 2015 was located in small solar generation corresponding to the cells installed in residences. However, in 2015, SPVSs above 400 kW increase in a 440% (from 38 to 170 MW approximately) and it will continue increasing in the future [52] [53].

In 2012, the government goal for 2020 for the SPVS capacity installed was 200 MW, which now it can be seen as a non-ambitious goal since by the end of 2016 the installed SPVS capacity in Denmark was estimated in more than 800 MW. However, the incredible increase of 30 times the installed capacity in 2012 was obviously not expected. By those years, it was thought that Denmark's solar would reach 1 GW by 2020 and 3,4 GW by 2030. In early 2016 the Danish Energy Agency forecasted that SPVSs will reach 1,75 GW by 2020 and more than 3 GW by 2025. One of the main reasons of the incredible growth in the solar

capacity was the net metering implemented in 2010. This policy allows the SPVS owners to generate and store the surplus production in the public grid. Consequently, it makes the variable generation of the solar more attractive so the energy generated in a shiny day could be used at night.

The scenario considered in this study developed by ENTSO-E, that is explained in the next chapter, is conservative and contemplate a SPVS capacity installed by 2030 of 1,4 GW, when this installed capacity will be probably achieved in 2020. The installed capacity in DK1 by the given scenario is 985 MW and it is considered that all the capacity is online and operating in the study. Given the 3,4 GW of SPVS capacity reviewed in the literature, having 985 MW online in the grid is considered a feasible scenario.

Some studies start including and analysing the solar in frequency stability analysis [54] [55] [56]. The main challenge when integrating solar, and also wind to the power system, increasing the RES penetration replacing conventional power plants is the loose of inertia and the variable power dispatching related to the maximum power point tracking (MPPT). To deal with the capabilities of the PV to support the frequency control, a delta power control can be used. In order to implement this control scheme, there are three approaches: integrating energy storage systems, applying a dump load to dissipate excess power or limiting the extracted PV power by modifying the MPPT algorithms.

The loose of inertia is introduced in this study as a problem for the renewable penetration because of the faster frequency excursions when an imbalance happens, hence, a need for faster deployment of FCR. However, full controlled generation as the SPVSs can achieve high ramp rates on the power output that can help the power system to response faster against a frequency deviation. There is a proposal found to denote the frequency stability support capability of inertia-less generation units during primary frequency control after major power imbalances known as fast frequency response (FFR) [56]. The favourable conditions for PV generation and the decreasing investment costs will probably lead to a continued implementation of PV generation even if the Danish road map is focused on WPP.

WPPs are in the focus for the green transition of Denmark for the next years. The power generated from wind power has been increasing from its beginning in the seventies and it experienced a fast raise in late nineties to the present. In Figure 3.4, the electricity generation by WPPs is shown with the wind power share of the net electricity production from 2000 to 2016, while Figure 3.5 presents the wind installed capacity and the number of wind turbines active. Both figures based on data from [57] and [58]. Denmark set a new world record in 2015 with a total share of 51% of the net production and 42% of the total electricity consumption being the top country in wind share in the world [59]. However, a reduction on the power produced can be seen in 2016 caused by a low windy year. The variability of an intermittent

generation like the wind, and also the solar, is present, but the wind share was still above 44% of the net production and 37% of the domestic consumption.

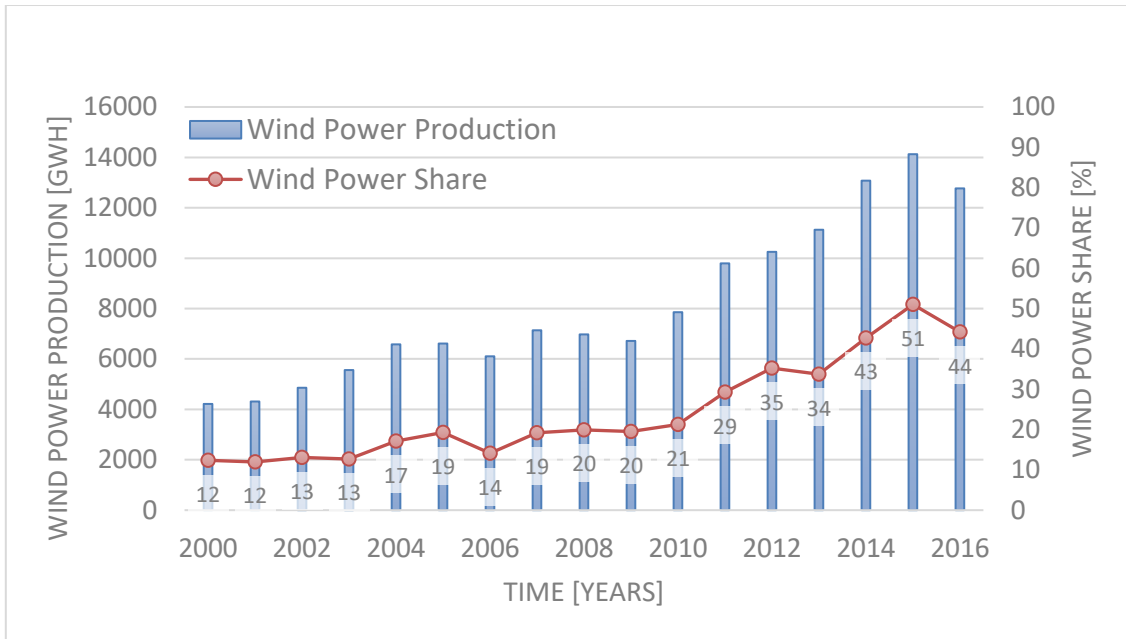


Figure 3.4 Wind power electricity production and wind share in the net electricity production [57] [58]

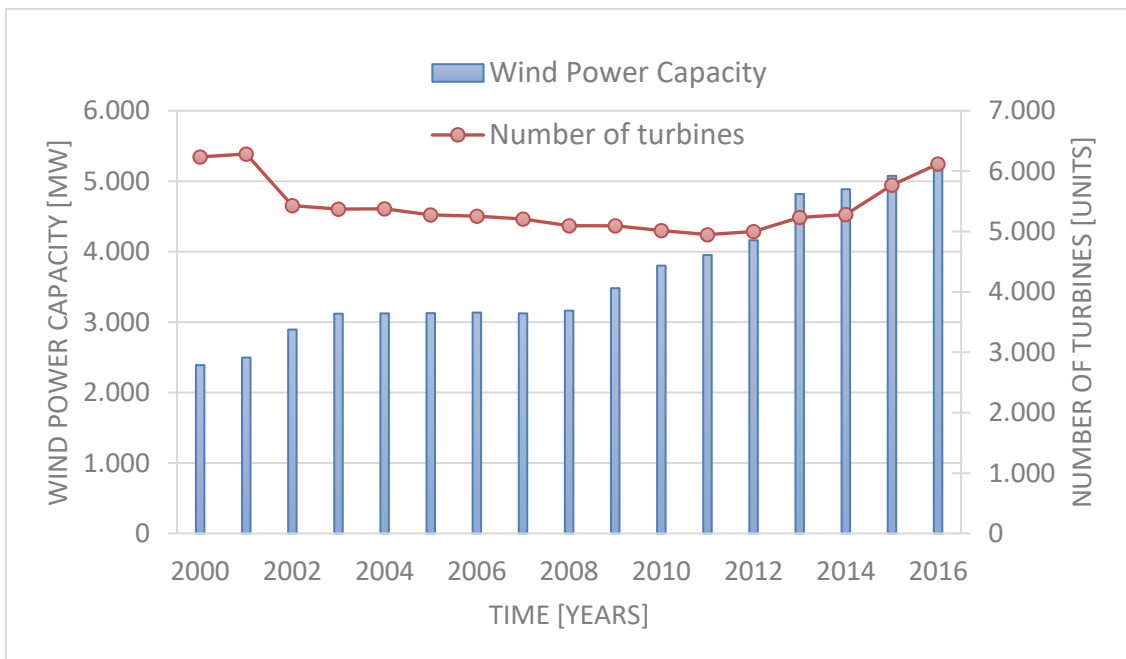


Figure 3.5 Wind power installed capacity and number of turbines active [57] [58]

What is more, the capacity installed is increasing year by year from a 2390 MW in 2000 to 5245 MW the last year, 2016. Although, while the number of turbines was kept between 5 and 6 thousand, the capacity

was increasing every year by the continuous commission and decommission of new and old turbines to increase the nominal power of the turbines installed. As an example of the huge generation that the WPPs installed in Denmark can achieve, some special days are mentioned: the power from WPPs shared 140% of Denmark's electricity demand in a particular day in July of 2015, in 15 October of 2016 a 139% wind share was reached and in 22 February of this year (2017) WPPs shared 104% of the domestic power consumption [60] [61] [62] [63]. Denmark is not normally capable to supply their entire needs with wind power if DK1 and DK2 are considered, despite it can be found some periods of the year that this happens if DK1 is focused. This specific days demonstrate that renewables can be a truly alternative to the conventional generators and a solid reference for the green transition that Europe is focusing. The surplus of power generated by these windy days are normally stored in the hydro of the Nordic countries, despite some power can be exported or imported from Germany depending on their congestion in the northern part of the German grid where their WPPs are placed.

The different WPPs online in the system can be implemented with different technologies of the wind turbine-generator. Four standard types of wind turbine topologies are presented below [64] [65]:

- Type 1: it is described by a fixed-speed induction generator directly connected to the grid. This type of WT can have pitch angle control or not. This type of generator can absorb reactive power and some stages of capacitor banks are switched to correct the power factor.
- Type 2: it is similar to the Type 1, but the turbine is equipped with electronics to vary the rotor resistance. The dynamic of the rapidly rotor resistance control and the slower pitch control work to control the speed, reduce mechanical stress and improve stability during a disturbance.
- Type 3: it is a variable speed, double-fed asynchronous generator with rotor-side converter. This allow the system to control the dynamic characteristics by the power converter. They can operate in a wide range of speeds and control active and reactive power independently. The WT can participate in steady-state and dynamic voltage and reactive control and provide frequency control as well. This type and the next one also implement the pitch control to optimize energy capture.
- Type 4: it is the model where the generator is full decoupled from the grid by a full converter where the AC grid is switched to DC and then to a controllable AC wave connected to the generator. This allows to completely control the generator speed and the grid side converter separately.

For type 3 and 4, although the wind power is considered non-dispatchable because of its variable nature, the reactive power can be dispatchable within the capability of the WT and the WPP level of reactive compensation, what makes these types economically advantageous. This reason together with the increasing control capabilities when adopting these types of technology for WTs will lead to be the most deployed technologies in the future. However, these types do not provide any inertia to the power system since the generator is not directly connected to the grid as it happens for type 1.

In 2015, the capacity of WPPs was divided as 3625 MW onshore and 1272 MW offshore in Denmark [38]. However, the future changes on the Danish system suggest that it will be more increase of power installed on the offshore option. WPP facilities are the cornerstone of the future in the Danish power system and the green transition to a 100% renewable generation by 2050. The offshore wind capacity will increase in a 1400-1600 MW range to attain the 2020 goal of achieve a stable 50% power share by wind. Some new offshore are being under construction to meet this goal: Horns Rev 3 with a capacity of 400 MW and Krieger Flak with a capacity of 600 MW. The wind power capacity will increase till the 2030 goal reaching more than 12 GW in the best scenario made by ENTSO-E and Energinet.dk, presented in the next chapter. The wind expansion also considers 400 MW near-coast offshore installations and 500-600 MW of added capacity on land before 2020. This capacity will come for repowering 1300 MW to 1800 MW new land-based WTs [66]. Relying the power supply in WPPs can cause problems because of the forecasting errors that can deviate the power exchange from its schedule. This forecast errors may compromise the normal operation of the grid leading to balancing problems. Also, in extreme weather conditions, the excess of wind speed can bring to the disconnection of an important amount of wind generation for a meaningful time. These new challenges should be taken into account in the future.

### 3.2. Modelling the system interconnections

For this study, the HVDC connections are developed as an emergency block that will be activated if the frequency reaches 50,6 Hz and delivers the available capacity with a ramp rate of 1 pu/s. Also, the activation delay is 100 ms that corresponds to the measurement of the frequency by the HVDC. If the frequency goes below 50 Hz, the power deliver of the HVDC is deactivated [6]. Otherwise, all the available capacity will be dispatched. The chosen ramp rate is achievable given the fact that these connections are fully controlled, so they can achieve this fast deployment of power when the emergency control is activated. The scenario that is simulated in this study is a failure on the AC lines isolating DK1, so the AC lines are not modelled for this study.

### 3.3. Modelling CHP and must-run units

CHPs are large conventional power plants and are based on coal as a main fuel. The must-run units are the CHPs needed to be online in the system and qualified to provide ancillary services to the power system. These power plants are modelled with the dynamics of a steam turbine. An aggregated model of a steam power plant is implemented simplified for primary frequency control dynamic simulations. Despite both power plants perform a slow response against frequency deviations, the must-run units are implemented with faster response than the CHPs as long as they are thought to be online to provide specifically ancillary services.

A generic CHP model is taken from [33] and it is given in Figure 3.6. The model consists of a speed governor and a steam turbine together with a boiler and its control, but the relevant dynamics for this study are the performed by the speed governor and the steam turbine. The boiler and its control are also implemented, but since the primary frequency control is focused, their dynamics do not participate. However, it would be useful for future studies to implement the secondary frequency control to the model developed. The response of a must-run unit or a CHP depends on the type of technology used in the plant, the speed governor and also the operating mode of the turbine. However, the model is simplified to reduce the calculation effort and avoid the fast dynamics for focusing on frequency control simulations, keeping the main performance of the model to give a reliable primary frequency control.

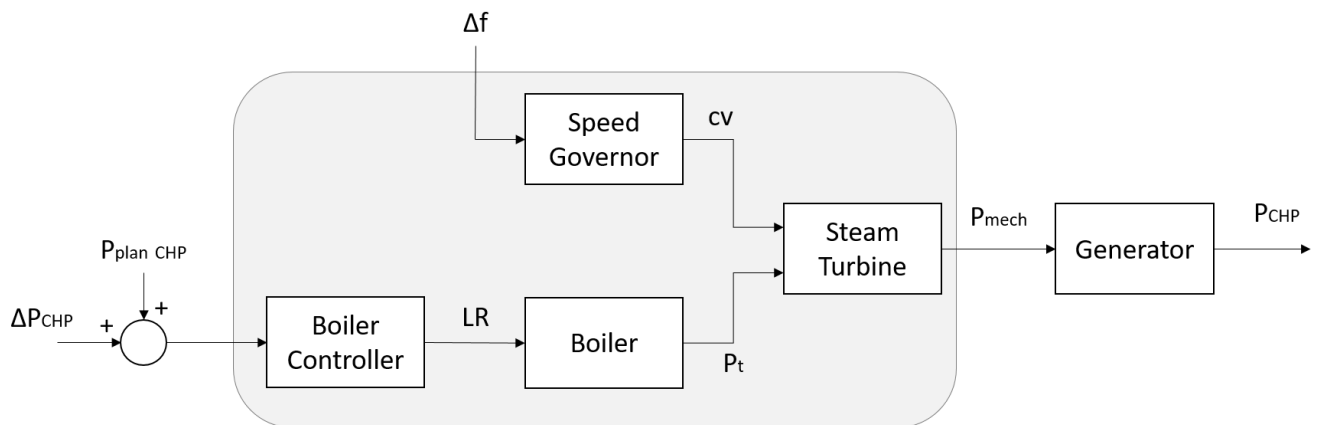


Figure 3.6 Aggregated CHP and must-run generic model

The boiler control model is implemented as a ramp rate that pretends to be the limiter of the thermodynamics and mechanical constrains of the boiler and the steam turbine. This setting is more sophisticated than the implemented, but simplified by means of this study. Values for this ramp limiter are found as 4% of the nominal power per minute. The signal LR calculated is the load reference to the boiler.

The boiler model is implemented as three first-order filters, or three first-order transfer functions, that add dynamics to the system corresponding to the series equivalent lumped storing steam. The detailed description for that model and its corresponding parameters are taken from [33] [67] [68]. Also, other parameters are set from these reports.

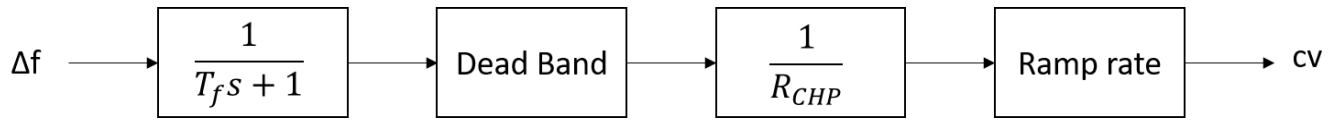


Figure 3.7 Speed governor for the must-run and CHP units

The speed governor implemented is the device in charge to respond when the system frequency deviates from its nominal value to provide primary frequency control and it is presented in Figure 3.7. The speed governor is simplified and it consists on a first-order filter that represent the measurement delay ( $T_f$ ), a dead band, a droop ( $R_{CHP}$ ) and a ramp rate. The measurement and communication delay of the frequency is considered 100 ms as described in the grid code and the dead band for the frequency control is considered to act between 49,8 to 50,2 Hz. The droop is controlled by the TSO, but it is fixed to a standard value of 6% as set in the grid code for plants above 11 kW. This study is decreasing the inertia in the grid so fast frequency excursions will take place and the ramp rate is added due to not considered delays or to ensure that the power plant will not perform too fast response [69]. The speed governor controls the position of a valve (cv) that permits to regulate the power output of the turbine.

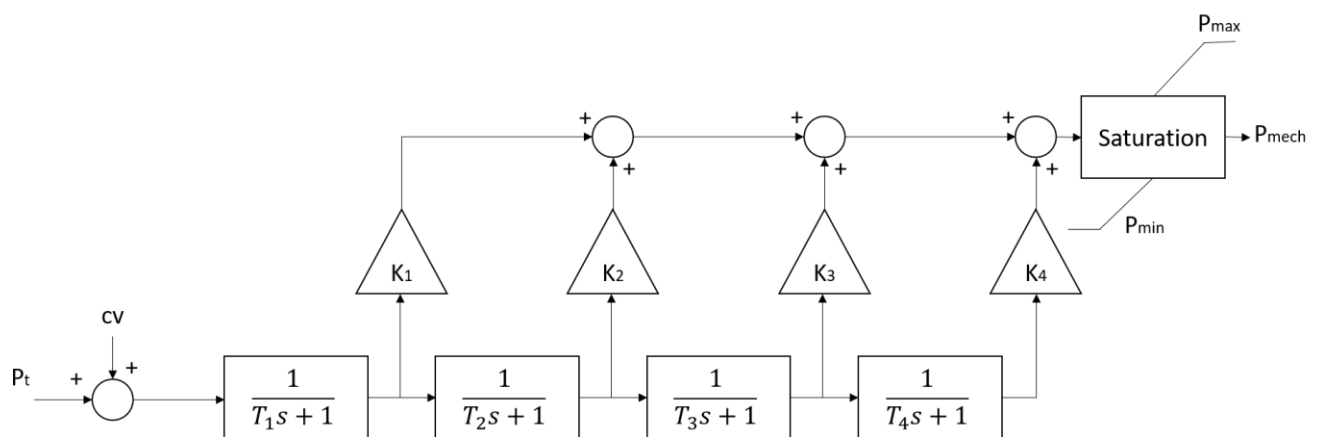


Figure 3.8 General turbine model for the must-run and CHP units

The steam turbine is the device that converts the energy stored in the steam in form of pressure and temperature into mechanical energy. The turbine consists of alternative vanes which are the rotating blades of the rotor and the stationary blades fixed to the stator. There are a lot of types of steam turbines

and each one has its particularities related to the thermodynamic cycle. Examples of types of steam turbines are: a tandem-compound with single or double reheat or a cross-compound with single or double reheat. A general turbine model is implemented and shown in Figure 3.8. The four time constants ( $T_1$  to  $T_4$ ) in the first-order filters represent the delays of the chest and inlet piping, the two reheating and the crossover piping. The four fractions ( $K_1$  to  $K_4$ ) represent the portion of the total power delivered by the turbine in the various cylinders: very high pressure, high pressure, intermediate pressure and low pressure.

The CHPs and the must-runs are modelled as double reheat steam turbine units, but the parameters of the must-run units are chosen to be faster than the CHP plants. Following [69] and the simplifications done in the steam turbine model, every double reheat turbine and every single reheat turbine has the same values without considering if it is a tandem compound or a cross compound. The values for both types of turbines can be taken from [33] [69] and they are shown in the appendix.  $P_{mech}$  is the mechanical power output of the steam turbine that will be transformed into electrical power through the generator.

### 3.4. Modelling DCHP units

The main fuel for the DCHP units is gas. So, the DCHPs are implemented in the model based on the gas turbine technology. Again, what is interesting from gas turbines is the speed controller and the prime mover that are the two main devices involved in the primary frequency control. An aggregated DCHP model based on a gas turbine is presented simplified by the aim of this research.

Different gas turbine models have been reviewed in [67] [70] [71]. A simple model as GAST is chosen due to the simplified implementation. This model was used by the Western Electricity Coordinating Council (WECC) and the Eastern Interconnection in North America. An illustration of the GAST model is shown in Figure 3.9.

This model fits the needs of the study because it assumes a simple droop control and it also implements a power limiter and the gas turbine dynamics. The dynamics of the prime mover and the power limiter are implemented with three first-order transfer functions which consist in three time constants. The speed governor implemented in the GAST model follows the same strategy than the made for the CHP. It contains a droop ( $R_{DCHP}$ ) with a standard value of 6%, a time constant that models the measurement and communication delay ( $T_f$ ) of the frequency, considered as 100 ms, the same dead band between 49,8 and 50,2 Hz and a ramp rate of 0,1 pu/s that prevents and unreliable power change given by not included controllers like the temperature control, the fuel system or the acceleration control.

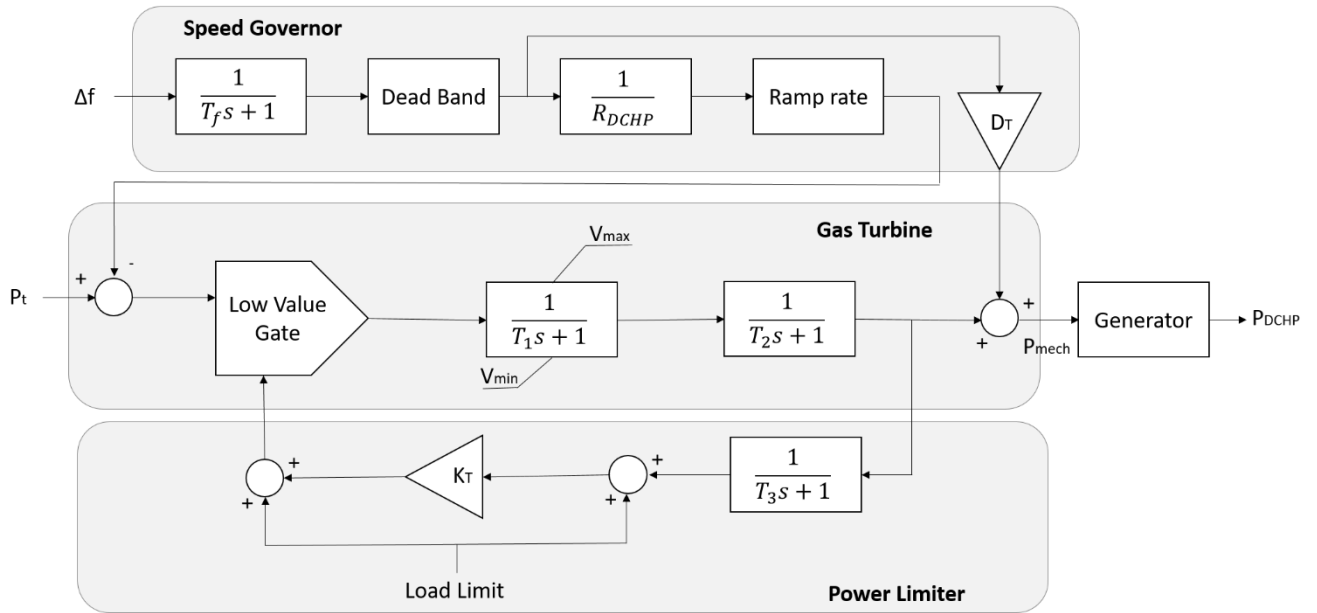


Figure 3.9 GAST model to simulate the aggregated DCHP units

Three time constants are implemented to provide the dynamic of the gas turbine: the fuel valve response time ( $T_1$ ) and the turbine response ( $T_2$ ) for the prime mover and one to represent the load limit response ( $T_3$ ). The dynamics also implement a saturation for the maximum and minimum power deployed. These three time constants simulate the power limitation control of the turbine and the mechanical response of the gas turbine.

The dynamics implemented by the GAST model, in fact, adds delay to the frequency response of the DCHP model and completely neglects all aspects of the physics of a heavy-duty gas turbine. There are hundreds of little DCHP units spread around DK1 so the capacity of each gas turbine is way smaller compared to the steam turbines implemented in the CHP units. Together with the reason that only primary frequency control is in the focus, this model is considered suitable for the study. Compared to the steam turbines, the gas turbines can deploy faster response. The values for this model are taken from [71] and shown in the appendix.

### 3.5. Modelling the SPVSs

The following aggregated SPVS model implemented is a simplified version for frequency stability studies and is based on [72]. The model contains the typical components of a SPVS: PV modules, a grid converter and a system control. The MPPT algorithm and the current and voltage controls for the grid side converter are not implemented as the model is used for frequency stability studies. The model is also simplified to

neglect different operation points for all the PV modules, the transformer and other filters at the point of common coupling (PCC), shadow effects, the reactive power contribution and the operation point is considered at maximum power production. The model developed is presented in Figure 3.10.

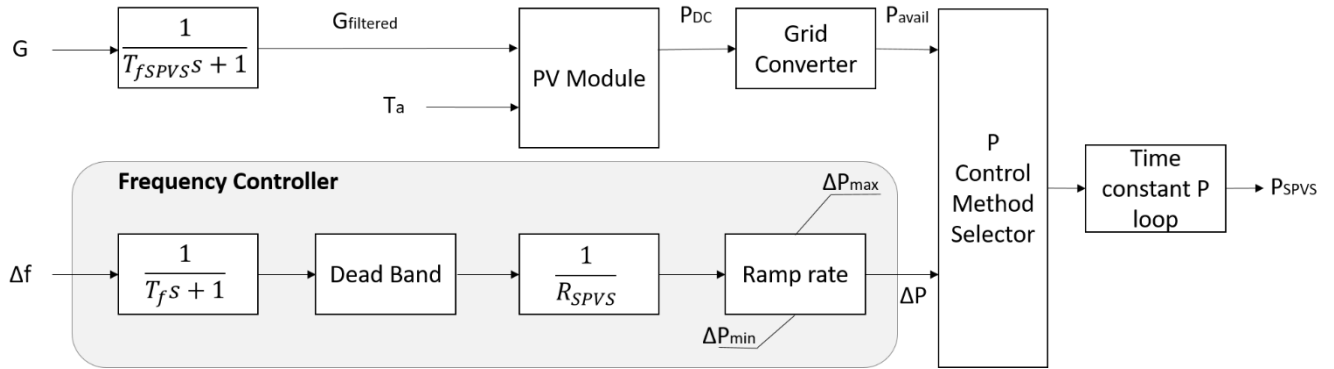


Figure 3.10 Aggregated SPVS model

A low pas filter is used to correlate single point solar irradiance measurements with power output of the SPVS. Equation (5) used for the cut-off frequency of the filter.

$$f_{cut-off} = aP_{installed}^b \text{ [Hz]} \quad (5)$$

Where  $a$  and  $b$  are parameters determined based on curve fitting techniques using measured data for several years from SPVS of different sizes. They are 0,26 and -0,499 respectively [72].  $P_{installed}$  is the installed power capacity of the SPVS in the PCC in kW. Hence, the time filtering constant for the low pas filter is expressed by:

$$T_{fSPVS} = \frac{1}{2\pi f_{cut-off}} \text{ [s]} \quad (6)$$

The PV module model uses the following equations to estimate the power output by means of calculating the estimation of the MPPT that is considered in a constant voltage algorithm. Finally, an efficiency factor of the converter is added to obtain the power available of the SPVS. The equations that compute the power at MPPT are:

$$V_m = V'_m \left[ 1 + c(T - T_{ref}) + \ln \left( 1 + b \frac{G - G_{ref}}{G_{ref}} \right) \right] \quad (7)$$

$$I_m = I'_m \frac{G}{G_{ref}} [1 + c(T - T_{ref})] \quad (8)$$

$$T = T_a + \frac{G}{800} NOCT - 293 \quad (9)$$

Where  $V_m$  [V] and  $I_m$  [A] are the voltage and current of the PV modules at MPPT,  $T$  [K] is the temperature of the PV modules,  $V'_m$  [V],  $I'_m$  [A] and  $NOCT$  [K] are parameters depending on the PV module and  $a, b, c, G_{ref}, T_{ref}$  and  $T_a$  are parameters of the model given by [73]. The parameters of the model developed are shown in the appendix.

The frequency controller implemented in the SPVS model consists in the same structure presented with the speed controller of the conventional power plants, shown in Figure 3.7. It contains a time constant corresponding to the measurement and communication delay of the frequency, a dead band that prevents the power plant to provide frequency control for small oscillations of the frequency in normal operation and only providing frequency control when an outage happens. A droop determined by Energinet.dk with a standard value of 4 % and a ramp rate with a saturation to limit the frequency response of the SPVS to overfrequency events are implemented as well.

In this study, the SPVSs are providing all the power available, working without leaving any reserves as it could be seen in the last chapter (Figure 2.7). Thus, they are only providing primary frequency control downgrading the power dispatched. The curtailment of the power output starts at the standard value of 50.2 Hz, according to the grid code. The ramp rate of this type of facilities can be really high because of the null inertia and the fast response in a full converter generation. A ramp rate of 1 pu/s is used in the study.

The last blocks of the model are the power control method, where the amount of power injected into the grid can be chosen, and a first-order transfer function representing the power control of the grid side converter. The operation mode of the SPVS in this study is to inject the available power, with the curtailment given by the primary frequency control if needed to maintain the system frequency stability. However, the model can also follow an active power reference or just inject all the available power without curtailment into the grid. Some considerations of this model for the study are that the solar irradiation and the temperature are set as constant so the power in the PV modules is 1 pu constant during the simulations, despite the model can support solar irradiancies and temperature data as inputs.

### 3.6. Modelling the WPPs

The aggregated model for WPPs is based on the developed for the SPVSs. The model implemented is focused on both frequency controller and prime mover of the WPPs. It is a simplified version for frequency stability studies and some considerations are made to decrease the operational effort of the simulations. The basic control architecture of a WPP consists in two different levels: the WPP control level and the wind turbine (WT) control level.

In the WPP control level, signals sent by the TSO, which establish the operation mode and the active services in the WPP, and measurements on the PCC are treated to calculate the active and reactive power references for the WTs. This level of the control architecture includes the different control options that a WPP can deploy such as: power ramp rate control, frequency control, delta control or voltage control. This study is focused on frequency control with the participation of the inertial response and takes out of scope the rest of the control services included in this control layer. The active and reactive power references calculated by the controllers in this layer are compared with the measurements on the PCC to adjust the power references sent for the WTs, normally by a PI controller. Then, the active and reactive power references are dispatched into different power references for the WTs.

A general control structure for a WT type 4 control level is presented in [74] [75] [76] (and also in the IEC 61400-27 standard). The main controllers that deal with the frequency control and the inertial response are the pitch controller, to control the pitch angle, and the rotor speed controller, hence, to control the generator speed.

The operation point is not considered in the delta model and only some of the controllers of the WT layer are relevant so the control structure for the WTs is aggregated in a first-order transfer function with a single time constant. With this consideration, it is supposed that the rest of the controllers are faster than the pitch controller so the time constant considered is reliably enough to provide an approximation of the dynamic response. The time constant for the pitch controller is considered as 2,2 seconds in [74]. Then, to include other delays of controllers not considered, the time constant that is taken for this study is 3 seconds. The ramp rate implemented will limit the rate of change in the power supplied by other restrictions related to topics not considered in the model such as current or mechanical dynamics. The model implemented is presented in Figure 3.11.

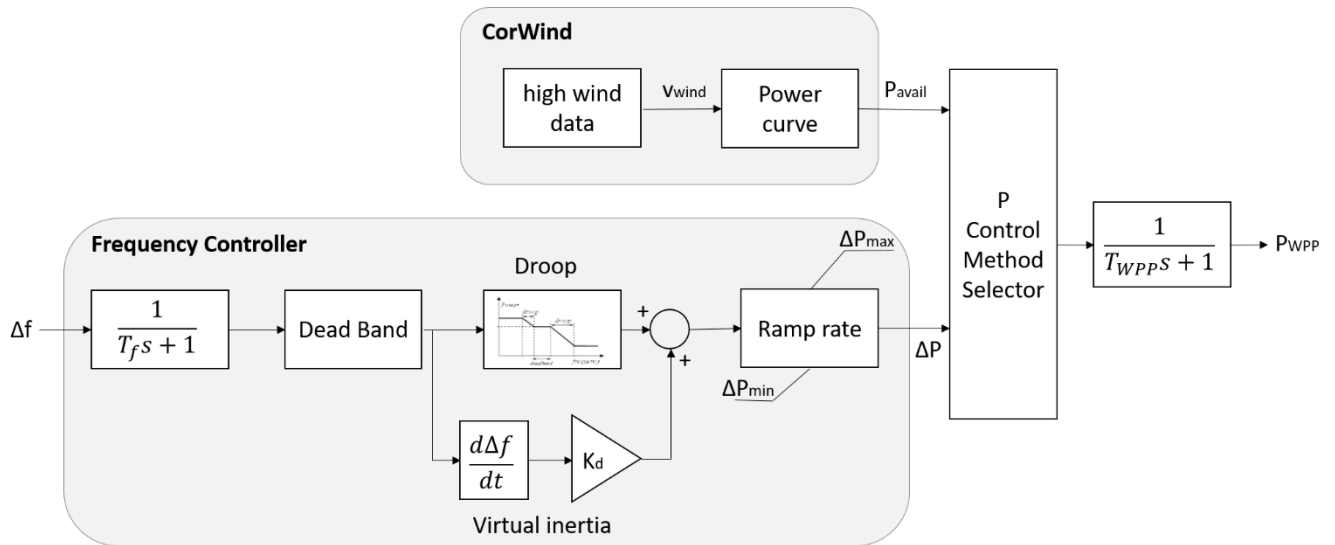


Figure 3.11 Aggregated WPP model

The model uses data provided by CorWind [6] which uses historical data of wind measurements and a power curve to provide the active power available to the model. Other characteristic settings implemented are: the frequency controller, the power control method and a first-order filter that aggregates the controls of the WTs. The model is a simplification for frequency stability studies and does not consider current or voltage controls, so, electrical connections from the PCC to the WTs are not implemented. The reactive power control is simplified too.

The frequency controller implemented follows the same structure as the other power plants explained before and it contains: a first-order transfer function with a time constant that represents the measurement and communication delay of the frequency and a dead band to avoid frequency control for small frequency deviations in normal operation. It also contains a ramp rate with a saturation that limits the velocity of the power dispatched and a module which calculates the power deviation from the droop and the virtual inertia for the primary frequency control.

The WPPs are modelled as an aggregated power plant that curtails the power available in order to control the injected power to the grid. The primary frequency control that they can provide is either increasing or decreasing the power generated for underfrequency or overfrequency events, respectively, as it can be seen in Figure 2.8. The dead band on frequency measurement operate from 49,8 to 50,2 Hz, as standard values on the grid code of Energinet.dk. The ramp rate, the droop and the virtual inertia are parameters explored on the sensitivity studies presented.

The power control method allows the model to operate injecting all the power available, curtail the wind power and allow the WPP to perform frequency control or follow an external power reference. By the mean of this study, the WPP is set in the control method where the power available is curtailed and the frequency controller down or upregulate the power reference. Although, the power deviation for underfrequency events is limited by the power reserves leaved from the total available power. The last block is explained at the beginning of this section and consists of a first-order filter that aggregates all the delays in the WT controls to a time constant that is considered to be 3 seconds.

### 3.7. Single bus model, load model and outage

The DK1 network topology is based on the equation of motion of a synchronous generator. In case of a sudden outage, the amount of kinetic energy which is stored in the rotating masses of the generators connected to the system will change until the imbalance is solved. Equation (101) is a well-known equation normally used in frequency stability simulations [77] [78] [79] [80] and it is right for delta modelling in per unit.

$$\Delta P_{gen} - \Delta P_{load} = M \frac{d\Delta f}{dt} \quad (10)$$

Where  $\Delta P_{gen}$  is the deviation on the power generated,  $\Delta P_{load}$  is the deviation on the power consumed,  $M$  is the inertia constant and  $\Delta f$  is the deviation on the system frequency. The inertia constant shows the kinetic energy that the rotating masses of the grid can store and inject. Another way to name the inertia constant is  $H$  where  $M=2H$ .

Moreover, the load is normally sensitive to the frequency deviation so it is modelled in two parts: the frequency dependent and the frequency independent. These two components are presented in equation (11) for a delta signal and per unit model:

$$\Delta P_{load} = \Delta P_1 + D \cdot \Delta f \quad (112)$$

Where  $\Delta P_1$  is the deviation on the frequency independent component of the load and  $D$  is the damping coefficient that models the variation in the demand under a frequency deviation. That parameter gives an idea of the amount of load that is frequency dependent. This damping parameter is considered as 1 %/Hz of the total load as a common acceptable value of this parameter, referred in [81].

Finally, combining the two equations for a delta signal model, the next equation is obtained and this is the equation for the single bus model and load model for the network topology. The equation in Laplace domain can be also seen.

$$\Delta P_{\text{gen}} - \Delta P_1 - D \cdot \Delta f = M \frac{d\Delta f}{dt} \quad (12)$$

$$\Delta f = \frac{\Delta P_{\text{gen}} - \Delta P_1}{Ms + D} \quad (13)$$

It can be seen in equation (13) that for a power balance situation ( $\Delta P_{\text{gen}}$  is equal to  $\Delta P_{\text{load}}$ ), the model does not experiment any frequency deviation. When the AC lines are disconnected and there is an interruption of the power exported, the generation is bigger than the load. So, the synchronous generators will accelerate until the imbalance disappears. Otherwise, if the load increases or the generation decreases, the system frequency will decrease. This equation gives the inertial response of the system until the power plants online deviate its power generated during the first seconds after an imbalance. In the end, the synchronous generators are used as energy buffer in the power system. The main reason against large frequency deviations from the nominal value is the loss of synchronism which would lead to a disconnection and might result on a chain reaction resulting in a black out.

Simplifying the inertial response of the grid and also considering the model in Figure 3.1 comes with the assumption that the frequency is uniform over the highly interconnected DK1, all the loads are aggregated in an equivalent load with an equivalent damping  $D$  and all the inertial response of the generators are aggregated in a single inertial parameter  $M$ . The frequency deviation is used as a feedback for the primary frequency control in the model for the power plants. All the delta signals of the power outputs for the different power plants are added to make the delta power generated.

As Denmark is expected to be a net exporter country, it is a logical reasoning to think that there will be more probability to have overfrequency imbalances, if an AC/HVDC interconnection fails. The generation will increase as Denmark will produce enough power to meet its demand and export the rest of the energy, so underfrequency imbalances can also happen by a disconnection of a generator. However, it is considered an islanding event as the critical scenario for frequency stability studies and that is the reason of focusing on the overfrequency events. If DK1 is not islanded, the large CE grid would provide inertia and reserves to the Danish grid for a generator disconnection, so the frequency deviation would be low.

An islanding event is an outage considered faster than the different delays on the measurement of the frequency and the dynamics of the power plants modelled so the outage is implemented as a step in the power exchanged leading to a surplus of generation.

# Chapter 4

## Scenario description and test cases

This chapter explains the scenario and the test cases that are simulated in this research. The key parameters considered in the sensitivity studies are presented and the evaluation criteria of the results is mentioned as well. At the end of the chapter, a Danish islanding event is presented as an example of a failure scenario isolating DK1.

### 4.1. Definition of the scenario

Denmark has a roadmap to 2050 where the energy supply will become fossil fuel independent. The political consensus agrees that the energy supply in Denmark must be based on renewable energy and it is also a high priority that this transition must take place without putting Denmark's competitiveness under pressure due to rising prices of energy services ensuring the security and reliability of the power supply [38].

The wind power is going to be the dominant RES on the transition, but the development environment of this green growth is costlier than the fossil fuel growth. Several challenges and opportunities need to be studied to reduce the economic cost of the transition to renewable energy so it can be competitive with the fossil energy growth.

The government's goal of fossil fuel independent electricity and heating is set on 2035 [4]. Energinet.dk is continuously analysing the development of the energy sector due to the changes done in the world energy system with the aim of ensuring the best possible transition to the Danish electricity system. Changes in the surrounding countries and in Europe have impact on the development of the Danish power system. Four scenarios were made by Energinet.dk based on the ENTSO-E scenarios which are designed in two dimensions: international integration of renewables and environment focus. These scenarios are four descriptions of how the Danish energy system will look in 2030 and it can be seen in Figure 4.1.

By means of this study where the research is focused on the capabilities of the WPPs, the scenario that considers the highest RES penetration and a European environment focus is chosen.

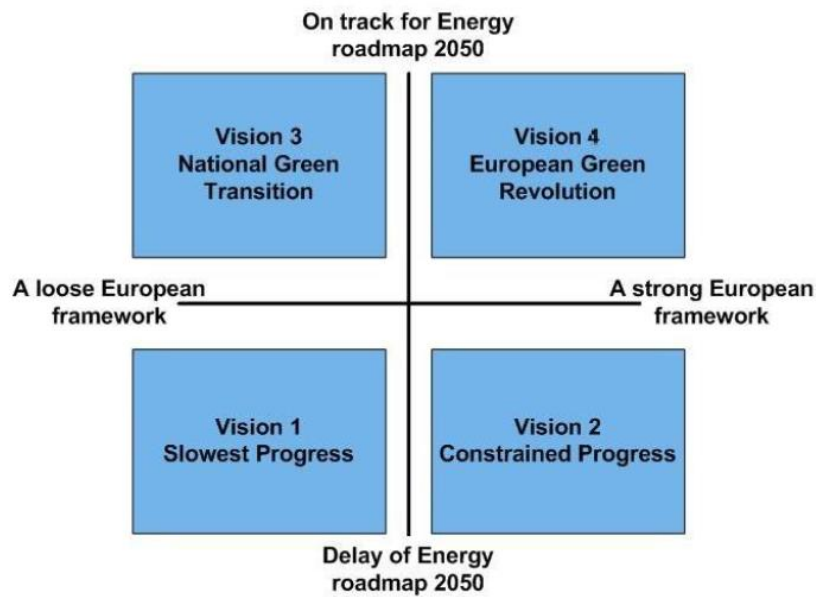


Figure 4.1 The four scenarios for the Danish energy system in 2030 [26] [82]

The Green Europe scenario works towards an 80-95 % reduction in greenhouse gases by 2050 so Europe is in its way into the green transition. RES are being optimized and investments are made to increase their generation. Moreover, areas with good conditions for RES can export energy. This scenario maintains the security of the power supply through European initiatives and consumer disconnections. Denmark is one of Europe’s most highly wind power dominated zones and the Nordic region synergize as a storage facility with hydroelectric power stations.

According to ENTSO-E and Energinet.dk, the installed capacity in Denmark and DK1 for the Green Europe scenario by energy source is shown in Table 4.1.

Table 4.1 Installed Capacities for Denmark and DK1 in 2030 in the Green Europe scenario [42]

Energy Source	Denmark 2030 [MW]	DK1 2030 [MW]
Biofuels	1400	395
Gas	3746	2446
Hard Coal	410	410
Hydro	9	9
Oil	735	-
Wind	12825	8186
Solar	1405	985
Other RES	260	160

In this study, the hydro power plants and the “other RES” are neglected because of their low presence in the power system. The biofuels are aggregated with gas to set the installed capacity for the DCHP units corresponding to 2841 MW. The hard coal energy source corresponds to CHP and the wind and solar energy sources are modelled as WPP and SPVS respectively.

ENTSO-E provides a data base for the scenario which describes hourly the electricity import, export and consumption for DK1 and DK2 [42]. The system is studied in a specific hour chosen in this data base under high wind scenario. The summary of the power flow for the hour chosen to do the study is seen in Table 4.2. The specific hour is chosen such as the system is operating at the peak load, DK1 is exporting in a high level and there are little imports. Hence, these are some typical requirements in a high consumption hour in high wind conditions.

Table 4.2 Power flow of the specific hour in 2030 scenario chosen [42]

Consumption [MW]	Power exported [MW]	Power imported [MW]	Total power generated [MW]
3917	5197	178	8936

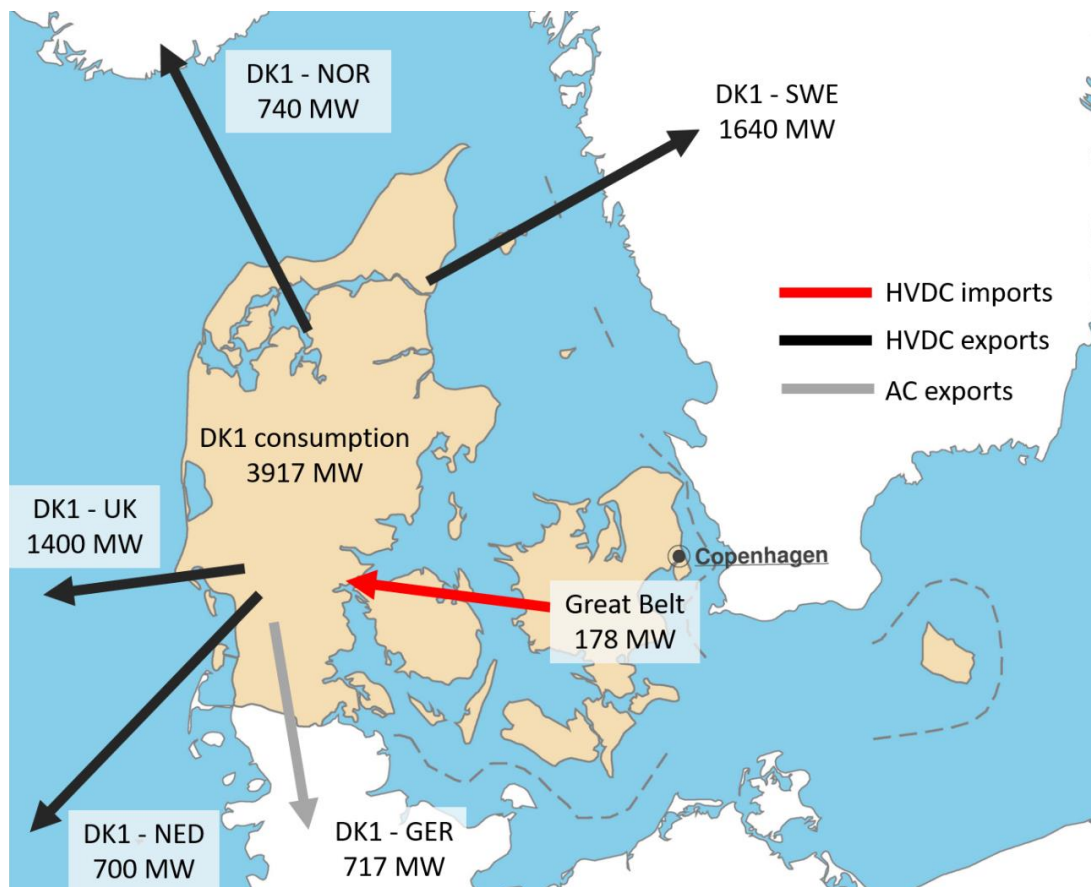


Figure 4.2 DK1 2030 scenario considered for the study based on data from [42]

In this scenario, the power system is generating more than 2 times the pick load of DK1 in 2030. It is worth mentioning that only the Great Belt is importing power to DK1 and all the other connections are exporting energy. From all the power exported, 717 MW is the power exported to Germany through the AC lines and that will be the outage simulated when isolating DK1 to CE. Underlining again that the primary reserves for DK1 is set in 30 MW, this outage is much larger and will bring the system to an emergency state. The scenario is illustrated in Figure 4.2.

## 4.2. Definition of test cases

From the scenario explained before, the test cases for the simulations are established. The system is tested in a base case, when the must-run units are online and all the power plants that provide inertia are also online in the grid, and then, the must-run units are decommissioned and replaced by other CHP and DCHP capacity reducing the inertia contribution in the power system. The RES penetration is increased in each test case until finding the case where the frequency excursion does not satisfy the evaluation requirements mentioned above. There are many options to calculate the RES penetration, but they are focused on using the capacity installed or the power production [83] [84]. In this study, the RES penetration is defined in the next equation:

$$\% \text{ RES penetration} = \frac{\text{RES power production}}{\text{Total load}} \cdot 100 \quad (144)$$

There are some studies that suggest that WPP Type 1, fixed speed induction generators (FSIGs), can provide some inertial response [77] [85]. Although, the future WPPs are supposed to be doubly fed induction generators (DFIGs) or in full scale converter (FSC) and, in both cases, the WTs are not going to provide inertia. Also, SPVSS are facilities fully decoupled from the grid by a converter and they will not provide inertia.

The conventional power plants are found to have inertia constants ( $M$ ) between 20 and 11,4 MWs/MVA [78] [79]. Furthermore, there are studies taking  $H$  as 6 seconds like an accepted value (*remembering that  $M=2H$* ) [86]. Given these range of values, the must-run units are considered to have 8 MWs/MVA of inertia constant ( $H$ ) and 6 MWs/MVA will be considered for the rest of the conventional generators. The inertia of a must-run unit is chosen higher than the rest of the conventional power plants to underline the importance on providing inertia to the system.

The system inertia of each test case will be calculated with the following equations:

$$Kinetic\ energy\ stored\ [MWs] = \sum_{i=1}^N P_i \cdot H_i \quad (15)$$

$$H\ [MWs/MVA] = \frac{Kinetic\ energy\ stored}{S_{base}} \quad (16)$$

Where  $i$  is the type of power plant implemented in the model,  $H_i$  [s] is the individual inertia constant of each power plant,  $P_i$  [MW] is the online power of each power plant,  $N$  is the number of power plants online, and  $S_{base}$  [MVA] is the power base of the system. An approximation is commonly done considering  $S_{base}$  approximately equal to  $P_{base}$  and then the measurement units of the inertia constant become [s] from [MWs/MVA].  $P_{base}$  is considered to be the total load.

The total installed capacity of conventional power plants in 2030 scenario will be 3251 MW as it is seen in Table 4.2. Test cases are developed increasing the RES penetration by 5% for each step from the base case with all the inertia connected. In the base case, a capacity online of 1000 MW for the must-run units is supposed and it replaces the hard coal and part of the gas installed capacity. The other 2251 MW are placed as DCHP capacity as it comes from gas facilities. On the other hand, the first test case keeps the RES penetration from the base case and decommissions all the must-run units to change them into CHP for the hard coal and DCHP for the gas installed capacities according to Table 4.1. From this case, the RES penetration is increased while the CHPs and DCHPs are being shut down. The test cases are shown in Table 4.3.

The conventional power plants are considered to work on 90% of the total capacity. There are several reasons that support this decision. One argument is the need of a market model that can provide a feasible set point for that type of power plants agreeing economical requirements. A high production point is set to this power plants to avoid set points not economically achievable. Another main reason is that reducing the set point of a conventional power plant, maintaining the power generation, leads to an increase of the capacity online, so the inertia will also increase. Although, low set points for the conventional power plants are used nowadays to increase the RES production without losing the inertia in the system, choosing a set point of 90% for the generation is considering the worst case in the frequency stability study. The 10% of the online power capacity that is not dispatched is considered as a mix of the power reserves and the power not sold in the market.

Table 4.3 Test cases to be simulated in the sensitivity studies

RES Penetration [%]	Type of power plant	Capacity online [MW]	Generation Set point [MW]	Kinetic energy stored [MWs]
<b>Base Case (67%)</b>	Must-run	1000	900	21506
	DCHP	2251	2026	
	SPVS	985	985	
	WPP	8186	5025	
<b>67</b>	CHP	410	369	19506
	DCHP	2841	2557	
	SPVS	985	985	
	WPP	8186	5025	
<b>70</b>	CHP	410	369	17872
	DCHP	2569	2312	
	SPVS	985	985	
	WPP	8186	5270	
<b>75</b>	CHP	-	-	14893
	DCHP	2482	2234	
	SPVS	985	985	
	WPP	8186	5717	
<b>80</b>	CHP	-	-	11915
	DCHP	1986	1787	
	SPVS	985	985	
	WPP	8186	6164	
<b>85</b>	CHP	-	-	8936
	DCHP	1489	1340	
	SPVS	985	985	
	WPP	8186	6611	
<b>90</b>	CHP	-	-	5957
	DCHP	993	894	
	SPVS	985	985	
	WPP	8186	7057	

In the specific snapshot studied, a fixed solar irradiation is considered that will not change in the test cases. The SPVSs are delivering all the power available because they do not provide frequency regulation and only downregulate the power when deploying frequency control. Finally, in a high wind scenario it is considered that all the WPPs capacity is available and this power is curtailed to adjust the power dispatched. The power dispatched from RES is increased in each test case and the conventional power plants are replaced, so the inertia is reduced. WPPs are supposed to supply not only primary frequency control, but secondary too in the future, so the power dispatched from WPPs can be theoretically increased until the power curtailed is equal to the primary and secondary reserves. Although, in this study the RES penetration is increased up till the system does not meet the success criteria explained in the next section, where the power curtailed would be bigger than the needed reserves from the WPPs.

### 4.3. Definition of key parameters and success criteria

To study the WPP capabilities on the frequency control, some KPIs are evaluated in their standard range to improve the understanding of the frequency stability support coordinated with the other power plants. The coordination is done by studying the parameters and doing recommendations depending on the configuration of the power plants in the power system (related with the RES penetration). The key parameters are listed below and some of them can be seen in the frequency controller of the WPP model in Figure 3.11:

- % RES penetration in the power system.
- Ramp rate that limits the rate of change in the power deviation.
- The droop used to calculate the power deviation of the WPP with the frequency deviation in the power system.
- The gain of the virtual inertia ( $K_d$ ). In the first sensitivity study, this control is inoperative and then is activated with a certain gain in the frequency controller.

Other parameters that are studied, related with the power system rather than with the WPPs, are:

- Frequency support of HVDC connections with neighbour countries.
- Delay in the communications and measurement of the frequency.

An increase on the RES penetration, decreases the system inertia by the replacement of conventional power plants which will make the frequency excursion faster and, presumably, increase the maximum instantaneous frequency that the system will reach. The evaluation of the parameters tested is considered successful if they achieve the goal of keeping the frequency excursion below 51 Hz and above 49 Hz and the RoCoF below 2,5 Hz/s. Although these limits are larger than the allowed for the primary control (50,8 and 49,2 Hz), they are considered good values to avoid a defence plan such as in the Danish isolation in 2007, presented in the following chapter, as long as the system is leaded to an emergency state where the operational limits are reached but still not losing the stability.

The WPP capabilities and limitations are explored with the ramp rate and the droop sensitivity study to find the operational limits when operating without must-run units. These key parameters regulate how fast the WPP can provide frequency control. The range for the droop is taken between 2 and 12 % as said in the grid code and the ramp rate is going to be varied between 0,1 and 0,5 pu/s range. These values are supposed to be achievable by WPPs in 2030. The gain of the virtual inertia is also studied to analyse the improvement with this new setting in the frequency controller.

Other parameters are explored such as the support of the HVDC interconnectors for frequency control in test cases with low inertia because of their fast response regulating their power flow given an imbalance. The delay on the communication and measurement of the frequency is studied to show how this parameter affects to the frequency excursion in high RES penetration of the power system.

#### 4.4. Danish islanding event 29.05.2007

In this study, an islanding event is simulated and the power system capabilities to handle this severe event are investigated. An example of an islanding event in Denmark is the event that took place in 29.05.2007. Normally, an outage in the power system cannot be only categorized in one of the three stability phenomena: voltage, rotor angle and frequency stability. An event threatening one stability scene can come with a problem in the other 2 stabilities. In this Danish islanding event, a small-disturbance angle stability ended in a disconnection of Denmark and Germany leading to a frequency instability issue. This example also agrees with the possibility of Denmark being islanded that is studied in this research. The sequence of events in the incident is listed below [9]:

- An explosion of a current transformer leads to a double bus bar failure in 380 kV Wilster substation (Germany).

- Disconnection of all 380 kV lines in substation Wilster and in particular the both two 380 kV lines that connect CE to DK1. Only two 220 kV lines remained connecting Denmark and Hamburg area. By all four lines, Denmark was exporting 1500 MW before the incident. Due to the disconnection of two lines, large power oscillations occurred with a negative damping.
- By overload phenomena during the oscillations, the two 220 kV lines were trip after 28 seconds from the failure of the 380 kV, leaving DK1 isolated from CE. Then the frequency of Denmark increased reaching 51 Hz by the exporting interruption and the frequency in CE decreased in a range of mHz to balance the imported power.
- 59 seconds after the explosion of the current transformer, the Baltic cable tripped by emergency protection control increasing the loss of power importation for UCTE to 2200 MW (frequency went down to 49,95 Hz). The Baltic cable unify Germany with Sweden.
- Finally, 5 minutes before the first event, the 380 kV lines resynchronised the system.

The sequence of events can be seen in Figure 4.3 with the resulting measurements and oscillations of this failure.

This outage is a good example also for showing the cascading nature of different kind of phenomena that took place from a failure in the German power system, leading to a Danish frequency instability problem. In Figure 4.3, the voltage stability is recovered from the oscillations produced by the short circuit when DK1 and CE were disconnected, even leaving DK1 with a problem of frequency instability.

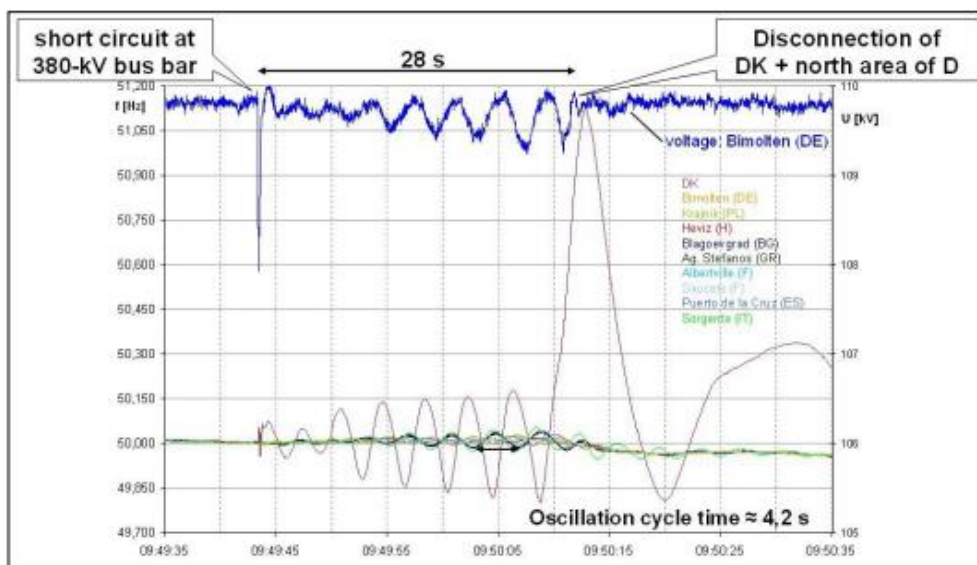


Figure 4.3 Measurement values for the Danish islanding in 29/05/2007 [9]

With the 1500 MW loss of power export by the islanding of DK1 from CE, the situation was led to an overfrequency phenomena [9]. The frequency reached 51 Hz in a few seconds and this power was covered by the primary frequency control of the power system and the automatic adaptation of the power flow in the HVDC links between Denmark and Sweden/Norway. When DK1 had this huge surplus of generation, it was not enough with the primary frequency control of the power plants online and other corrective actions were needed to avoid the loss of stability. These corrective actions were the participation of the HVDC automatic regulation of the power flow, but it could also be another defence plan like a tripping strategy of the generators to reduce the power generated.

This event provides back-up information and corroborates the chosen frequency limit of 51 Hz for the study presented below in this project. Also, the frequency excursion for both DK1 and CE can be compared and it is seen how the same power imbalance produce a small frequency deviation in the large CE power system while a defence plan is needed for DK1. The frequency in DK1 reached 51 Hz while for the CE, however, the decrease of the frequency is very low, reaching 49,95 Hz when the total loss of import was around 2200 MW. The difference between the frequencies reached by the power system gives an idea of how large is the CE power system compared with DK1. Nevertheless, the frequency excursion is also faster in DK1 compared with the excursion in CE and it is an indicator of the inertia online in the power system. Energinet.dk does not consider the inertia a critical factor for a safe operation and both DK1 and DK2 normally rely their inertia on the contribution of CE and NE, respectively [28]. With the islanding event, the inertia in DK1 suffer a high decrease what led to faster frequency excursions.

A final comment to this disturbance is the participation of the HVDC supporting the grid as a defence plan. In this study, the participation of HVDC in low inertia test cases is also tested to see if they should increase its importance for frequency stability in a future power system with high RES penetration.

# Chapter 5

## Sensitivity studies

The different sensitivity studies of the power system and the WPP capabilities are presented in the following sections. First, the base case is simulated and commented to show how the frequency excursion would be with full inertia online in the power system. Then, a study on the droop and the ramp rate is presented when increasing the RES penetration in each test case. The virtual inertia is applied as well to show the improvements in the frequency excursion. After exploring the WPP capabilities, a study on the HVDC connections between DK1 and the neighbour countries is presented to understand how these facilities can contribute in the frequency control between the HVDC interconnections and the power system. Finally, the delay on the measurement and communication of the frequency controller is investigated.

### 5.1. Simulation of the base case

As mentioned on the definition of the test cases, the base case is the one where the must-run units are online and they provide a substantial amount of inertia. Two simulations are tested in the base case: the one where the RES generation is not participating on the frequency control and the other where the RES is participating. These two simulations are shown in Figure 5.1.

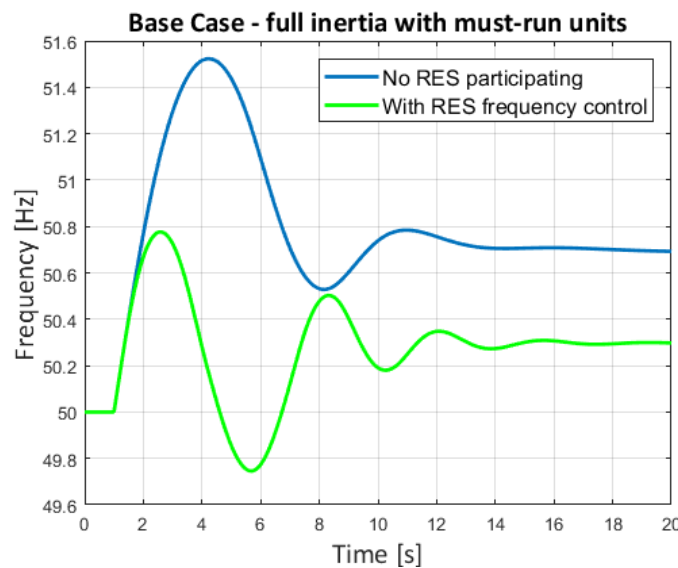


Figure 5.1 Frequency excursion for the base case with and without RES participation

Figure 5.1 shows that only with the must-run units and the DCHPs providing frequency control in a 67% of RES penetration, the system will remain stable. However, the frequency reaches 51,5 Hz and it is threatening the disconnection of some generators to maintain the frequency in normal operation range. In contrast, when the RES is participating in the frequency control with the must-run active and full inertia in the grid, it can be seen that the frequency excursion is faster and the maximum instantaneous frequency does not overcome the limit of 50,8 Hz established in [81] by ENTSO-E.

These simulations show that in a future scenario where RES will have a big share in the power system, it is important to introduce these power plants into the ancillary services. The simulation with the RES participating and must-run units online, done with the recommended values in the grid code of Energynet.dk, shows that the system will remain stable and within the normal operation range for a severe disturbance. For the rest of the test cases: the must-run units are decommissioned and substituted by other CHP and DCHP at first, and then the increasing RES penetration will replace the conventional power plants.

## 5.2. Study on the droop and the ramp rate

The power system is stressed in this study by increasing the RES penetration and decreasing the inertia online. The WPP droop is changed in every simulation from 2 to 12 %, as established in the grid code, and the ramp rate is varied from 0,1 to 0,5 pu/s. The highest ramp rate considered in the study is difficult to achieve nowadays, but it is expected that the future WPPs will achieve it easily.

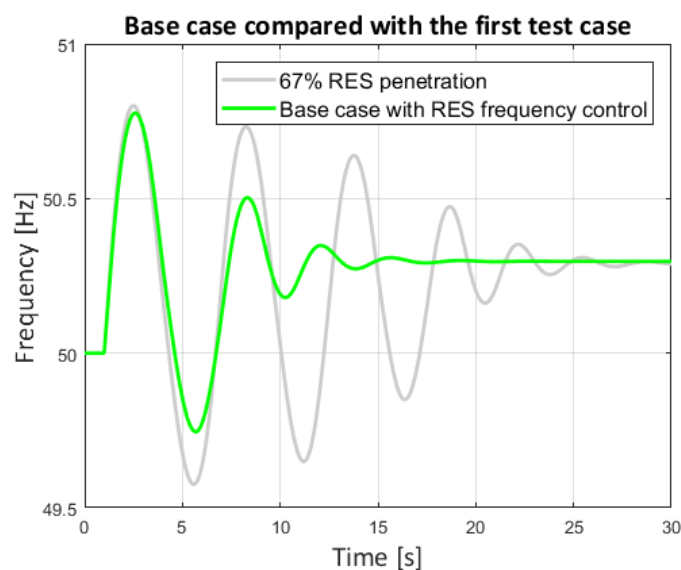


Figure 5.2 Comparison between the base case and the test case with the same RES penetration

For the first test case, the penetration is maintained and the must-run units are replaced by CHP and DCHP, losing part of the inertia that the must-run were supplying. The frequency excursion for the base case with RES frequency control and the first test case (67% of RES penetration) for the same droop and ramp rate parameters can be seen in Figure 5.2.

It is clear in Figure 5.2 that the inertia lost by the must-run replacement has big effects on the power system response, even if the system runs with the same parameters, the same power online and the same RES penetration. The maximum instantaneous frequency (maximum instantaneous deviation or frequency peak) is higher in the first test case than in the base case, but the notable difference between the two simulations is the oscillations in the frequency excursion. The oscillations are caused by the slow reaction of the power system compared with the current inertia online in the grid. Then, the power system can operate without the must-run units, but the droop and ramp rate are studied to find the technical capabilities and limitations when running without these power plants. In further studies, the virtual inertia is found as a good solution to reduce these oscillations. In Figure 5.3, the system is stressed reducing the inertia by increasing the RES penetration and it is tested for 0,5 pu/s ramp rate and 0,04 pu droop.

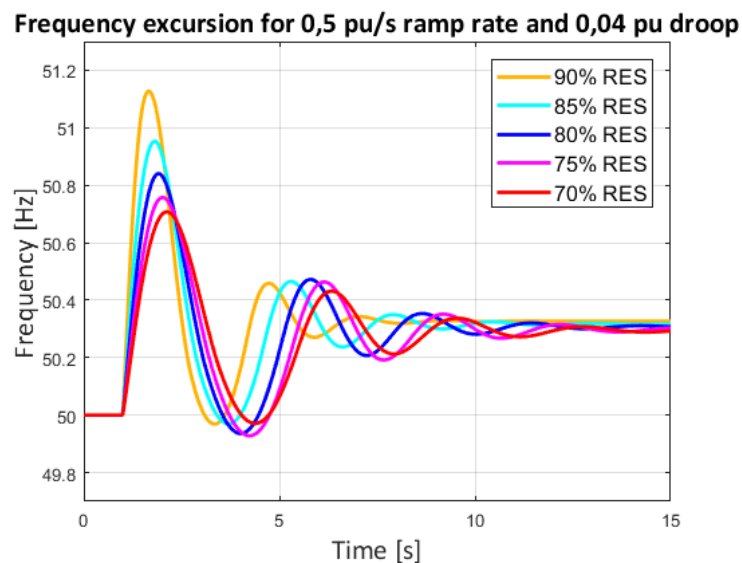


Figure 5.3 Frequency excursion for 0,5 pu/s ramp rate and 0,04 pu droop by RES penetration

The simulations reveal that the frequency excursion and the stabilization time are faster when the RES penetration increases, hence, the inertia decreases by the replacement of CHP and DCHP capacity. The WPPs and SPVSs can deliver power faster than the conventional power plants and this is why they can achieve a faster response and also a low stabilization time. However, the maximum frequency deviation is increasing with the RES penetration, as expected when the inertia is reduced. Moreover, the difference

between the frequency peak in each simulation by the same ramp rate and droop is increasing with the RES penetration, despite the difference in the RES penetration is kept constant in 5% for each test case.

Taking all the maximum instantaneous frequency points reached in the simulations changing the ramp rate and the droop and bringing all these points into a surface for each penetration allows to make the 3D Figure 5.4.

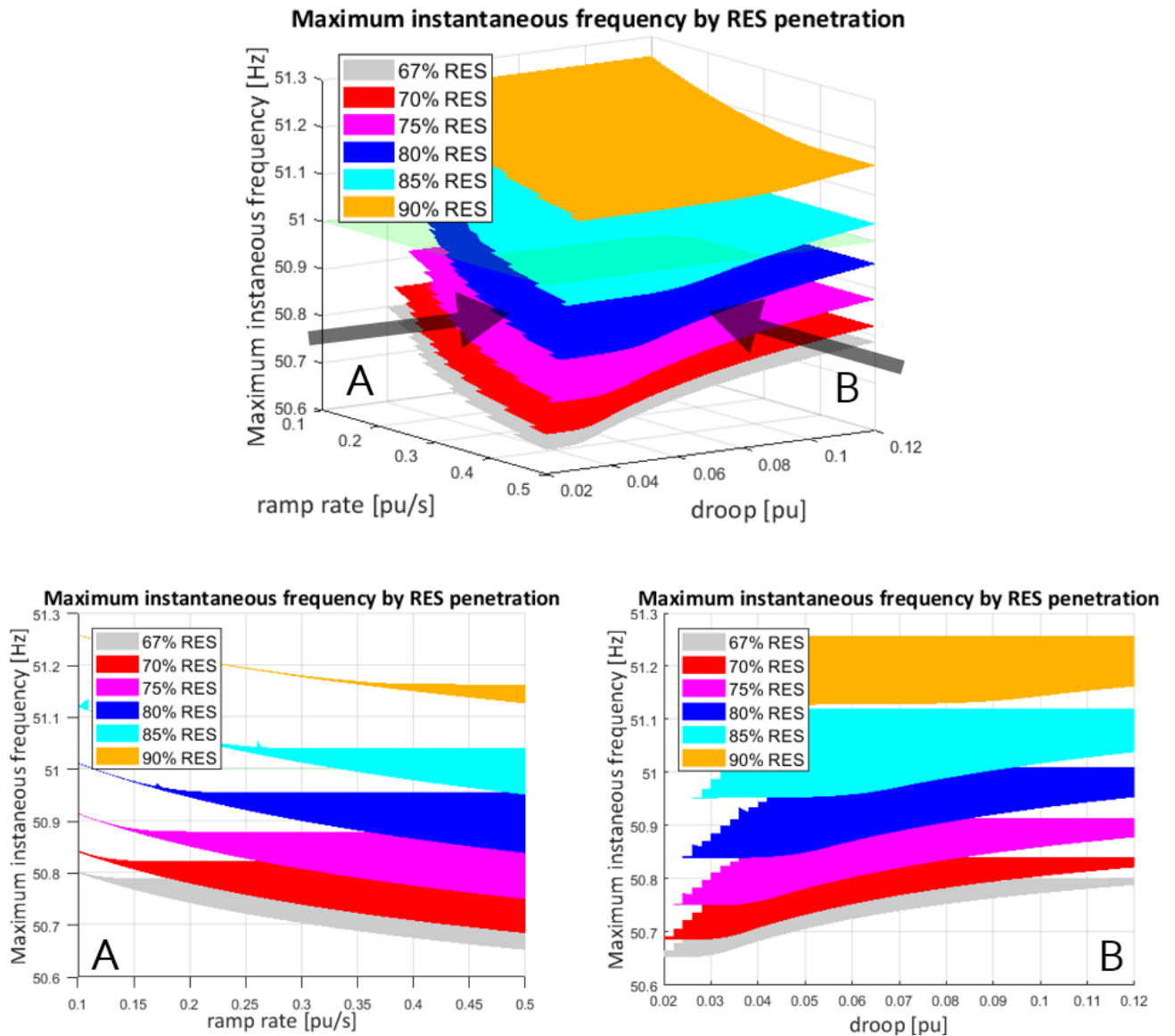


Figure 5.4 Maximum instantaneous frequency by ramp rate, droop and RES penetration

Figure 5.4 is shown in 3 different perspectives to improve its understanding: one 3D perspective where a global overview can be seen and two projections, a frequency-droop projection is shown by 0,5 pu/s ramp rate and a frequency-ramp rate projection by 0,02 pu droop. The highest maximum instantaneous

frequency for each test case is reached for low values of ramp rate. When the ramp rate increases, the maximum instantaneous frequency increases with the droop. The higher the droop is, the higher the maximum frequency will be. It makes sense because the higher is the droop and the lower is the ramp rate, the slower is the response of the power plants against the frequency deviation and it leads to increase the maximum frequency deviation. Also, the oscillations in the frequency excursion increase for low droop values when the ramp rate is not high enough. This happens because the frequency controller with low droop tries to calculate a fast change in the power output of the WPP, but the power plant has a slower reaction by the ramp rate that limits the rate of change of the power. This fact, together with the delay in the frequency controller, desynchronises the frequency deviation with the change in the power output and it leads to increase the oscillations. High ramp rates are needed for the usage of low droops.

In the frequency-ramp rate projection, a decrease on the maximum frequency is observed when the ramp rate raises. What is more, it can be seen a frequency band covered by each RES penetration that has a relation with the second projection of frequency-droop. In this other projection, an increase in the maximum frequency is seen when the droop is increasing and this is more predominant for lower RES penetration tested. The thickness of the frequency bands covered in the projection of the left is the aggregated points that are achieved for all the droops tested by a given ramp rate. By the same reason, the thickness of the bands in the right projection is the aggregated points that are achieved for all the ramp rates with a fixed droop.

The thickness of the lines in the right projection increases with the ramp rate. For low values of ramp rate, this parameter limits the maximum frequency deviation and the droop affects only on the oscillations of the frequency excursion. For high values of ramp rate, the droop is the one that starts limiting the frequency excursion. The thickness is bigger for the 67% RES penetration and it covers less frequency while the penetration raises. This means that the droop control is more important for low RES penetration, because the system is slow enough so the ramp rate does not affect in the same level than the droop. For high RES penetration, the ramp rate is the parameter that limits the maximum frequency deviation, diminishing the sensitivity on the frequency droop. The higher ramp rate the WPPs can achieve, the lower droop can the frequency controller perform and the maximum instantaneous frequency is decreased.

To provide more understanding, Figure 5.5 is shown. Two zones can be identified easily: the zone where the limiting parameter is the ramp rate and the other where it is the droop. For a given ramp rate, the maximum instantaneous frequency is constant from low droop values until a limit point where the ramp rate does not affect to the response. Then, the maximum frequency is constant when increasing the ramp rate for a fixed droop. The higher RES penetration, the less sensitivity can be seen for the droop.

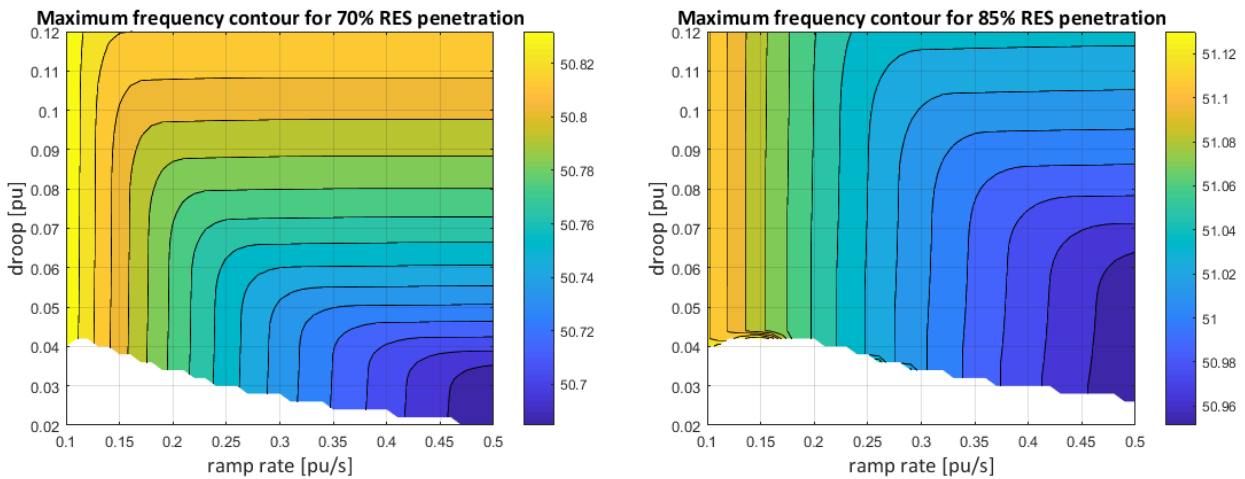


Figure 5.5 Maximum frequency by droop and ramp rate in 70% and 85% RES penetration

The points that are not plotted in all the figures are simulations that the frequency excursion became unstable or had the maximum frequency out of the range given these specific parameters, so a defence plan would be needed. An 85% of RES penetration can be achieved but only for a range of values that can be seen in the 3D Figure or in the contour plots for the values under 51Hz. Higher RES penetrations will not accomplish the goal of maintaining the frequency under this limit.

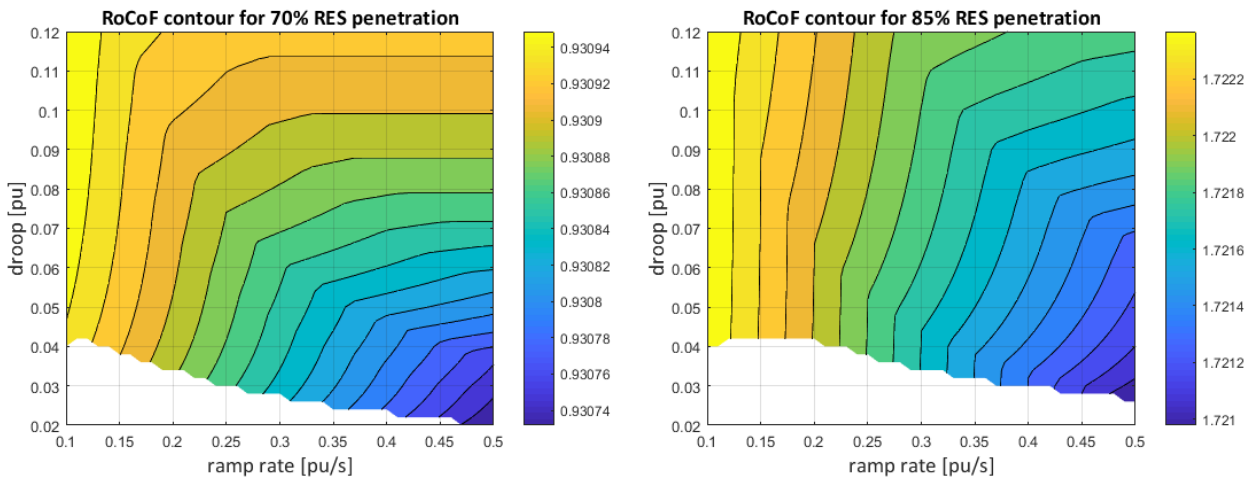


Figure 5.6 RoCoF contour plot by droop and ramp rate in 70% and 85% RES penetration

The RoCoF also increases with the RES penetration and the highest RoCoF appears during the first seconds from the introduction of the outage. The power system response at the first seconds after an outage is called inertial response. The RoCoF for 70% and 85% test cases are shown in Figure 5.6. The contour plots presented are similar to the Figures displayed for the maximum instantaneous frequency, so the recommendations to control the frequency deviation can be valid to control the RoCoF as well. For the 85% RES penetration test case, the RoCoF is below 2,5 Hz/s so the generators will not disconnect either by

maximum frequency or RoCoF limit. Although, the differences observed changing the droop or the ramp rate cannot be compared with the difference from one RES penetration to another. An increase of 15% on the RES penetration (70-85%) leads the RoCoF to almost double its value. So, the strong sensitivity for the RoCoF is related with the system inertia.

*Recommendations on the droop*

*Table 5.1 Recommended droop for WPPs by RES penetration and ramp rate performed*

<b>RES Penetration [%]</b>	<b>Ramp rate [pu/s]</b>	<b>Droop [%]</b>
<b>67</b>	0,1	12
	0,2	6
	0,3	4
	0,4	3
	0,5	2
<b>70</b>	0,1	12
	0,2	7
	0,3	4,5
	0,4	3,5
	0,5	2
<b>75</b>	0,1	12
	0,2	7,5
	0,3	5
	0,4	4
	0,5	3
<b>80</b>	0,15	12
	0,2	9,5
	0,3	6
	0,4	4
	0,5	3,5
<b>85</b>	0,35	7
	0,4	6
	0,5	4

Some recommendations are presented to set the droop by RES penetration and ramp rate. To avoid unnecessary oscillations on the frequency excursion and ensure the lowest instantaneous frequency for each RES penetration test case, the droop setting chosen is the one in the edge between the two zones

found: the ramp rate dependent and the frequency droop dependent. In Table 5.1, these recommendations are summarized.

The droop indicated in Table 5.1 is chosen by direct inspection of the plots done in the study. A certain variation ( $\pm 0,5\%$ ) would also provide a good performance on the frequency control. Droops below these limits will produce more oscillations leading to instabilities if it is too low. Droops above the indicated will lead to an increase in the frequency peak of the response and also the steady-state value of the frequency after the imbalance. Also, very low ramp rates are not achievable for 80 and 85% of RES penetration because the performance reaches a maximum instantaneous frequency above 51 Hz and they are not values within the design limits.

### 5.3. Study on the virtual inertia implementation

A similar study is done, but now, the virtual inertia is implemented at the frequency controller of the WPP model.  $K_d$  is the parameter that refers to the gain of the virtual inertia and it is expressed in pu. In Figure 5.7, the system is tested in 67% RES penetration and different inertia gains are compared with the frequency excursion of the base case and the simulation without virtual inertia.

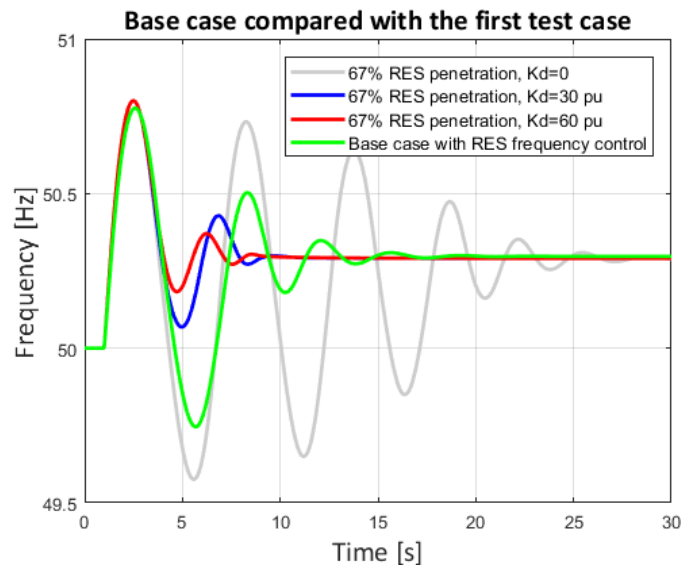


Figure 5.7 Frequency excursion for the base case and 67% RES penetration by virtual inertia gain ( $K_d$ )

The simulation given by the parameters of the base case with the virtual inertia activated does not affect the maximum frequency reached in the simulations. However, the virtual inertia reduces the oscillations of the response achieving even better attenuation than the performed in the base case where the inertia was

higher with the must-run. Hence, the virtual inertia allow the WPPs to control the oscillations of the frequency excursion providing inertial response and allowing the power system to handle faster frequency excursions in low inertia without the must-run units.

In Figure 5.8, the maximum frequency deviation with ( $K_d=60$ ) and without ( $K_d=0$ ) virtual inertia implemented is shown and it can be seen how the maximum deviation is reduced for high ramp rates. Two zones were identified in the previous study: the zone where the maximum frequency was dependent on the ramp rate and the zone where it was dependent on the droop. The virtual inertia is able to reduce the maximum frequency deviation only in the droop dependent zone. The sensitivity of the maximum instantaneous frequency on the droop is almost lost when implementing the virtual inertia, if the gain is high enough, as it can be seen in Figure 5.8 b).

Other studies, like [23], show that for a low virtual inertia gain, 0 to 5 pu, the maximum frequency deviation is considerably reduced. However, there is not a big reduction between two high values like 30 and 60 pu. When the RES penetration is set to a low value, the difference between a virtual inertia gain of 30 and 60 is more significant than in a high RES test cases. For high RES test cases, the power reference is curtailed by the ramp rate limiter and apparently big values of virtual inertia perform the same maximum frequency deviation. However, the oscillations of the frequency excursion are dependent on the virtual inertia and the droop.

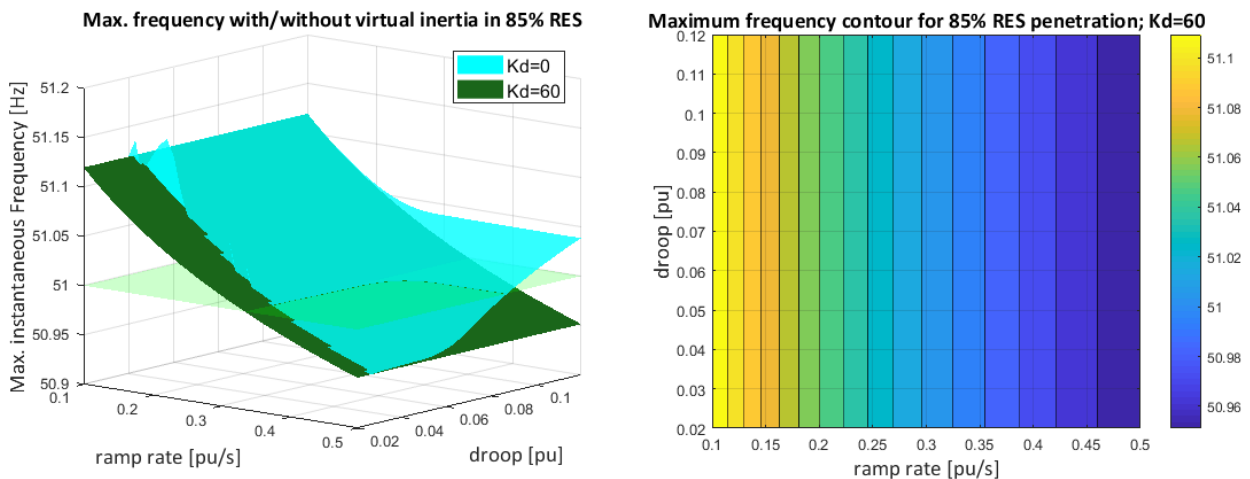


Figure 5.8 a) Maximum frequency reached in every simulation with and without virtual inertia. b) Maximum frequency contour plot with virtual inertia ( $K_d=60$ )

Figure 5.9 shows the effect of the virtual inertia gain for 67% of RES penetration for a gain value for the virtual inertia of 5 and 30 pu (a gain of 60 pu for the 67% test case perform a contour plot identical to the 85% test case showed in Figure 5.8 b)).

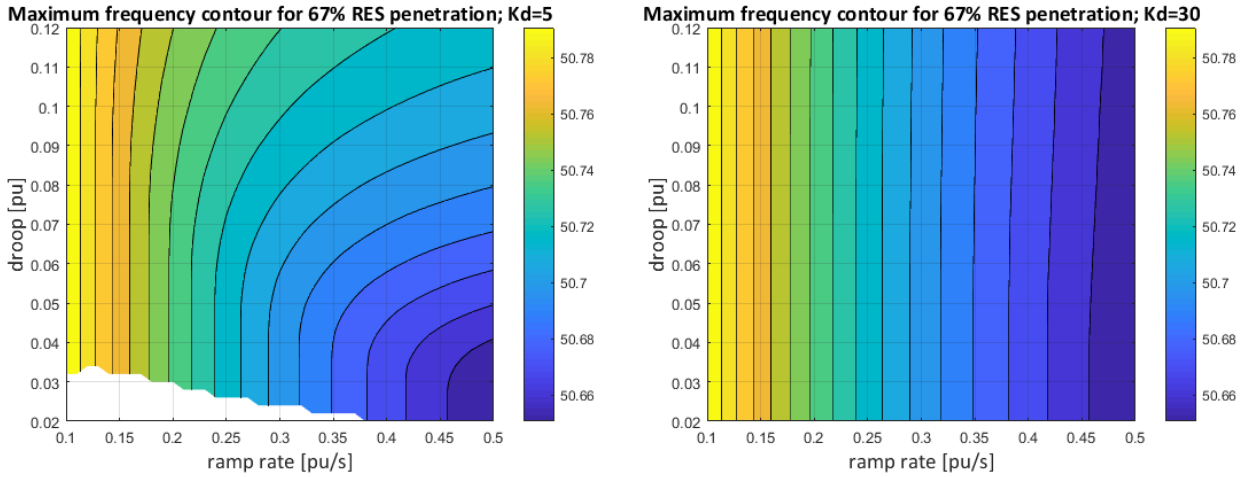


Figure 5.9 Maximum instantaneous frequency in 67% RES penetration by virtual inertia gain

Avoiding the sensitivity on the droop for the maximum instantaneous frequency allows to have more flexibility in the power system. Apart from the reduction in the oscillations of the excursion when the WPP controller is upgraded with virtual inertia, enabling this performance ensures that the maximum instantaneous frequency will be constant for every droop given a ramp rate. Hence, an error on setting the droop is not a critical issue. The power system increases its robustness to this problem.

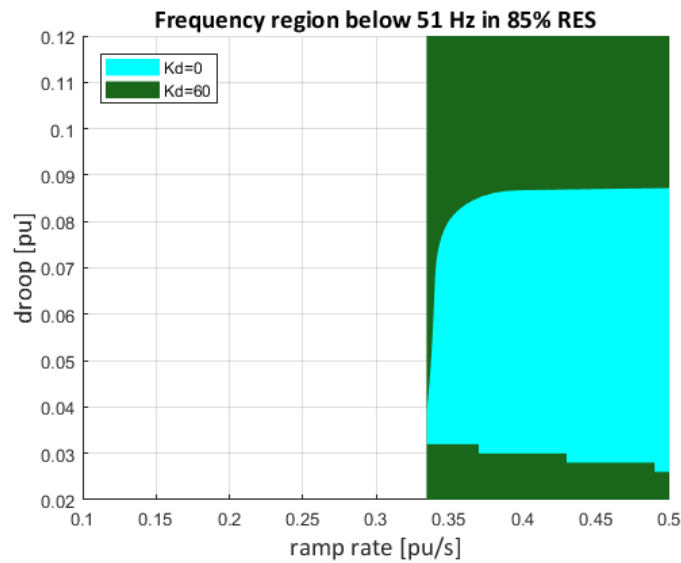


Figure 5.10 Area with maximum frequency below 51 Hz by virtual inertia in 85% RES penetration

The area of available points that maintain the frequency below 51 Hz is presented in Figure 5.10 where it can be easily noticed that the area below 51Hz with virtual inertia completely covers the area with no virtual inertia. However, an increase on the RES penetration is not found on this study. So, an 85% is still reachable as in the previous study and 90% performs peak frequencies out of the design limits.

Even if the sensitivity in the droop for the maximum frequency deviation is avoided, this parameter is still important on the attenuation of the frequency excursion as it can be seen in Figure 5.11 for 70 and 85% RES penetration. This means that too low droops will lead to an increase of the oscillations, but a lower steady-state frequency value. Too many oscillations on the frequency excursion might not be desirable as well.

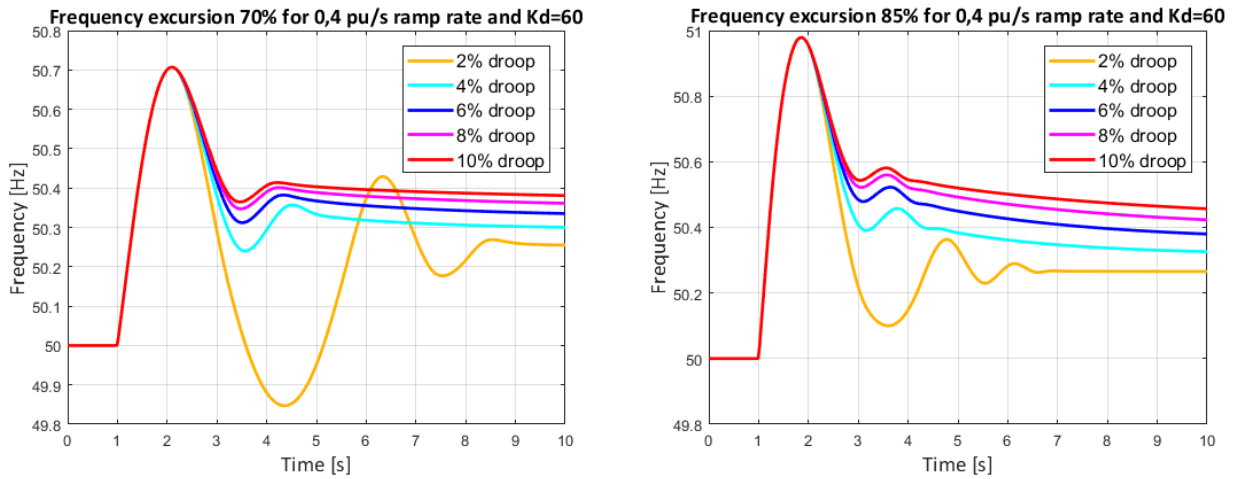


Figure 5.11 Oscillations in the frequency excursion by using a too low droop

As it happened with a too low droop when the ramp rate was low in the previous study, a too high gain in the virtual inertia can cause a little increase in the oscillations when the ramp rate limits the power reference calculated in the frequency controller. These increase on the oscillations appears as a consequence of the delay between the frequency measurement and the change of the power output. Too high gains in the virtual inertia lead the power reference in the frequency controller to change too fast for the ramp rate performed and the delay on the frequency controller cause these little oscillations. As an example of these fact, Figure 5.12 shows this effect for 80% RES penetration. This fact shows that the gain for the virtual inertia has to be controlled in a proper value. Gains between 30 and 60 resulted high enough to eliminate the droop sensitivity and perform well frequency attenuation in high RES penetration.

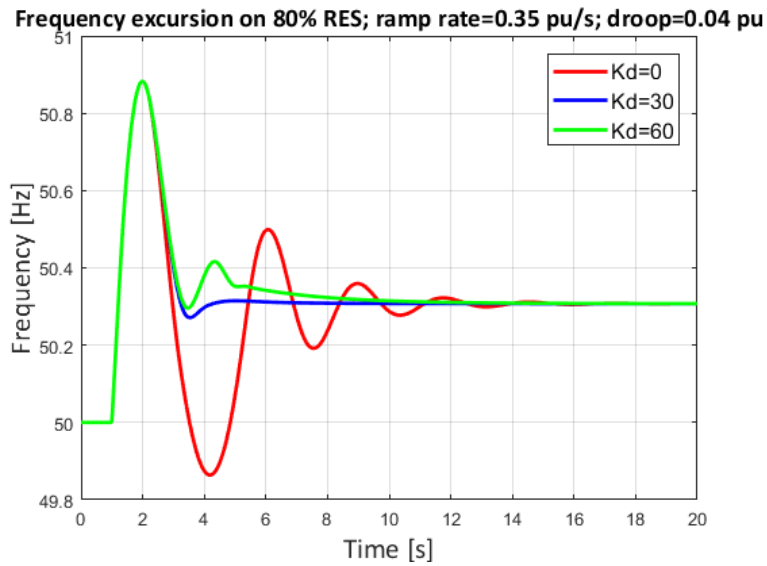


Figure 5.12 Frequency excursion in 80% RES penetration for 60 pu, 30 pu and 0 gain for virtual inertia

The virtual inertia also helps with the maximum RoCoF achieved in the simulations as it does with the maximum instantaneous frequency and the reduction of the sensitivity on the droop. The sensitivity on the ramp rate for the RoCoF dominates over the sensitivity on the droop when the virtual inertia gain is sufficiently high (30-60 pu). The RoCoF increases with the RES penetration and, in Figure 5.13, the RoCoF for 85% RES penetration with and without virtual inertia is shown for a virtual inertia gain of 60 pu. The same conclusion reached for the maximum instantaneous frequency is valid for this parameter: the use of the virtual inertia is advisable, increasing its importance, when the RES penetration increases.

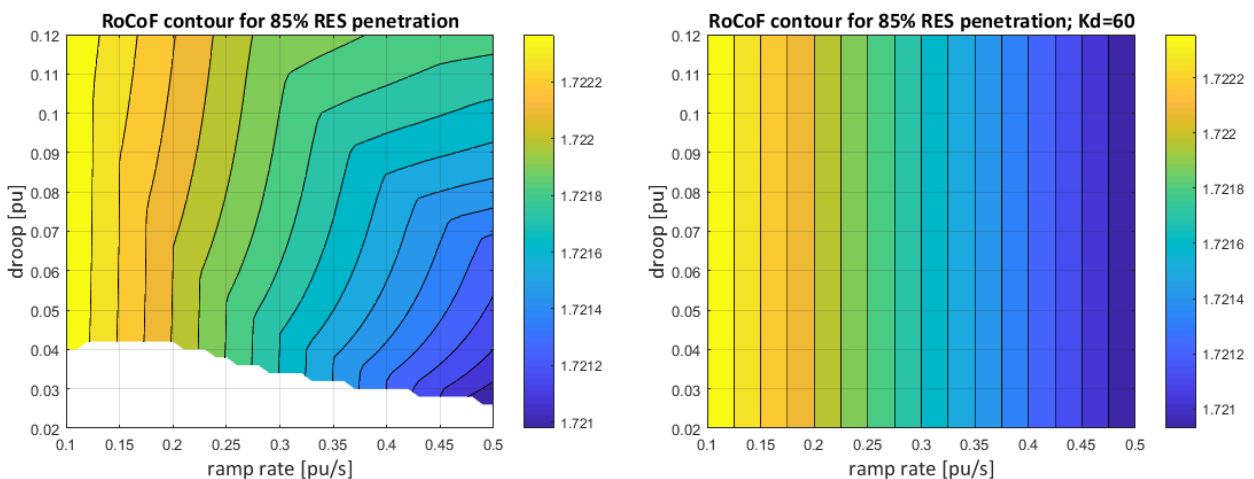


Figure 5.13 RoCoF contour plot for 85% RES penetration with and without virtual inertia (Kd=60)

## 5.4. Study on frequency support of the HVDC cross-border connections

The previous analysis explores the capabilities of the WPP to provide primary frequency control coordinated with the composition of the rest of the power system given a scenario based on the islanding of DK1. The HVDC interconnections of DK1 to neighbour countries, and the Great Belt that is connected to DK2, are considered to operate with almost all the capacity focused on exporting energy under high wind scenario. Also, the participation in the frequency control of these HVDC connections is not considered in the previous studies, so they are explored in this section.

In this study, the WPP model is implemented with the virtual inertia online in a high value so the frequency excursion has only sensitivity on the ramp rate and not on the droop. The rest of the parameters are kept in their standard range as it can be seen in the appendix. In this scenario, where an overfrequency event is studied, the HVDC connections are supposed to increase the power exported so the excess of generation disappears. Hence, the HVDC connection model is considered as an aggregated model of all the connections and a total capacity available is established in order to increase the power exported. A market model is needed to confirm if this power reserved in the connections is a cheaper solution than leaving a generator to trip. However, defence plans including HVDC participation are already in use, so it is a possible scenario. Still, by its fast change in their power flow, the HVDC contribution is studied so they might increase its importance in the future for frequency control purposes in a highly interconnected power system exporter of RES generation.

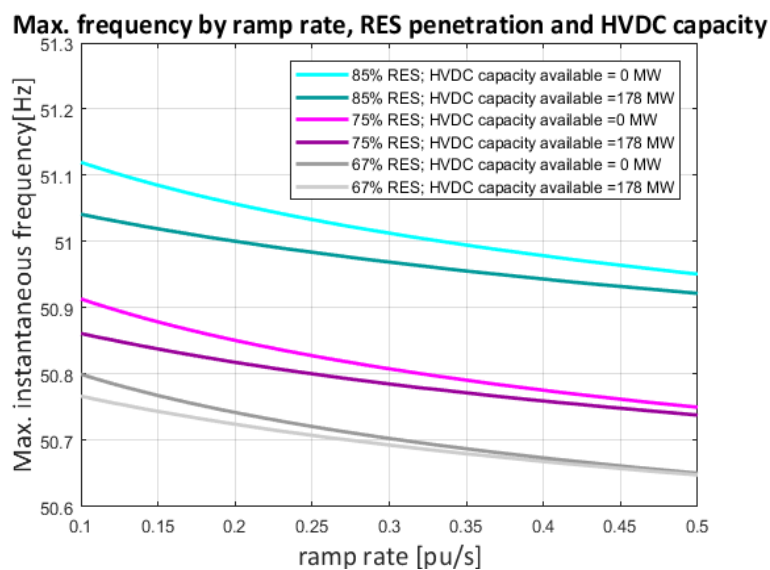


Figure 5.14 Maximum instantaneous frequency by ramp rate, RES penetration and HVDC capacity

In Figure 5.14, the maximum instantaneous frequency is plotted by the ramp rate when the imports are cut down. This means that 178 MW of power capacity is available for the HVDC connections to downgrade the power exchanged. It is thought this measure before reserving HVDC capacity from the exports because it is supposed that cutting the imports is cheaper than curtailing the power that can be exported.

When the ramp rate is low, the support from the HVDC reduce the maximum frequency deviation considerably. The difference in the maximum instantaneous frequency between the simulations with and without HVDC support decreases when the ramp rate is set in high values. Moreover, when the RES penetration increases, the difference in the peak frequency between the simulations with and without HVDC support increases as well. These behaviours are related to two concepts: the velocity of the system response, obtaining less reduction of the maximum deviation for higher ramp rates, and how fast the response should be when the system inertia goes down, more significant reduction on the maximum frequency when decreasing the inertia by increasing the RES penetration.

A low ramp rate on the WPPs makes the response of the system slower, what leads to a higher maximum frequency. The HVDC increases the power exported faster than the response of the power system downregulating the generation and this makes the system to reach lower values for the frequency. When the ramp rate increases, the response of the power system is faster and the velocity of the power dispatched is approaching the fast deploy of the HVDC interconnections. This fact makes that the difference on the maximum instantaneous frequency decreases for high ramp rates. Nevertheless, when the RES penetration is increasing and the inertia goes down, a faster response to frequency deviations is needed and the HVDC support raise its importance with the increase of the RES penetration as it can be seen in Figure 5.14.

To sum up, HVDC connections are found as interesting devices to provide frequency control when the system inertia decreases due to an increase of the RES penetration. The importance of adding HVDC support to the system increases with the RES penetration as lower values of maximum frequency are reached. What is more, the HVDC frequency support is also more important when the ramp rate performed by the WPPs is low because these devices can make the system response to be faster. Coordinating the HVDC support with the power system allows to increase the penetration of RES.

However, the HVDC available capacity reserved for frequency control cannot be too high because of economic problems, where leaving too many reserves would make the system operation expensive. For frequency control purposes, if there is too much available capacity dispatched, the system can present high oscillations, as it can be seen in Figure 5.15 for a HVDC capacity of 300 MW. The system maximum

frequency deviation decreases when increasing the HVDC available capacity, but oscillations on the frequency excursion should be considered. By modelling the HVDC connections as an emergency bloc, all the available power will be dispatched in short time. Thus, for outages smaller than the available capacity in the HVDC interconnections, an overfrequency problem will be lead to an underfrequency problem. For high RES test cases, alternative control strategies to create primary frequency control with these devices should be contemplated to avoid the problems of dispatching too many available power when the HVDC connections are modelled as an emergency block.

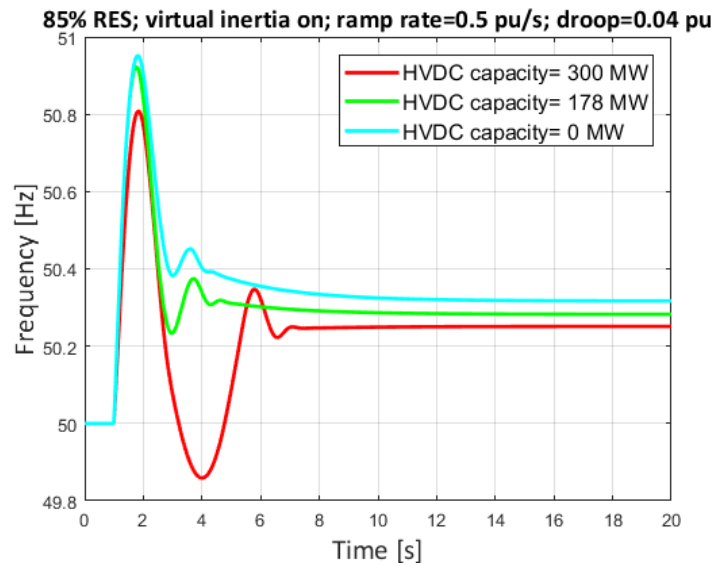


Figure 5.15 Frequency excursion in 85% RES penetration by HVDC capacity available

## 5.5. Study on the delay in the measurement and communications

The last key parameter that is tested by its influence on the frequency control is the delay on the measurement and communication of the system frequency from the point of common coupling to the frequency controller or to the speed governor, depending on the power plant. For CHPs or DCHPs, this time delay is referred to the direct measurement of the frequency and the communication to the speed governor that is based on an 80-100 ms measuring period as described in the grid code. For WPPs and SPVSSs, the time delay is established on 80-100 ms as described in the grid code for these type of power plants as well, but the communications are more complicated than in the conventional power plants. This is because the WPP governor has to communicate the power reference with each WT governor, so the delay can increase easily if a problem happens.

A reduction in the peak frequency seems logic if the delay time in the measurement and the communication is reduced. However, this is not considered in this study because a reduction in the measurement time might not be possible for a correct measurement of the frequency as it is done by taking the mean value calculated during this period. A reduction on the time measurement might bring to a wrong calculation of the mean frequency of the grid.

On the other hand, an increase of the time delay will lead to an increase in the peak frequency, but this study is done to enhance the understanding of the consequences of a problem in this delay. The study is done increasing the time delay of 100 ms, considered the base time, to 200 and 300 ms, 2 and 3 times the base time respectively. In Figure 5.16, the maximum frequency deviation is plotted for a high RES penetration and for a low RES penetration.

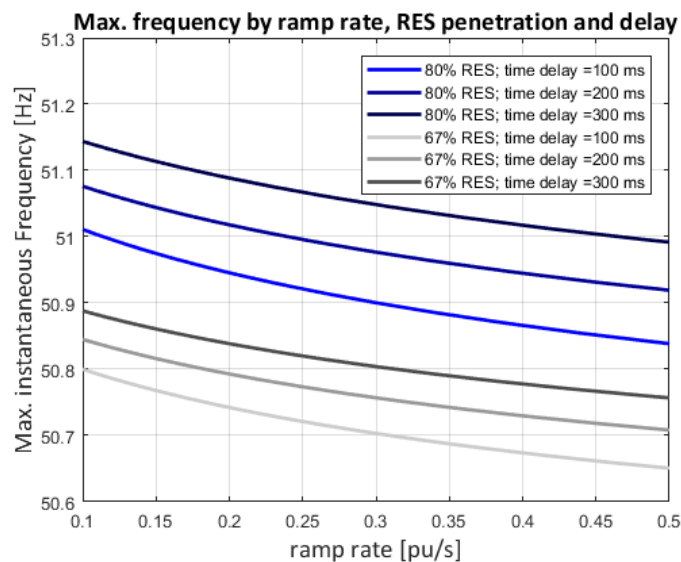


Figure 5.16 Maximum frequency deviation by ramp rate, RES penetration and time delay

The maximum instantaneous frequency increases when the time delay is enlarged. The frequency peak seems to change with a constant value when the delay is increased. However, the difference between one curve and another has a slight increase when the ramp rate is high than when it is low. This is the opposite behaviour than the observed in the HVDC interconnections where the difference was high in low ramp rates rather than in high ramp rates. Furthermore, the maximum instantaneous frequency increases a lot when the delay increases in a high RES test case. However, this difference is less prominent in the lower RES test cases. This fact can be explained relating the delay with the inertia of the grid. With low RES penetration, high inertia is online in the system so the delay does not affect much because of the slow frequency excursion. On the other hand, with high RES penetration, the frequency excursion reaches high

values of frequency faster because of the low inertia, so a change in the delay is more significant and can cause the system to achieve undesirable frequency peaks leading to a defence plan. An 80% of RES penetration is almost not achievable as it can be seen in Figure 5.16 when the delay increases from 100 ms to 300 ms, where an 85% was achievable with the base time delay of 100 ms. What is studied increasing the delay, can also be extrapolated to understand the behaviour if the frequency delay could be reduced. For a high RES test case, a small decrease on the time delay can cause a big decrease on the frequency deviation, but a smaller decrease on the maximum instantaneous frequency if the system is in a low RES test case.

The time delay not only affects the maximum instantaneous frequency but on the frequency excursion. In Figure 5.17, two frequency evolutions are shown with the difference on the virtual inertia implementation.

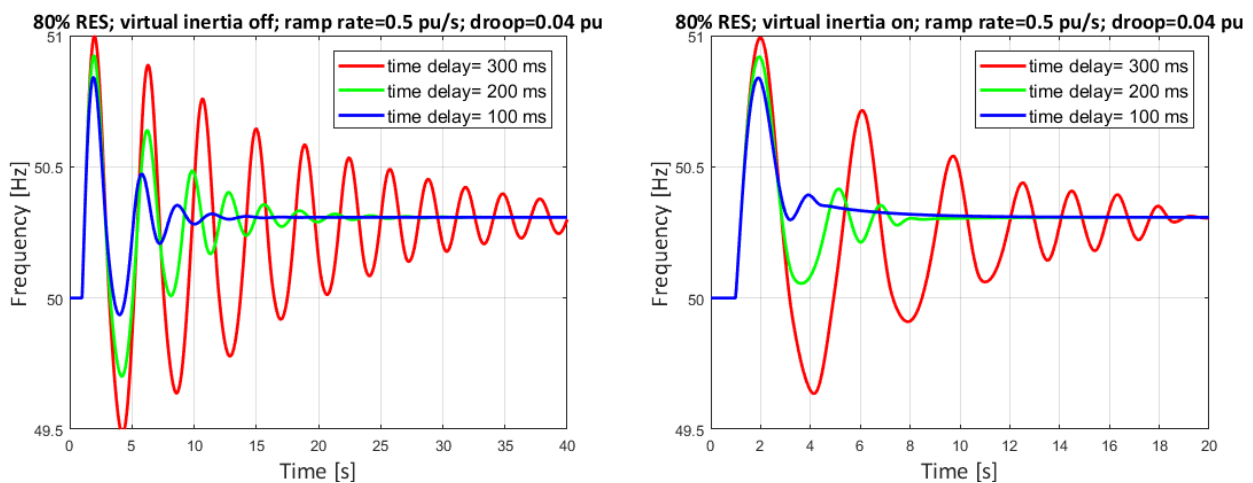


Figure 5.17 Frequency excursion in 80% REs penetration with and without virtual inertia

In Figure 5.17, the Figure on the left shows three frequency evolutions where the delay is increased and the virtual inertia is offline. The three frequency excursions are dominated by the oscillations and the stabilisation time increases a lot with the increase of the delay. These oscillations lead to a continuous change in the power output of the power plants, so, many oscillations in the frequency excursion are not desired. These oscillations are not appearing with that importance in low RES test cases, so the problem increases its importance when the inertia is reduced. This parameter results on being a critical value to consider in the frequency control when a high RES penetration is tested. In the Figure of the right, the virtual inertia of the WPP is online in a high value, where the sensitivity for the droop disappears. The excursion is performing fewer oscillations and the stabilisation time is also lower than in the simulations without virtual inertia. This means that the virtual inertia increases the robustness of the system against the delay, improving the frequency control in case that the delay raises.

## 5.6. Summary

The main points of this chapter are summarised in the following list:

- The base case with all the inertia online in the grid is established and the impact of the RES participating or not in the frequency response is shown so the difference is clearly noticed in the two different simulations.
- The first sensitivity study of the power system explores the effect of the ramp rate, the droop and the RES penetration on the frequency control. The power system can operate without must run units within some limitations and some recommendations on the droop are displayed according to the results. Low RES penetration allows the system to have lower droops than for high RES penetration. High ramp rates performed admits lower droops than low ramp rates. 85% of RES penetration can be achieved for a restricted range in the droop for this particular event without the need of a defence plan, but the ramp rate needs to be higher than 0,3 pu/s.
- The same recommendations than in the droop study can be applied with the virtual inertia online. However, a high enough gain in this setting (30-60 pu) allows the droop to be higher without affecting the maximum instantaneous frequency but increasing the frequency deviation in steady state. Too low droops should not be chosen in high RES scenarios, even if the peak frequency is accepted, because of the increase in the oscillations and low attenuation of the frequency excursion in the power system. The virtual inertia is crucial in high RES penetration to increase the robustness of the system against these oscillations and provides flexibility to the power system on choosing the droop.
- The HVDC cross-border links are tested to allow them to perform frequency control and interesting capabilities are found from these facilities by its converter-based structure. A fast deployment of power reserves is achieved and a reserve plan for the HVDC connections will help the power system to add more RES penetration and handle power imbalances with low inertia. A study on the reserve plan is needed because the power dispatched should be in accordance with the outage, otherwise a big amount of power dispatched can produce oscillations in the frequency excursion.
- The delay on the measurement and communication of the frequency is also tested and an increase in its importance is found when the RES penetration augments. When the system inertia is low, there is a need for faster response against frequency deviations and the delay hinders the

performance of the power system. However, by technical reasons, this delay is needed to measure and filter the frequency properly, so, the delay has to be as low as possible. When the delay increases, it takes more time to mitigate an imbalance between the generation and the load and the peak frequency reaches higher values. Also, by this desynchronization between the measurement of the frequency and the power output, the attenuation of the frequency excursion will be lower and the system frequency will present non-desired oscillations. The virtual inertia gives robustness to the system and reduces this effect of the delay.

# Chapter 6

## Conclusions and future work

This last chapter summarizes the ideas of the research and the recommendations for every study are included in the following section. Ideas and directions for future work in the topic are also mentioned at the end of the chapter.

### 6.1. Main conclusions

This study “Frequency control in power systems without must-run units” explores the primary frequency control of the western Danish (DK1) power system in 2030 with a high RES scenario where the must-run units are decommissioned. The objective of this study is to answer if the power system can operate without must-run units and under which technical capabilities and limitations. This study is focused on overfrequency events when the power system is islanded as a result of a severe disturbance given by a failure of the alternative current (AC) lines connecting Denmark to Germany. The wind power plant (WPP) capabilities are investigated and sensitivity studies are made to increase the knowledge and understanding of this topic for a power system with extensive RES penetration. Also, the participation of the high voltage direct current (HVDC) interconnections for primary frequency control is tested.

In the following list, the main conclusions of the study are presented:

- The sensitivity studies show that the composition of power plants online in the power system not only has influence on the system inertia of the grid, but to the capabilities to handle a power imbalance. Even if the system inertia is being reduced by decommissioning must-run units, the system can handle a fast frequency excursion because of the RES generation (wind and solar) which can dispatch power reserves faster than the conventional power plants. The key parameters chosen for the study such as the system inertia, the governor droop setting, the ramp rate, the gain of virtual inertia, the measurement and communication delay and the cross-border HVDC support are decisively important in controlling the frequency peak and the frequency attenuation. This research shows that the frequency control can improve its performance varying those parameters independently. However, a proper solution needs to consider all the parameters due to the

different correlations in the primary frequency control. So, both key parameters studied and configuration of the power system are important to understand the frequency control.

- A control of the governor droop setting is needed to ensure a desired primary frequency control. An increase on the RES penetration leads to a need of a faster deploy of frequency reserves to secure the stability of the power system and prevent the generators to trip. The study shows limitations of the power system when exploring the droop and the ramp rate of the power plants to increase the RES penetration in the grid. Choosing always the lowest droop to calculate the fastest power deviation is not a good practice since the system can be unstable for some parameters. A conformity between the ramp rate performed by the power plants and the governor droop setting has to be ensured. If the ramp rate is low, the droop should be high and if high ramp rates are achieved, the droop can be low. The recommendations given in chapter 4 for choosing the droop by the ramp rate and the RES penetration improve the recommended standard value of 4% given in the grid code by Energinet.dk. The low RES penetration test cases allow the system to have lower governor droop setting in the frequency controller, while this parameter needs to increase reaching high values to allow a power system operation with high RES penetration. However, in the higher RES penetration test cases, too high droop forces the system to have a non-desirable instantaneous frequency peak, so the droop has to be chosen in a proper range. What is more, the decrease in the inertia demands high ramp rates to power plants so the primary frequency control can be faster. The maximum RES penetration found with a frequency peak below 51 Hz is around 85% and it can only be achieved for a small range of ramp rates and droop values. A market model is needed to verify if a defence plan such as a tripping strategy of generators is costlier than curtailing the RES penetration.
- Nowadays, the primary frequency control described in the Danish grid code is based on the governor droop setting. However, very high RES penetration can only be achievable for high ramp rates in the WPP, and generally, in the power plants online that provide frequency control. The droop value is being limited when the RES penetration goes above 80%. The virtual inertia has been proved as an advisable setting to implement when the RES penetration is low by its help in the attenuation on the oscillations of the frequency excursion and in the frequency peak for high droops. For low droops in high inertia, the virtual inertia provides low performance. On the other hand, with high RES penetration, higher droops are needed so the virtual inertia is considered crucial to control the maximum frequency deviation and the attenuation of the frequency

excursion. The virtual inertia increases the power system flexibility and enables the usage of higher droops when needed without increasing the maximum frequency deviation.

- In a future scenario where a power system based on renewables will be able to export a big amount of power to neighbour countries, the risk of large imbalances increases by the failure of the cross-borders HVDC and AC connections. HVDC cross-border connections are found as interesting devices, for its participation on the primary frequency control, to handle power imbalances in a high RES scenario because of the fast deployment of reserves that they can achieve. HVDC cross-border connections are recommended to increase its importance in the future by providing ancillary services in high interconnected power systems, where exports and imports are high, rather than only participating as a defence plan. The more HVDC reserves are available and dispatched, the more time is needed to stabilize the system frequency. Thus, a compromise between the reserves dispatched and the imbalance would be needed together with further studies on HVDC dispatch strategies for frequency stability.
- The delay on the measurement and the communication is found as a critical value for the attenuation of the frequency excursion, whether it has its influence on the frequency peak as well. An increase or decrease on the delay will lead to an increase or decrease of the frequency peak, but also a huge effect on the attenuation of the frequency excursion. The delay raises its importance when the system inertia is low. An increment on the delay makes the system response slower and desynchronizes the power output with the measurement of the frequency. This effect increases the time where the imbalance is present on the power system and has big impact on the stabilization time. Keeping the delay in a low value is imperative recommended for an appropriate frequency peak and attenuation of the frequency excursion. The virtual inertia provides robustness to the system and the effect of the delay is lower with this controller active. The virtual inertia increases the attenuation of the frequency excursion compared with the scheme without virtual inertia, thus, these are even more reasons to advice the implementation of the virtual inertia for the frequency controller.

## 6.2. Future work

The research for this project is accomplished within the scope and limitations, but some open questions came across at the end of the investigation. The suggestions for future research are listed below:

- An AC failure completely isolating DK1 is considered as an extreme case for frequency stability. However, the power imbalance can be caused by many sources like load disconnections, errors in wind power forecast, errors in solar photovoltaic forecast, HVDC disconnections, among others. These studies can be done in the future to compliment this research.
- Using aggregated models of the different power plants in the system does not allow to study the power system with a particular configuration for each power plant such as testing different wind speeds in each WPP, studying critical weather conditions, testing the system with de connection/disconnection of generators when a defence plan is needed or considering the congestion of the lines.
- Economic studies can be done in the future to decide which of the proposed recommendations are economically suitable for the market and reduce the costs of the power system operation.
- DK1 would be a net exporter country so most of the time DK1 will be exporting power. Despite the power system would import energy when there is low wind power available, underfrequency studies can be done to identify the maximum RES penetration achievable coordinated with the load shedding.
- The participation of RES in secondary control can also be a subject for future investigation. This fact would allow the power system to ensure ancillary services with WPPs and to increase the flexibility of the power system.
- This project is focused on frequency stability and further studies can include other developments for voltage and rotor angle stability for high RES penetration in future power systems. The reactive power can be added to the system to perform the two types of stabilities mentioned as well.
- The HVDC cross-border connections are found as interesting facilities to help the power system with primary frequency control in high RES future scenarios. For full converter power sources, such as a solar photovoltaic system (SPVS), a fast ramp rate in the power dispatched is achievable and the primary frequency control can counterbalance the loss of inertia. Additional studies on innovative frequency control strategies for HVDC links are recommended as it would increase its importance for power balancing together with the RES generation.

## References

- [1] pwc, "Moving towards 100% renewable electricity in Europe – North Africa by 2050," [Online]. Available: <http://www.sefep.eu/activities/projects-studies/2011-05-11-100-%20renewables.pdf>. [Accessed 21 06 2017].
- [2] International Energy Agency, "Electricity generation by fuel, Denmark," [Online]. Available: <https://www.iea.org/stats/WebGraphs/DENMARK2.pdf>. [Accessed 04 04 2017].
- [3] B. V. Mathiesen, H. Lund, K. Hansen, I. R. Skov, S. R. Djørup, S. Nielsen, .... and P. A. Østergaard, "IDA's Energy Vision 2050: A Smart Energy System strategy for 100% renewable Denmark," 2015. [Online]. Available: [http://vbn.aau.dk/files/222230514/Main\\_Report\\_IDAs\\_Energy\\_Vision\\_2050.pdf](http://vbn.aau.dk/files/222230514/Main_Report_IDAs_Energy_Vision_2050.pdf). [Accessed 04 04 2017].
- [4] Danish Energy Agency, "Energy scenarios for 2020, 2035 and 2050," 03 2014. [Online]. Available: [https://ens.dk/sites/ens.dk/files/Analyser/energiscenarier\\_uk.pdf](https://ens.dk/sites/ens.dk/files/Analyser/energiscenarier_uk.pdf). [Accessed 04 04 2017].
- [5] P. Kundur, J. Paserba, V. Ajjarapu, G. Andersson, A. Bose, C. Canizares, .... and V. Vittal, "Definition and Classification of Power System Stability," *IEEE Transactions on Power Systems*, vol. 19, no. 2, pp. 1387-1401, 2004.
- [6] K. Das, P. E. Sørensen, A. D. Hansen and H. Abildgaard, "Integration of Renewable Generation in Power System Defence Plans," *DTU Wind Energy PhD*, vol. 0058, 2016.
- [7] P. Kundur, *Power System Stability and Control*, McGraw-Hill, Inc., 1994.
- [8] NERC, "Reliability Concepts," 19 12 2007. [Online]. Available: [http://www.nerc.com/files/concepts\\_v1.0.2.pdf](http://www.nerc.com/files/concepts_v1.0.2.pdf). [Accessed 21 06 2017].
- [9] ENTSO-E, "Technical background and recommendations for defence plans in the continental europe synchronous area," 26 10 2010. [Online]. Available: [https://www.entsoe.eu/fileadmin/user\\_upload/\\_library/publications/entsoe/RG\\_SOC\\_CE/RG\\_CE\\_ENTSO-E\\_Defence\\_Plan\\_final\\_2011\\_public.pdf](https://www.entsoe.eu/fileadmin/user_upload/_library/publications/entsoe/RG_SOC_CE/RG_CE_ENTSO-E_Defence_Plan_final_2011_public.pdf). [Accessed 06 04 2017].
- [10] P. Didsayabuttra, W.-J. Lee and B. Eua-Arporn, "Defining the Must-Run and Must-Take Units in a Deregulated Market," *IEEE Transactions on Industry Applications*, vol. 38, no. 2, pp. 596-601, 2002.
- [11] California Energy Commission, "Glossary of energy Terms," [Online]. Available: <http://www.energy.ca.gov/glossary/glossary-r.html>. [Accessed 05 04 2017].

- [12] Ercot, "Reliability-Must-Run Procedures," 05 2016. [Online]. Available: [http://www.ercot.com/content/wcm/lists/89476/OnePager\\_RMR\\_May2016\\_FINAL.pdf](http://www.ercot.com/content/wcm/lists/89476/OnePager_RMR_May2016_FINAL.pdf). [Accessed 05 04 2017].
- [13] Danish Energy Agency, "Flexibility in Power System - Danish and European experiences," 10 2015. [Online]. Available: [https://ens.dk/sites/ens.dk/files/Globalcooperation/flexibility\\_in\\_the\\_power\\_system\\_v23-Iri.pdf](https://ens.dk/sites/ens.dk/files/Globalcooperation/flexibility_in_the_power_system_v23-Iri.pdf). [Accessed 05 04 2017].
- [14] ENTSO-E, "Mid-term Adequacy Forecast Edition 2016," [Online]. Available: [https://www.entsoe.eu/Documents/SDC%20documents/MAF/ENSTOE\\_MAF\\_2016.pdf](https://www.entsoe.eu/Documents/SDC%20documents/MAF/ENSTOE_MAF_2016.pdf). [Accessed 05 04 2017].
- [15] Ea Energy Analyses, "Ea (2015): The Danish Experience with Integrating Variable Renewable Energy. Study on behalf of Agora Energiewende.," 09 2015. [Online]. Available: [https://www.agora-energiewende.de/fileadmin/Projekte/2015/integration-variabler-erneuerbarer-energien-daenemark/Agora\\_082\\_Deutsch-Daen\\_Dialog\\_final\\_WEB.pdf](https://www.agora-energiewende.de/fileadmin/Projekte/2015/integration-variabler-erneuerbarer-energien-daenemark/Agora_082_Deutsch-Daen_Dialog_final_WEB.pdf). [Accessed 05 04 2017].
- [16] H. Abildgaard and N. Qin, "Synchronous Condensers for reliable HVDC operation and bulk power transfer," 2015. [Online]. Available: <http://www.ieee-pes.org/presentations/gm2015/PESGM2015P-003046.pdf>. [Accessed 05 04 2017].
- [17] Energinet.dk, "Market Model 2.0 - Final report," 2015. [Online]. Available: <https://www.energinet.dk/SiteCollectionDocuments/Engelske%20dokumenter/El/Final%20report%20-%20Market%20Model%202.0.pdf>. [Accessed 05 04 2017].
- [18] DNV-GL, "Integration of Renewable Energy in Europe," 12 06 2014. [Online]. Available: [https://ec.europa.eu/energy/sites/ener/files/documents/201406\\_report\\_renewables\\_integration\\_europe.pdf](https://ec.europa.eu/energy/sites/ener/files/documents/201406_report_renewables_integration_europe.pdf). [Accessed 05 04 2017].
- [19] W. Prügler, C. Obersteiner, K. Zach, H. Auer, L. Olmos, R. Cossent, J. de Joode, ... and B. Doersam, "Scenarios for DG/RES energy futures on case study, country and European level. Energy Research Centre of the Netherlands," 2009. [Online]. Available: [http://orbit.dtu.dk/files/3791524/Scenarios%20for%20DG\\_RES%20energy%20futures.pdf](http://orbit.dtu.dk/files/3791524/Scenarios%20for%20DG_RES%20energy%20futures.pdf). [Accessed 05 04 2017].
- [20] A. D. Hansen, "Evaluation of power control with different electrical and control concept of wind farm Part 2 – Large systems. Project UpWind," 2010. [Online]. Available: <http://orbit.dtu.dk/files/5246113/UpWind%20part%202.pdf>. [Accessed 05 04 2017].
- [21] A. D. Hansen, M. Altin and F. Iov, "Provision of enhanced ancillary services from wind power plants - Examples and challenges," *Elsevier Renewable Energy*, vol. 97, pp. 8-18, 2016.

- [22] L. Zeni, P. E. Sørensen, A. D. Hansen, B. Hesselbak and P. C. Kjar, "Power system integration of VSC-HVDC connected wind power plants," 2015. [Online]. Available: [http://orbit.dtu.dk/files/116284450/Power\\_system\\_integration.pdf](http://orbit.dtu.dk/files/116284450/Power_system_integration.pdf). [Accessed 05 04 2017].
- [23] I. D. Margaritis, S. A. Papathanassiou, N. D. Hatziargyriou, A. D. Hansen and P. Sørensen, "Frequency control in autonomous power systems with high wind power penetration," *IEEE Transactions on sustainable energy*, vol. 3, no. 2, pp. 189-199, 2012.
- [24] A. Molina-García, I. Muñoz-Benavente, A. D. Hansen and E. Gómez-Lázaro, "Demand-side contribution to primary frequency control with farm auxiliary control," *IEEE Transactions on Power Systems*, vol. 29, no. 5, pp. 2391-2399, 2014.
- [25] A. D. Hansen, M. Altin, I. D. Margaritis, F. Iov and G. C. Tarnowski, "Analysis of the short-term overproduction capability of variable speed wind turbines," *Renewable Energy*, vol. 68, pp. 326-336, 2014.
- [26] ENTSO-E, "TYNDP 2016 Scenario Development Report," 03 11 2015. [Online]. Available: <https://www.entsoe.eu/Documents/TYNDP%20documents/TYNDP%202016/rgips/TYNDP2016%20Scenario%20Development%20Report%20-%20Final.pdf>. [Accessed 27 04 2017].
- [27] G. Yang and O. J. Oleson, "Secure operation of sustainable power system: WP1: future scenario description, system in context and specifications," *iPower Consortium*, 2013.
- [28] Energinet.dk, «Amendment to Energinet.dk's ancillary services strategy,» 2013.
- [29] European Commission, "Establishing a guideline on electricity transmission system operation, final draft version," 2016. [Online]. Available: <https://ec.europa.eu/energy/sites/ener/files/documents/SystemOperationGuideline%20final%28provisional%2904052016.pdf>. [Accessed 15 06 2017].
- [30] J. Merino, I. Gómez, E. Turienzo, C. Madina, C. Iñigo, A. Morch, H. Saele, K. Verpoorten, ... and D. Siface, "SmartNet: Ancillary service provision by RES and DSM connected at distribution level in the future power system, D1.1," 2016.
- [31] S. De Boeck, D. Van Hertem, K. Das, P. E. Sørensen, V. Trovato, J. Turunen y M. Halat, «Review of Defence Plans in Europe: Current Status, Strengths and Opportunities,» *CIGRE Transactions on Science & Engineering*, vol. 5, pp. 6-16, 2016.
- [32] Energinet.dk, "Energinet.dk's ancillary services strategy," 2011. [Online]. Available: [http://kom.aau.dk/project/smartcool/restricted\\_files/2012.11.06-AAU/Energinet\\_Ancillary\\_Services\\_Strategy\\_Aug2011\\_en.pdf](http://kom.aau.dk/project/smartcool/restricted_files/2012.11.06-AAU/Energinet_Ancillary_Services_Strategy_Aug2011_en.pdf). [Accessed 08 06 2017].

- [33] A. Basit, A. D. Hansen, P. E. Sørensen and M. Altin, "Wind power plant system services," 12 2014. [Online]. Available: [http://orbit.dtu.dk/en/publications/wind-power-plant-system-services\(1262239d-fbb2-4df4-8201-72d1b1776358\).html](http://orbit.dtu.dk/en/publications/wind-power-plant-system-services(1262239d-fbb2-4df4-8201-72d1b1776358).html). [Accessed 07 06 2017].
- [34] Energinet.dk, "Technical regulation 3.2.3 for thermal plants above 11 kW," 10 01 2017. [Online]. Available: [www.energinet.dk/EN/EI/Forskrifter/Technical-regulations/Sider/Forskrifter-for-nettilslutning.aspx+&cd=1&hl=ca&ct=clnk&gl=dk](http://www.energinet.dk/EN/EI/Forskrifter/Technical-regulations/Sider/Forskrifter-for-nettilslutning.aspx+&cd=1&hl=ca&ct=clnk&gl=dk). [Accessed 20 05 2017].
- [35] Energinet.dk, "Technical regulation 3.2.2 for PV power plants above 11 kW," 14 07 2016. [Online]. Available: [www.energinet.dk/EN/EI/Forskrifter/Technical-regulations/Sider/Forskrifter-for-nettilslutning.aspx+&cd=1&hl=ca&ct=clnk&gl=dk](http://www.energinet.dk/EN/EI/Forskrifter/Technical-regulations/Sider/Forskrifter-for-nettilslutning.aspx+&cd=1&hl=ca&ct=clnk&gl=dk). [Accessed 20 05 2017].
- [36] Energinet.dk, "Technical regulation 3.2.5 for wind power plants above 11 kW," 22 07 2016. [Online]. Available: [www.energinet.dk/EN/EI/Forskrifter/Technical-regulations/Sider/Forskrifter-for-nettilslutning.aspx+&cd=1&hl=ca&ct=clnk&gl=dk](http://www.energinet.dk/EN/EI/Forskrifter/Technical-regulations/Sider/Forskrifter-for-nettilslutning.aspx+&cd=1&hl=ca&ct=clnk&gl=dk). [Accessed 20 05 2017].
- [37] ENTSO-E, "Total Load Forecast - Month Ahead," ENTSO-E, [Online]. Available: <https://transparency.entsoe.eu/load-domain/r2/monthLoad/show?name=&defaultValue=false&viewType=TABLE&areaType=BZN&atch=false&dateTime.dateTime=01.01.2017+00:00|UTC|MONTH&biddingZone.values=CTY|10Y1001A1001A65H!BZN|10YDK-1-----W>. [Accessed 28 06 2017].
- [38] Energinet.dk, "System Plan 2015," 2015. [Online]. Available: <http://www.energinet.dk/SiteCollectionDocuments/Engelske%20dokumenter/Om%20os/System%20Plan%202015.pdf>. [Accessed 29 05 2017].
- [39] H. Lund, F. Hvelplund, P. A. Østergaard, B. Möller, B. V. Mathiesen, ... and H. H. Lindboe, "Danish Wind Power Export and Cost," 02 2010. [Online]. Available: [http://www.pfbach.dk/firma\\_pfb/ceesa\\_danish\\_wind\\_power.pdf](http://www.pfbach.dk/firma_pfb/ceesa_danish_wind_power.pdf). [Accessed 2016 06 06].
- [40] Techconsult, "Analysis of Wind Power in the Danish Electricity Supply in 2005 and 2006," 10 08 2007. [Online]. Available: <http://docs.wind-watch.org/dk-analysis-wind.pdf>. [Accessed 06 06 2017].
- [41] Paul-Frederik Bach, "German Market Policy Limits Electricity Exchange," 14 04 2015. [Online]. Available: [pfb\\_german\\_market\\_policy\\_limits\\_exchange\\_2014\\_04\\_14](http://www.pfbach.dk/firma_pfb/ceesa_danish_wind_power.pdf). [Accessed 06 06 2017].
- [42] ENTSO-E, "TYNDP 2016 downloads," ENTSO-E, [Online]. Available: <http://tyndp.entsoe.eu/reference/#downloads>. [Accessed 28 06 2017].
- [43] Nordic Operations Development group (NOD), "Evaluation of the ramping restriction in the energy market," 24 09 2010. [Online]. Available: [http://www.statnett.no/Documents/Nyheter\\_og\\_media/Nyhetsarkiv/2010/Ramping%20report.pdf](http://www.statnett.no/Documents/Nyheter_og_media/Nyhetsarkiv/2010/Ramping%20report.pdf). [Accessed 24 06 2017].

- [44] Danish Energy Agency, "Regulation and planning of district heating in Denmark," 12 2015. [Online]. Available: <http://stateofgreen.com/files/download/1975>. [Accessed 06 06 2017].
- [45] M. Altin, X. Han, A. D. Hansen, R. L. Olsen, N. A. Cutululis and F. Iov, "Technical Feasibility of Ancillary Services provided by ReGen plants," 30 09 2015. [Online]. Available: [http://orbit.dtu.dk/files/118349095/Technical\\_Feasibility.pdf](http://orbit.dtu.dk/files/118349095/Technical_Feasibility.pdf). [Accessed 07 06 2017].
- [46] Dong Energy, "Where we operate," Dong Energy, [Online]. Available: <http://www.dongenergy.com/en/our-business/bioenergy-thermal-power/where-we-operate>. [Accessed 07 06 2017].
- [47] Statensnet, "Case: Viborg CHP Plant," [Online]. Available: <http://www.statensnet.dk/pligtarkiv/fremvis.pl?vaerkid=329&reprid=0&filid=16&iarkiv=1>. [Accessed 07 06 2017].
- [48] Wikiwand, "Fyn Power Station," [Online]. Available: [http://www.wikiwand.com/en/Fyn\\_Power\\_Station](http://www.wikiwand.com/en/Fyn_Power_Station). [Accessed 07 06 2017].
- [49] Vattenfall, "Nordjylland Power Station," Google Cache, [Online]. Available: [https://webcache.googleusercontent.com/search?q=cache:ClcSdjBtZr8J:https://corporate.vattenfall.dk/globalassets/danmark/om\\_os/nordjyllandsvaerket\\_english.pdf+&cd=8&hl=ca&ct=clnk&gl=dk](https://webcache.googleusercontent.com/search?q=cache:ClcSdjBtZr8J:https://corporate.vattenfall.dk/globalassets/danmark/om_os/nordjyllandsvaerket_english.pdf+&cd=8&hl=ca&ct=clnk&gl=dk). [Accessed 07 06 2017].
- [50] DONG Energy, "Annual report 2016," 02 02 2017. [Online]. Available: [http://assets.dongenergy.com/DONGEnergyDocuments/com/Investor/Annual\\_Report/2016/dong\\_energy\\_annual\\_report\\_en.pdf](http://assets.dongenergy.com/DONGEnergyDocuments/com/Investor/Annual_Report/2016/dong_energy_annual_report_en.pdf). [Accessed 07 06 2017].
- [51] Jessen, Kasper; Green Energy, "DISTRICT HEATING in The Danish Energy System," [Online]. Available: <http://www.northsearegion.eu/media/1531/the-danish-energy-system-case-dh.pdf>. [Accessed 07 06 2017].
- [52] International Energy Agency, "PVPS annual report 2016," 18 05 2017. [Online]. Available: <http://www.iea-pvps.org/index.php?id=6>. [Accessed 09 06 2017].
- [53] Energinet.dk, "Solar power," [Online]. Available: <http://energinet.dk/EN/KLIMA-OG-MILJOE/Miljoerapportering/VE-produktion/Sider/Sol.aspx>. [Accessed 27 05 2017].
- [54] D. Wu, F. Tang, T. Dragicevic, J. M. Guerrero and J. C. Vasquez, "Coordinated primary and secondary control with frequency-bus-signaling for distributed generation and storage in islanded microgrids," in *In Proceedings of the 39th Annual Conference of the IEEE Industrial Electronics Society IEEE IECON'13*, Vienna, Austria, Nov. 2013.

- [55] A. Sangwongwanich, Y. Yang, F. Blaabjerg and D. Sera, "Delta power control strategy for multi-string grid-connected PV inverters," in *In Proceedings of the 8th Annual IEEE Energy Conversion Congress and Exposition, ECCE 2016*, IEEE Press, 2016.
- [56] C. Rahmann and A. Castillo, "Fast frequency response capability of photovoltaic power plants: the necessity of new grid requirements and definitions," *Energies*, vol. 7, no. 10, pp. 6306-6322, 2014.
- [57] Danish Energy Agency, "Data: Oversigt over energisektoren," 19 05 2017. [Online]. Available: <https://ens.dk/service/statistik-data-noegletal-og-kort/data-oversigt-over-energiesektoren>. [Accessed 12 06 2017].
- [58] D. E. Agency, "Energistatistik 2015: Data, tabeller, statistikker og kort," [Online]. Available: <https://ens.dk/sites/ens.dk/files/Statistik/energistatistik2015.pdf>. [Accessed 12 06 2017].
- [59] H. Jacobsen, "Denmark breaks its own world record in wind energy," 15 01 2016. [Online]. Available: <http://www.euractiv.com/section/climate-environment/news/denmark-breaks-its-own-world-record-in-wind-energy/>. [Accessed 12 06 2017].
- [60] A. Neslen, "Wind power generates 140% of Denmark's electricity demand," *The guardian*, 10 07 2015. [Online]. Available: <https://www.theguardian.com/environment/2015/jul/10/denmark-wind-windfarm-power-exceed-electricity-demand>. [Accessed 12 06 2017].
- [61] Wind Europe, "Daily Wind Power Numbers," 22 02 2017. [Online]. Available: <https://windeurope.org/about-wind/daily-wind-archive/2017-02-22/>. [Accessed 12 06 2017].
- [62] M. Andrei, "Denmark just ran a day entirely on wind energy," *ZME Science*, 03 03 2017. [Online]. Available: <http://www.zmescience.com/ecology/renewable-energy-ecology/denmark-wind-energy-03032017/>. [Accessed 12 06 2017].
- [63] Global Wind Energy Council (GWEC), "Global Wind Report: Annual Market Update 2016," 25 04 2017. [Online]. Available: <http://files.gwec.net/files/GWR2016.pdf>. [Accessed 12 06 2017].
- [64] WECC Renewable Energy Modeling Task Force, "WECC Wind Plant Dynamic Modeling Guidelines," 04 2014. [Online]. Available: <https://www.wecc.biz/Reliability/WECC%20Wind%20Plant%20Dynamic%20Modeling%20Guidelines.pdf>. [Accessed 12 06 2017].
- [65] NEPLAN, "Wind Turbine Models IEC 61400-27-1," [Online]. Available: [http://www.neplan.ch/wp-content/uploads/2015/08/NEPLAN\\_IEC-61400-27-1.pdf](http://www.neplan.ch/wp-content/uploads/2015/08/NEPLAN_IEC-61400-27-1.pdf). [Accessed 12 06 2017].
- [66] IEA Wind, "Annual Report 2015: Denmark," [Online]. Available: [https://www.ieawind.org/annual\\_reports\\_PDF/2015/Denmark.pdf](https://www.ieawind.org/annual_reports_PDF/2015/Denmark.pdf). [Accessed 12 06 2017].

- [67] CIGRE Task Force 25 of Advisory Group 02 of Study Committee C4, "Modeling of Gas Turbines and Steam Turbines in Combined Cycle Power Plants," 12 2003. [Online]. Available: <http://www.e-cigre.org/Order/select.asp?ID=236>. [Accessed 07 06 2017].
- [68] IEEE Working Group, "Dynamic models for fossil fueled steam units in power system studies," *IEEE Transactions on Power Systems*, vol. 6, no. 2, pp. 753-761, 1991.
- [69] IEEE Committee report, "Dynamic models for steam and hydro turbines in power system studies," *IEEE Transactions on Power Apparatus and Systems*, Vols. PAS-92, no. 6, pp. 1904-1915, 1973.
- [70] IEEE Task force on turbine-governor modeling, "Dynamic Models for Turbine-Governors in Power System Studies," 01 2013. [Online]. Available: <https://es.scribd.com/document/170578635/IEEE-PES-Dynamic-Models-for-Turbine-Governors-in-Power-System-Studies-PES-TR1-Jan-2013>. [Accessed 08 06 2017].
- [71] SIEMENS, "Dynamic Models Package „Standard-1“,” 10 2012. [Online]. Available: [https://www.energy.siemens.com/hq/pool/hq/services/power-transmission-distribution/power-technologies-international/software-solutions/BOSL\\_Controllers\\_Standard-1.pdf](https://www.energy.siemens.com/hq/pool/hq/services/power-transmission-distribution/power-technologies-international/software-solutions/BOSL_Controllers_Standard-1.pdf). [Accessed 08 06 2017].
- [72] F. Iov and L. Petersen, "Solar PV System Performance Model: Implementation Description," Smart Energy Systems Lab, Aalborg University, 2016.
- [73] C.-I. Ciontea, D. Sera and F. Iov, "Influence of Resolution of the Input Data on Distributed Generation Integration Studies.," in *14th International Conference on Optimization of Electrical and Electronic Equipment*, Brasov, Romania, 2014.
- [74] A. D. Hansen and I. D. Margaritis, "Type IV Wind Turbine Model," 2014. [Online]. Available: [http://orbit.dtu.dk/files/102281784/Type\\_IV\\_wind\\_turbine\\_model.pdf](http://orbit.dtu.dk/files/102281784/Type_IV_wind_turbine_model.pdf). [Accessed 11 06 2017].
- [75] M. Altin, A. D. Hansen, Ö. Göksu, N. A. Cutululis and P. E. Sørensen, "Wind Turbine and Wind Power Plant Modelling Aspects for Power System Stability Studies," in *In Proceedings of the International Conference on Wind Energy Grid-Adaptive Technologies 2014*, 2014.
- [76] A. D. Hansen, M. Altin and N. A. Cutululis, "Modelling of wind power plant controller, wind speed time series, aggregation and sample results," *DTU Wind Energy*, no. 0080, 2018.
- [77] J. Van de Vyver, J. D. M. De Kooning, B. Meersman, L. Vandeveldel and T. L. Vandoorn, "Droop Control as an Alternative Inertial Response Strategy for the Synthetic Inertia on Wind Turbines," *IEEE Transactions on power systems*, vol. 31, no. 2, pp. 1129-1138, 2016.
- [78] T. Inoue, H. Taniguchi, Y. Ikeguchi and K. Yoshida, "Estimation of Power System Inertia Constant and Capacity of Spinning reserve Support Generators Using Measured Frequency Transients," *IEEE Transactions on Power Systems*, vol. 12, no. 1, pp. 136-143, 1997.

- [79] A. Molina-García, I. Muñoz-Benavente, A. D. Hansen and E. Gómez-Lázaro, "Demand-Side Contribution to Primary Frequency Control With Wind Farm Auxiliary Control," *IEEE transactions on power systems*, 2014.
- [80] P.-K. Keung, H. Banakar and B. T. Ooi, "Kinetic Energy of Wind-Turbine Generators for System Frequency Support," *IEEE Transactions on power systems*, vol. 24, no. 1, pp. 279-287, 2009.
- [81] ENTSO-E, "P1 - Policy 1: Load-Frequency Control and Performance [C]," 19 03 2009. [Online]. Available: [http://kom.aau.dk/project/smartcool/restricted\\_files/2012.11.06-AAU/ENTSOE\\_UCTE\\_frequency\\_reserves.pdf](http://kom.aau.dk/project/smartcool/restricted_files/2012.11.06-AAU/ENTSOE_UCTE_frequency_reserves.pdf). [Accessed 05 04 2017].
- [82] Energinet.dk, "Energy scenarios for 2030," 04 10 2016. [Online]. Available: [http://www.energinet.dk/SiteCollectionDocuments/Engelske%20dokumenter/Klimaogmiljo/15-08958-165%20Energy%20Scenarios%20for%202030%20\(UK%20Version\)%203957068\\_3\\_1.PDF](http://www.energinet.dk/SiteCollectionDocuments/Engelske%20dokumenter/Klimaogmiljo/15-08958-165%20Energy%20Scenarios%20for%202030%20(UK%20Version)%203957068_3_1.PDF). [Accessed 29 05 2017].
- [83] F. W. Letson, "Wind Power Capacity Value Metrics and Variability: A study in New England," 2015. [Online]. Available: [http://scholarworks.umass.edu/cgi/viewcontent.cgi?article=1486&context=dissertations\\_2](http://scholarworks.umass.edu/cgi/viewcontent.cgi?article=1486&context=dissertations_2). [Accessed 25 06 2017].
- [84] FLSmidth, "High Penetrations of Renewable Energy for Island Grids," [Online]. Available: [http://www.homerenergy.com/White\\_Papers/High\\_Penetrations\\_of\\_Renewable\\_Energy\\_for\\_Island\\_Grids.pdf](http://www.homerenergy.com/White_Papers/High_Penetrations_of_Renewable_Energy_for_Island_Grids.pdf). [Accessed 25 06 2017].
- [85] M. Kayikçi and J. V. Milanovic, "Dynamic Contribution of DFIG-Based Wind Plants to System Frequency Disturbances," *IEEE Transactions on power systems*, vol. 24, no. 2, pp. 859-867, 2009.
- [86] F. Díaz-González, M. Hau, A. Sumper y O. Gomis-Bellmunt, «Coordinated Operation of Wind Turbines and Flywheel Storage for Primary Frequency Control Support,» *International Journal of Electrical Power and Energy Systems*, 2014.
- [87] Vanterfall, "Nordjylland power plant," Google Cache, [Online]. Available: [https://webcache.googleusercontent.com/search?q=cache:ClcSdjBtZr8J:https://corporate.vattenfall.dk/globalassets/danmark/om\\_os/nordjyllandsvaerket\\_english.pdf+&cd=8&hl=ca&ct=clnk&gl=dk](https://webcache.googleusercontent.com/search?q=cache:ClcSdjBtZr8J:https://corporate.vattenfall.dk/globalassets/danmark/om_os/nordjyllandsvaerket_english.pdf+&cd=8&hl=ca&ct=clnk&gl=dk). [Accessed 07 06 2017].

## **Appendix: Model parameters**

In this appendix, the parameters of all the models simulated are presented in the following tables. Parameters of the CHP and must-run units are shown in Table A.1. Parameters of the DCHP unit are shown in Table A.2. Parameters of the SPVS are shown in Table A.3. Parameters of the WPP are shown in Table A.4. Parameters for the HVDC interconnectors are shown in

Table A.5.

Table A.1 Parameters of the aggregated CHP and must-run unit

Model	Parameter	Description	Value for CHP	Value for must-run
Boiler model	Tb1	1 <sup>st</sup> Boiler time constant	5 s	5 s
	Tb2	2 <sup>nd</sup> Boiler time constant	30 s	30 s
	Tb3	3 <sup>rd</sup> Boiler time constant	40 s	40 s
Speed Governor	Ramp rate	Power ramp limiter	0,1 pu/s	0,1 pu/s
	T <sub>f</sub>	Measurement and communication delay	0,1 s	0,1 s
	Dband	Dead band	49,8-50,2 Hz	49,8-50,2 Hz
	R <sub>CHP</sub>	Droop	0,06 pu	0,06 pu
Steam Turbine	$K_1$	Very high pressure turbine power fraction	0,22 pu	0,22 pu
	$K_2$	High pressure turbine power fraction	0,22 pu	0,22 pu
	$K_3$	Intermediate pressure power fraction	0,28 pu	0,28 pu
	$K_4$	Low pressure power fraction	0,28 pu	0,28 pu
	$T_1$	Chest and inlet piping	0,4 s	0,2 s
	$T_2$	Re-heater time constant	11 s	8 s
	$T_3$	Crossover time constant	11 s	8 s
	$T_4$	Double re-heater time constant	0,5 s	0,4 s
	P <sub>max</sub>	Maximum power output	1 pu	1 pu
	P <sub>min</sub>	Minimum power output	0,1 pu	0,1 pu

Table A.2 Parameters of the aggregated DCHP unit

Model	Parameter	Description	Value
Speed Governor	Ramp rate	Power ramp limiter	0,1 pu/s
	$T_f$	Measurement and communication delay	0,1 s
	Dband	Dead band	49,8-50,2 Hz
	R <sub>DCHP</sub>	Droop	0,06 pu
	$D_T$	Turbine parameter	0
Gas Turbine	V <sub>max</sub>	Maximum load power output	1 pu
	V <sub>min</sub>	Minimum load power output	0,1 pu
	$T_1$	Fuel valve time constant	0,5 s
	$T_2$	Turbine time constant	0,4 s
Power Limiter	$T_3$	Load limit time constant	1 s
	KT	Load limit feedback gain	2 pu
	AT	Ambient temperature load limit	1 pu

Table A.3 Parameters of the aggregated SPVS

Model	Parameter	Description	Value
Speed Governor	Ramp rate	Power ramp limiter	1 pu/s
	$T_f$	Measurement and communication delay	0,1 s
	Dband	Dead band	49,8-50,2 Hz
	$R_{SPVS}$	Droop	0,04 pu
PV Module	Rated power	Rated power of the PV Module	360 W
	$V_m$	Voltage MPPT	38,4 V
	$V_{oc}$	Voltage open circuit	48,3 V
	$I_m$	Current MPPT	9,39 A
	$I_{sc}$	Short circuit current	9,84 A
	NOCT	Normal operating cell temperature	318 K
Grid Converter	$\eta$	Grid converter Efficiency	0,985 pu
Power Control Method Selector	$\Delta P_{curtail}$	Power curtailment	0
Time constant P loop	$T_p$	Active power loop time constant	0,1 s

Table A.4 Parameters of the aggregated WPP

Model	Parameter	Description	Value
Speed Governor	Ramp rate	Power ramp limiter	0,1-0,5 pu/s*
	$T_f$	Measurement and communication delay	0,1 s
	Dband	Dead band	49,8-50,2 Hz
	$R_{WPP}$	Droop	0,02-0,12 pu*
	$K_d$	Virtual inertia gain	0-60 pu*
	$\Delta P_{max}$	Maximum upregulation in active power	$\Delta P_{curtail}$
	$\Delta P_{min}$	Minimum downregulation in active power	$-(P_{nominal}-\Delta P_{curtail})$
Power Control Method Selector	$\Delta P_{curtail}$	Power curtailment	(0,39-0,14) pu*
Time constant P loop	$T_{WPP}$	Aggregated delay for the active power loop time constant	3 s

\* Depending on the test case simulated explained in chapter 4. When increasing the RES penetration, the power curtailment decreases and it is calculated as (1 pu – power set point [pu]).

Table A.5 Parameters of the aggregated HVDC interconnector and outage simulated

Parameter	Description	Value for HVDC
f <sub>act</sub>	Frequency when the HVDC activates the emergency support	50,6 Hz
f <sub>deact</sub>	Frequency when the HVDC deactivates the emergency support	50 Hz
CapAv	Capacity available to support the power system	0-300 MW*
Ramp rate	Power ramp limiter	1 pu
delay	Time delay after the activation of the emergency support	0,1 s
Parameter	Description	Value for the outage
P <sub>imbalance</sub>	Outage simulated in the model (Surplus of generation)	+717 MW

\* Depending on the scenario simulated explained in the sensitivity study of the HVDC interconnections support in chapter 4.